Exploring the role of aneuploidy in phenotypic variability

by

Christine Anne Moomau

B.S. Cell Biology and Molecular Genetics
University of Maryland

Submitted to the Department of Biology
in Partial Fulfillment of the Requirements for the Degree of

Doctor of Philosophy

at the

MASSACHUSETTS INSTITUTE OF TECHNOLOGY

February 2022

Signature of Author _____
Department of Biology
December 9, 2021

Certified by_____
Matthew Vander Heiden
Director, Koch Institute for Integrative Cancer Research
Lester Wolfe Professor of Molecular Biology
Thesis Supervisor

Accepted by_____
Amy Keating
Professor of Biology and Biological Engineering
Co-Director, Biology Graduate Committee

Exploring the role of aneuploidy in phenotypic variability

by

Christine Anne Moomau

Submitted to the Department of Biology on December 9th, 2021 in Partial Fulfilment of the Requirements for the Degree of Doctor of Philosophy in Biology.

ABSTRACT

Phenotypic variability is a noted feature of human trisomies. This is exemplified by the presentation of trisomy 21 (Down syndrome). The incidence of and severity of clinical features are highly variable in individuals with Down syndrome. These differences have long been attributed to genetic differences within the population altering the likelihood that particular phenotypes will develop. However, work in yeast and mouse models of aneuploidy suggest that phenotypic variability can be a consequence of aneuploidy itself in the absence of genetic heterogeneity.

By studying variability in induction of the GAL1-10 promoter in aneuploid strains of budding yeast, S. cerevisiae, we show that altering gene dosage can lead to variability. The endocytosis defect caused by a specific aneuploidy (Disome IX) is sufficient to increase variability in the GAL signaling pathway. The addition of a second copy of chromosome IX in haploid yeast increases the dosage of multiple genes involved in endocytosis. This leads to an endocytic defect that impacts the cell surface localization of hexose transporters, which ultimately leads to variability in uptake of hexose sugars and thus variability in induction of the GAL1-10 promoter.

Thesis Supervisor: Matthew Vander Heiden
Title: Director, Koch Institute for Integrative Cancer Research

This thesis is dedicated to my mom, Pam Moomau, and my mentor, Angelika Amon; two brilliant women I am lucky to have known.

Acknowledgments

First, I would like to thank my advisor, Angelika. She was a dedicated mentor and enthusiastic scientist who always made time for her students. Angelika's enthusiasm was infectious, she provided me with endless motivation and advice when I needed it most. I will always remember and share her passion for the best things in life: yeast, wine, chocolate, puzzles, and bunnies.

I have been lucky to work with an exceptional group of people in the Amon Lab. It was a great place to work, full of both hard work and fun. I have learned so much from lab members past and present and am grateful for the community we all share.

I would also like to thank Matt Vander Heiden for providing me a new science home when I needed one. Matt and his lab have been so helpful and welcoming over the last year, and I am glad I have gotten to know them better. I am also grateful to my thesis committee, Mike Laub and Gene-Wei Li, for their insights and support throughout this project, and Mike Springer who has been generous with his time, resources, and lab space over the years.

I am thankful to my friends for filling my life with laughter and fun. Thanks to Becca for the coffee breaks, long walks, and couch chats. Thanks to Summer, Franny, John, Allegra, and Juliet for the many adventures over the years. Thanks to Savannah, Nadia, Becky, and Theresa for a group chat filled with pet photos and encouragement. Thank you to Dan for the love and patience, for enduring grad school, and for making Cambridge feel like home from day one. And thank you to all of the animals: Luna, Duncan, Papaya, Bonnie, Artemis, Blueberry, Silas, Fern, Riley, Colby, and Mimi.

Finally, I would like to thank my family. My siblings, nieces, and nephews are a consistent source of support in my life and remind me that life exists outside of school. My parents have always been encouraging and loving, and I am grateful they instilled in me a love of learning.

Table of Contents

Chapter 1: Introduction

Aneuploidy is an imbalanced karyotype in which chromosomal content is not a multiple of the haploid complement, due to the gain or loss of one or more whole chromosomes. Most organisms are haploid (1n) having one copy of each chromosome, or diploid (2n) with two copies of each chromosome. Aneuploidy is distinct from polyploidy, in which full additional sets of chromosomes are present. For example, a diploid cell which duplicates but fails to segregate its chromosomes will become tetraploid (4n). In polyploidy, the copy number of all genes are altered, maintaining a constant ratio of dosage relative to one another. In contrast, aneuploidy results in an imbalanced karyotype, meaning the dosage of certain genes are increased or decreased relative to the rest of the genome. Aneuploidy has a variety of consequences at both the cellular and organismal level (Figure 1). Aneuploid cells have delayed cell cycle entry and proliferative defects (Bonney et al., 2015; Thorburn et al., 2013; Torres et al., 2007), proteotoxic stress (Oromendia et al., 2012; Stingele et al., 2012), genomic instability (Sheltzer et al., 2011; Zhu et al., 2012), and a unique gene expression signature (Sheltzer et al., 2012; Terhorst et al., 2020). On the organismal level, aneuploidy has widely negative effects. Very few whole chromosome aneuploidies are observed in nature and all are associated with developmental defects and reduced life span (Siegel and Amon, 2012).

In this introduction I will discuss an emerging consequence of aneuploidy – non-genetic variability. I will first discuss this in the context of mammalian aneuploidy, specifically human trisomies. Then, I will review variability in the context of aneuploid yeast. Finally, I will introduce the yeast galactose regulatory pathway as a context in which to study variability in transcriptional induction.

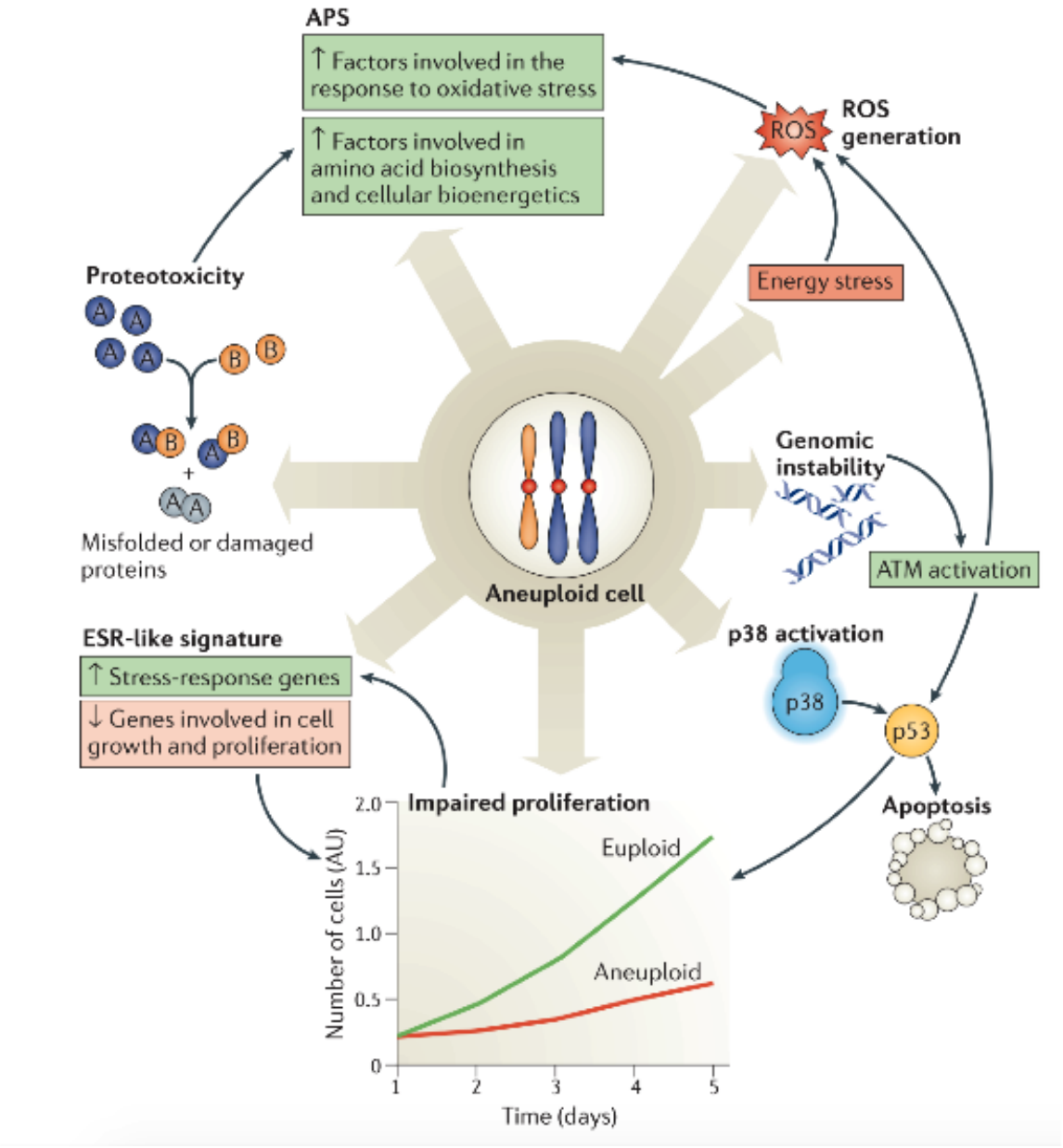

Figure 1. Aneuploidy induces many common phenotypes

(Figure adapted from Santaguida and Amon 2015).

ANEUPLOIDY IN MAMMALS

Aneuploidy and cancer

Aneuploidy is considered a hallmark of cancer, present in 90% of solid tumors, and 75% of hematopoietic tumors (Hanahan and Weinberg, 2000, 2011; Weaver and Cleveland, 2006). Tumors frequently have complex karyotypes with many chromosomal gains and losses. Aneuploidy in cancer is associated with chemotherapy resistance, higher rates of recurrence, and poor prognosis. Considering the many cellular defects associated with aneuploidy, this relationship with cancer is surprising (Pfau and Amon, 2012). Some cancers are particularly prone to specific chromosomal gains, indicating a fitness gain in the context of cancer that is not present in typical cells. Chromosome 8 is commonly gained in multiple cancers, including acute myeloid leukemia (AML), Wilm's tumor, and Ewing's sarcoma (Maurici et al., 1998; Ozery-Flato et al., 2011; Peres et al., 2004). In Ewing's sarcoma, the gain of RAD21 on chromosome 8 mitigates replication stress caused by the EWS-FLI1 oncogene which drive the cancer (Su et al., 2021).

Human trisomies

Aneuploidy is the leading cause of miscarriage in humans, accounting for up to 85% of spontaneous abortions (Jia et al., 2015). Very few human aneuploidies are viable. There are no chromosomal losses, with the exception of sex chromosomes, and very few chromosomal gains that are tolerated. Trisomy is the most common chromosomal abnormality observed in humans, about 4% of recognized pregnancies are identified as trisomic and about 0.3% of live born infants are trisomic (Hassold and Jacobs, 1984). The only autosomal trisomies which have

been identified at birth are trisomies 13, 18, 21. Trisomy 18, Edwards syndrome, is the second most common trisomy at birth, occurring in around 1 in 5,000. The condition is marked structural defects and cardiac lesions (Lin et al., 2006). Trisomy 13, Patau syndrome, occurs in approximately 1 in 20,000 live births and is characterized by cleft palate, microphthalmia, and polydactyly (Hsu and Hou, 2007). Both Edwards and Patau syndrome are typically fatal within the first year of life.

Trisomy 21, Down syndrome, is the most common, occurring in about 1 in 750 live births. Down syndrome is associated with a number of phenotypes including congenital heart disease, childhood leukemias, Alzheimer's disease, cognitive impairment, and shortened life span, although many individuals with Down syndrome live well into adulthood (Roizen and Patterson, 2003). Exactly how the gain of chromosome 21 leads to these phenotypes has been a topic of debate. There are two hypotheses for how the Down syndrome genotype relates to phenotype – "gene dosage hypothesis" and "amplified developmental instability hypothesis" (Pritchard and Kola, 1999).

Gene dosage hypothesis

The "gene dosage hypothesis" posits that the phenotypes associated with chromosomal gain are due to the increased dosage of specific genes on that chromosome. In Down Syndrome, this would mean that the increased dosage of a few genes on chromosome 21 are responsible for the majority of phenotypes. Work focused on identifying these genes has led to the discovery of the "Down syndrome critical region" (DSCR), a region on HSA21q22 believed to be responsible for the majority of Down syndrome phenotypes based on sequence analysis of

individuals with partial trisomy 21 (Delabara et al., 1993; Kahlem, 2006; Korenberg et al., 1990; Rachidi and Lopes, 2007, 2008). The DSCR is further supported by mouse models of Down syndrome. Down syndrome is typically modeled in mice by segmental trisomy 16, Ts65Dn, but the critical region can be modeled in Ts1Rhr mice which are trisomic for 33 genes corresponding to the DSCR. Trisomy in the Ts1Rhr segment causes significant changes in 20 of 48 phenotypes associated with typical Down syndrome models (Belichenko et al., 2009). However, the Ts1Rhr segment is not sufficient, to produce the impaired hippocampal function seen in Ts65Dn (Olson et al., 2007). While some Down syndrome phenotypes have been successfully mapped to the DSCR or other smaller segments of chromosome 21, others cannot be attributed to specific trisomic genes (Korbel et al., 2009; Olson et al., 2004, 2007).

An example of gene dosage directly leading to a phenotype in Down syndrome is Alzheimer's disease. Nearly every individual with Down syndrome develops Alzheimer's disease pathology by age 40, with dementia developing as they age (Hartley et al., 2015). This can be traced to the increased dosage of amyloid precursor protein (APP) on chromosome 21. Duplication of the APP locus in otherwise euploid individuals causes early onset Alzheimer's disease with autosomal dominant inheritance (Rovelet-Lecrux et al., 2006). Conversely, a rare individual with Down syndrome due to partial trisomy 21 who lacked triplication of the region of chromosome 21 containing APP, did not develop Alzheimer's, nor the associated dementia, plasma Aß, or neuritic plaques (Doran et al., 2017). In this case, there is a clear and demonstrable link between gene dosage and a specific phenotype, where a locus on the chromosome is both sufficient to cause a phenotype and necessary for that phenotype in Down syndrome.

It is also possible for gene dosage to have less direct consequences (Reviewed in Roper and Reeves, 2006) (Figure 2). Trisomic genes can directly affect the function of a differentiated cell or alter development of undifferentiated cells. Trisomic gene can also affect the gene expression of disomic genes. For example, cells trisomic for transcription factor RUNX1 have increased levels of hemogenic epithelium markers Tie-2 and c-Kit, potentially contributing to the high risk of leukemia in children with Down syndrome (De Vita et al., 2010).

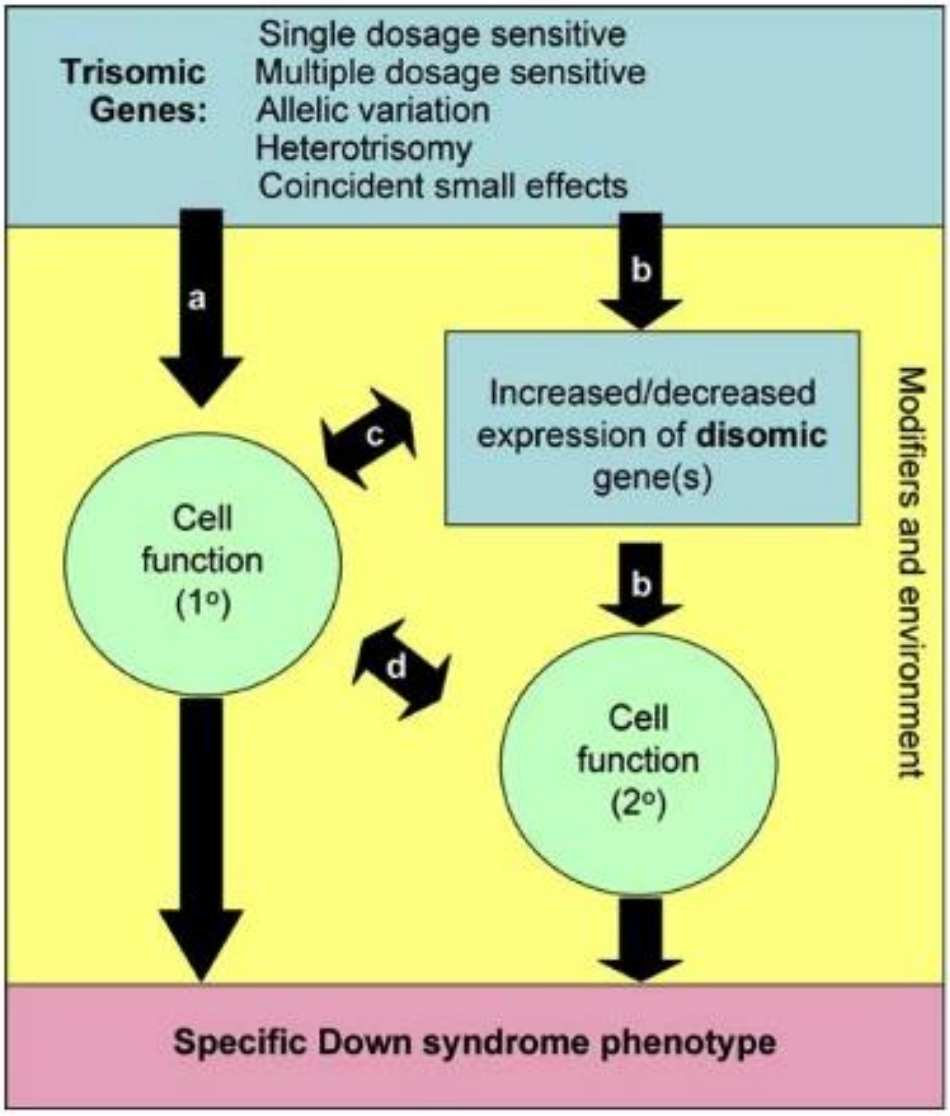

Figure 2. Trisomic gene dosage produces phenotypes in a number of ways

Trisomic genes can directly alter cell function (a) or alter the development of undifferentiated cells (d). Trisomy of regulatory elements may alter expression of disomic genes (b) which can themselves alter primary or secondary cell function (b,c). All of these pathways interact with each other and the environment to ultimately produce phenotypes. (Figure adapted from Roper and Reeves 2006).

Amplified developmental instability hypothesis

An alternate, but not mutually exclusive, hypothesis for how trisomy generates phenotypes is the "amplified developmental instability hypothesis." It states that altering the dosage of many genes at once disrupts cellular homeostasis which propagates through development to produce a wide range of phenotypes (Rachidi and Lopes, 2007; Shapiro, 1975, 1994). This is supported by the fact that the only viable human aneuploidies are in the three chromosomes with the fewest open reading frames (ORFs). In mice, the only trisomy which is not embryonic lethal is in chromosome 19, the smallest autosome (Lorke, 1994). This relationship between degree of aneuploidy and severity of phenotype would suggest that the consequences of aneuploidy scales with the number of genes altered, rather than the specific identity of those genes.

Many commonalities exist between human trisomies (Hall, 1965; Shapiro, 1975, 1994). Cardiac defects, developmental delay, and cognitive impairment are common to trisomies 13, 18, and 21. It is possible that these overlapping phenotypes represent general consequences of aneuploidy that result from the addition of many genes, regardless of the identity of those genes. The alternate must also be considered that the mechanism by which these characteristics are produced are unique to each chromosome (Pritchard and Kola, 1999). In that case, the commonalities between different trisomies would be indicative of complex phenotypes which are sensitive to gene dosage in several processes which contribute to the phenotype.

Variability in aneuploidy

A striking feature of all human aneuploidies is the wide variability in incidence and severity of characteristics observed across trisomic individuals. 75% of trisomy 21 embryos result in spontaneous miscarriage, but individuals with Down syndrome live well past 60 (Hassold and Jacobs, 1984; Roizen and Patterson, 2003). All people with Down syndrome will develop Alzheimer's plaques by age 40, but age of dementia onset varies widely, with 70% developing dementia by ago 60 (Hartley et al., 2015). 40-50% of people with Down syndrome have a congenital heart defect, with the exact anomaly varying (Cohen, 2003; Roper and Reeves, 2006).

In trisomy 18, some characteristic traits such as clenched hands and malformed ears are almost universal, occurring in about 90% of cases. However, other phenotypes are quite variable between individuals, for example around half of babies have microcephaly, around one third have hypertelorism, and around 10% of cases have corneal opacity (Lin et al., 2006).

Trisomy 13 is also marked by phenotypic variability. Patau syndrome is classically characterized by a "clinical triad" of cleft palate, microphthalmia, and polydactyly, however, individuals rarely have all three, and some have none (Caba et al., 2013; Hsu and Hou, 2007).

Genetic variability

The marked phenotypic variability in trisomies is often thought to be due to genetic heterogeneity. Individuals with Down syndrome all have a third copy of chromosome 21, but are otherwise genetically diverse with the typical array of alleles and mutations present in all

people. Allelic differences in disomic genes and trisomic genes could impact the severity of Down syndrome phenotypes.

Mutations in specific disomic genes can increased the incidence of congenital heart disease (CHD) in trisomy 21 (Dunlevy et al., 2010; Li et al., 2012; Maslen et al., 2006). Studies of people with atrioventricular septal defects (AVSD) in both euploid and Down syndrome groups led to the discovery of missense mutations in CRELD1. In the euploid population, these mutations confer a susceptibility for AVSD with incomplete penetrance. CRELD1 mutations were also identified in the Down syndrome population in 5% of participants with AVSD, and none who did not also have AVSD (Maslen et al., 2006). This relationship is present in mouse studies as well. Ts65Dn mice have a higher incidence of CHD when in combination with loss of function mutations in CREDL1 or HEY2. Ts65Dn Creld1$^{+/-}$ and Ts65Dn Hey2$^{+/-}$ mice have significantly higher chance of septal defect than Ts65Dn, Creld1$^{+/-}$ or Hey2$^{+/-}$ mutants alone (Li et al., 2012).

Allelic differences in disomic genes affect mandible size and embryo body size in the mouse Down syndrome model Ts1Rhr (Deitz and Roper, 2011). Ts1Rhr mice which are crossed into different background genotypes display phenotypic differences. Expression of three genes associated with Down syndrome craniofacial phenotypes, Dyrk1a, Rcan1, and Ets2 (Arron et al., 2006; Hill et al., 2009), are higher in mixed background mice than inbred (Deitz and Roper, 2011). These differences indicate that alleles outside of the trisomic chromosome can affect expression of the trisomic genes, and therefore alter phenotypes.

Mutations on chromosome 21 could also induce variability in the Down syndrome population. Single nucleotide polymorphisms (SNPs) and copy number variations (CNVs) are common points of genetic heterogeneity in the general population and are known to affect gene expression. Therefore, SNPs and CNVs on chromosome 21 could have big effects on the severity of Down syndrome phenotypes (Letourneau and Antonarakis, 2012; Smith et al., 2010). For this reason, SNPs and CNVs that fall within loci already associated with disease are good candidates for potential sources of phenotypic variability.

Another hypothesis for the source of phenotypic variability in Down syndrome is that genomic instability stochastically causes heterogeneity across cell types in individuals. In yeast, all constitutive aneuploidies display some sort of genomic instability (Sheltzer et al., 2011). Chromosomal instability in aneuploid cells is thought to be a driver of cancer, providing a fitness advantage in rapidly changing environments (Birkbak et al., 2011; Pfau and Amon, 2012; Zhu et al., 2012). In Alzheimer's disease models, exposure to Aß peptide induces chromosome mis-segregation leading to mosaic aneuploidies. Due to the APP locus on chromosome 21, excess Aß is constantly produced in Down syndrome, potentially leading to differing karyotypes across tissues and cell types (Potter, 2016). Depending on what chromosomal alterations occurred in what cell type, the resulting phenotypes could be quite different between individuals.

Non-genetic variability

Much less work has been done exploring the possibility that phenotypic variability is a consequence of aneuploidy itself. In humans it is impossible to study genetically homogenous

populations, however, laboratory models of aneuploidy provide that opportunity. Aneuploid yeast display non-genetic individuality in a number of metrics which will be discussed in more detail later in this chapter. Briefly, populations of yeast with chromosomal gains and losses are more variable in G1 duration, S and early M phase duration, activation of stress responses, and transcriptional induction (Beach et al., 2017)

Non-genetic variability can be observed in mice as well. Gross morphology of trisomy 13 and trisomy 19 embryos is more variable than their euploid littermates (Figures 3A, C). The thickness of nuchal edema is more variable in trisomy 19 embryos, with a significantly higher standard deviation than euploid embryos (Figure 3B) (Beach et al., 2017). In a study of cerebellar phenotypes in multiple mouse models of Down syndrome there was greater phenotypic variability in mice with more trisomic genes (Olson et al., 2004). Ts65Dn mice are more variable in cerebellar volume, granule cell density, and Purkinje cell density than Ts1Cje mice which are trisomic for 67% of the genes in Ts65Dn.

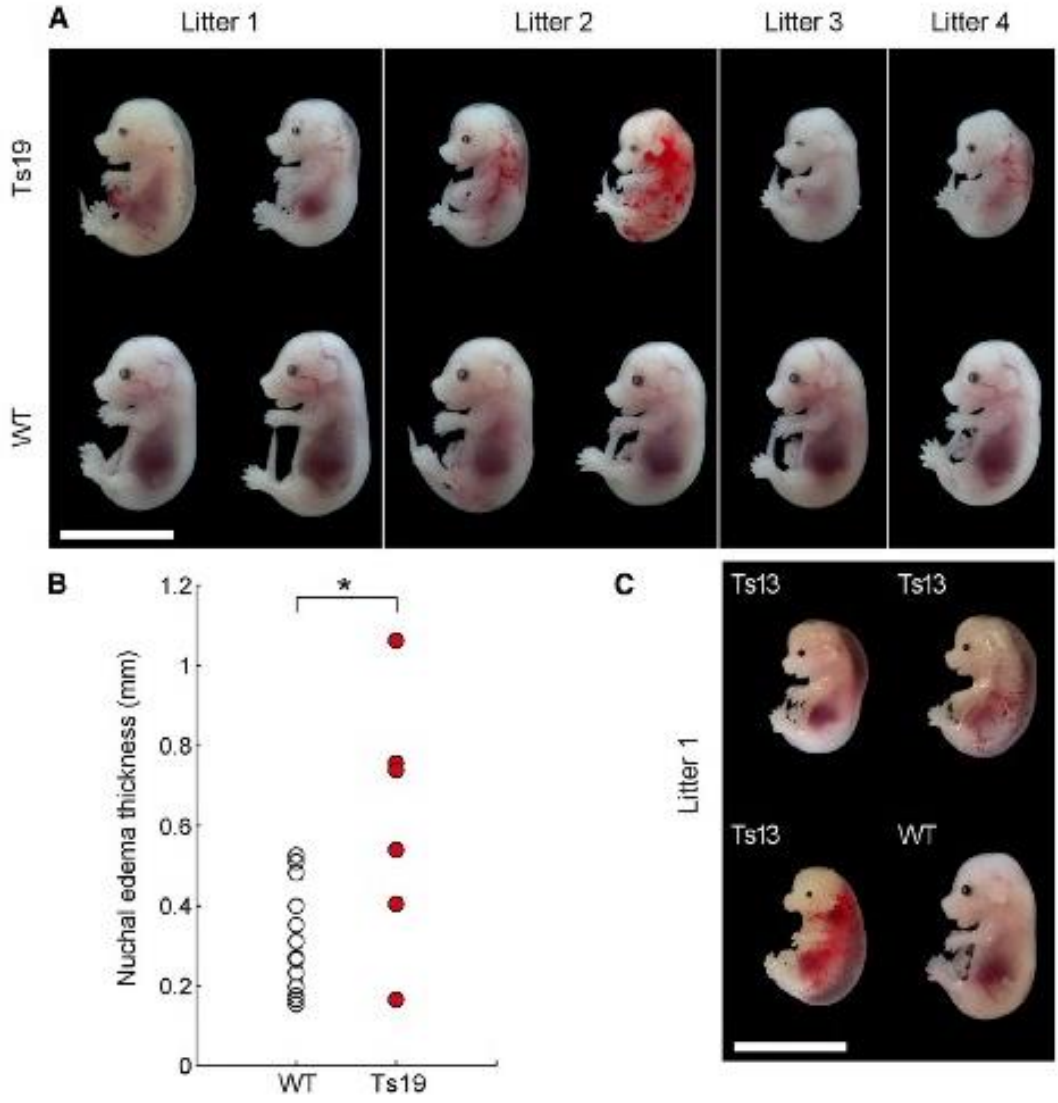

Figure 3. Variability in morphology of trisomic mouse embryos

(A) Trisomy 19 (Ts19) mice at embryonic day 15.5 and their euploid littermates (WT). (B) Quantification of nuchal edema thickness in embryos is (A). (C) Trisomy 13 (Ts13) mice at E15.5 and euploid (WT) littermates. (Figure adapted from Beach et al., 2017)

ANEUPLOIDY IN YEAST

Budding yeast, *Saccharomyces cerevisiae,* are a useful tool for studying the cellular effects of aneuploidy. The majority of work presented here was done in strains of haploid yeast containing and extra copy of specific chromosomes, known as disomes (Torres et al., 2007). Disomes were generated by random chromosome transfer induced by deletion of karyogamy gene KAR1 in one mating partner. Specific disomies were selected and maintained by placing selectable markers at the same locus in each mating partner. With dual selection, disomes can be maintained indefinitely.

Disomic yeast do not just contain extra DNA content, but the extra chromosome(s) are expressed. Increased copy number results in a corresponding rise in RNA and protein levels in disomic yeast (Dephoure et al., 2014; Stingele et al., 2012; Torres et al., 2007, 2010). There is no mechanism of dosage compensation in yeast as changes in gene dosage are tightly correlated with expression (Springer et al., 2010; Torres et al., 2016).

These stable disome strains are an excellent tool, but have a couple of important limitations. First, it is impossible to study chromosome loss through a similar method because nullisomes (n-1) and monosomes (2n-1) are not viable past a few divisions. Second, these disomes model the effects of being aneuploid over many generations and may be harboring compensatory mutations. To study the immediate effects of becoming aneuploid through chromosome gain or loss, conditional aneuploidies were made.

Conditional aneuploidies utilize a system to induce mis-segregation of specific chromosomes. In these strains, a GAL1-10 promoter is placed upstream of the centromere of

the chromosome of interest. When yeast are grown in glucose, their chromosomes segregate normally and they remain euploid. However, if the promoter is induced by media containing galactose, transcription at the centromere disrupts spindle assembly and that chromosome mis-segregates. In haploid yeast, this division will result in a nullisome and a disome. In diploid yeast, a trisome and a monosome are generated. GFP dots are used to track mis-segregation in individual cells by microscopy, allowing observation of the generations immediately following mis-segregation.

General consequences of aneuploidy

Using yeast models, we are able to observe phenotypes across gains and losses of many chromosomes. There are some phenotypes which are common to many or all aneuploidies, these are thought to be general consequences of aneuploidy. Rather than being the consequence of altered dosage of specific genes, these phenotypes are thought to be the result of the imbalanced karyotype or resulting imbalanced proteome, regardless of the specific genes involved. These generalized aneuploid phenotypes include proteotoxic stress, slowed cell cycle, genomic instability, and activation of a unique gene expression signature (Dephoure et al., 2014; Dodgson et al., 2016; Sheltzer et al., 2012; Thorburn et al., 2013; Torres et al., 2007).

Disomic yeast experience increased proteotoxic stress resulting from the excess protein produced by the increased copy number of many genes at once. As there is no dosage compensation in yeast, the addition of an extra chromosome increases the burden on protein quality control mechanisms (Springer et al., 2010; Torres et al., 2016). This is evident in the increase of Hsp104 associated aggregates observed in disomes (Oromendia et al., 2012).

Hsp104 is a molecular chaperone which colocalizes with aggregates of improperly folded proteins, increase Hsp104-eGFP foci are indicative of a stress response. Protein aggregation is induced only when excess DNA is expressed, yeast artificial chromosomes (YACs) containing human DNA that is not expressed in yeast do not cause an increase in aggregates. This aggregation represents an increased burden on the proteasome due to altered stoichiometry of protein complexes (Brennan et al., 2019). Increasing proteasome function by deletion of ubiquitin protease, UBP6, eases this burden, reducing aggregates in all disomes tested, and ameliorating growth defects in many disomes (Dephoure et al., 2014; Oromendia et al., 2012).

Aneuploid yeast also have a unique gene expression signature. Many disomes activate a transcriptional program characteristic of environmental changes such as temperature, osmotic stress, and starvation, known as the environmental stress response (ESR) (Gasch et al., 2000). In the ESR, ribosome biogenesis and RNA processing genes are down regulated as genes involved with protein folding and detoxification of reactive oxygen species (ROS) are upregulated, consistent with proteotoxic stress and ROS generation observed in aneuploid cells. Activation of the ESR reduces the number of ribosomes per cell, limiting mass accumulation throughout the prolonged cell cycle (Terhorst et al., 2020). Euploid yeast strains bearing non-expressed YACs also activated an ESR, suggesting that this phenotype is due to the presence of extra DNA rather than proteome imbalance (Torres et al., 2007).

Aneuploidy specific phenotypes

Other aneuploid phenotypes observed in yeast are the result of altered gene dosage. Phenotypes can be driven by a small number of dosage sensitive genes, or be the result of

altering dosage of many genes at once. In the simplest case, the overexpression of a single gene on a disomic chromosome produces a phenotype. This is true in Disome IX yeast which have an endocytic defect that is due almost entirely to the additional copy of a gene on chromosome IX, PRK1 (Dodgson et al., 2016).

Identifying the cause of slowed proliferation in disomes has been more complex. Using a "genetic tug of war" approach in 11 disomes, no genes were identified which are capable of recapitulating the proliferation defect of the full disomy (Bonney et al., 2015). Efforts to combine potential dosage sensitive genes also failed to produce significant defects. Therefore, the proliferation defects in disomes are the result of the mass action of genes which are not individually dosage sensitive.

Variability in aneuploid yeast

Much like in human trisomic populations, aneuploid yeast are more variable in a variety of phenotypes than euploid populations. Both chromosome gains and losses result in more variable G1 duration and S and early M phase duration. Stochastic DNA damage in aneuploid yeast leads to some cells getting held up at the DNA damage checkpoint, therefore prolonging S phase. Deleting RAD9, a checkpoint protein, reduces variability in these strains (Beach et al., 2017). Therefore, S phase variability in disomes and monosomes can be considered a general consequence of aneuploidy. Being aneuploid increases chances of DNA damage (Blank et al., 2015), which in turn inconsistently alters cell cycle length.

Disomic yeast are also variable in stress response and transcriptional induction (Beach et al., 2017) (Figure 4). Disomes I, IX, VIII, II, XIII, and XVI are variable in activation of the heat

shock response after 4 hours at 42˚. Similarly, Disomes IX, II, XIII, and XVI are variable in activation of the unfolded protein response after exposure to DTT. Disomes IX, II, and XIII have a higher standard deviation in induction at the GAL1-10 promoter when grown in galactose. Together, these data may suggest that disomes are generally noisy in transcription. However, these phenotypes are not universal; in all three conditions there were disomes tested which did not have an increased standard deviation compared to euploid cells. This indicates that variability is transcriptional induction is unlikely to be a generalized consequence of an imbalanced karyotype, and rather a gene dosage effect, dependent on the specific genes which are in excess. In Chapter 2, I investigate how a specific aneuploidy, Disome IX, induces GAL1-10 promoter variability.

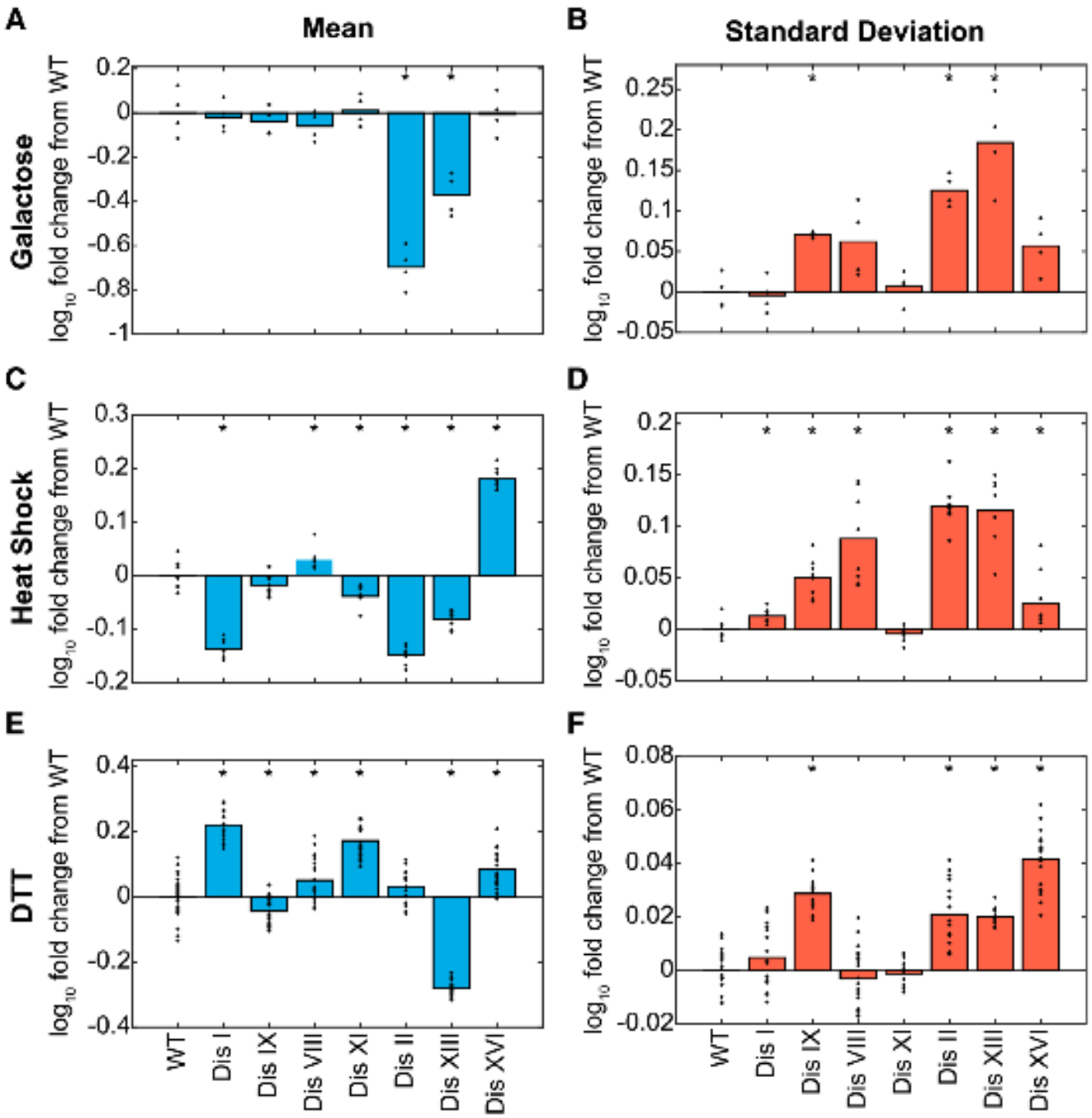

Figure 4. Disomes are variable in stress response and transcriptional induction

Mean (A, C, E) and standard deviation (B,D,F) of transcriptional induction in euploid (WT) and disome yeast. (A-B) Induction of the GAL1-10 promoter is measured using a fluorescent

reporter driven by the GAL1-10 promoter (GAL1pr-YFP) after induction in media containing galactose. (C-D) Activation of the heat shock response is measured using a fluorescent reporter driven by heat shock elements, (P_{4xHSE}-YFP) after heat shock at 39˚. (E-F) Activation of the unfolded protein response is measured using a fluorescent reporter driven by Hac1 sensitive unfolded protein response elements (P_{4xUPRE}-GFP) after incubation in media containing 0.625 mM DTT. (Figure adapted from Beach et al., 2017)

NOISE IN GENE EXPRESSION

Noise is inherent in gene expression and can have a number of phenotypic consequences (Raser and O 'shea, 2005) (Figure 5). Small fluctuations in gene expression can produce observable phenotypic heterogeneity in a population. This can occur through action of that gene itself or propagation of noise down a signaling pathway resulting in larger fluctuations in other genes. In some cases, this noise is be advantageous. In single cellular organisms, population heterogeneity can allow for adaptability in a changing environment without genetic diversity (Levy et al., 2012). In mice, noise is the basis for creating the sense of smell. Stochastic gene expression of an odorant receptors followed be inhibition of other receptors, results in an array of olfactory neurons each sensitive to a different smell (Chess et al., 1994; Serizawa et al., 2004). However, noise in expression of certain genes confer a fitness defect. In yeast, essential genes and protein complex members have less noise in gene expression than other genes, indicating selective pressure to reduce noise in more sensitive genes (Arias and Hayward, 2005; Fraser et al., 2004).

Gene expression noise can be characterized as intrinsic, global extrinsic, or pathway-specific extrinsic (Elowitz et al., 2002; Raj and Van Oudenaarden, 2008; Raser and O 'shea, 2005). Intrinsic noise is the result of stochasticity of chemical reactions which occur during transcription, such as chromatin remodeling and promoter binding. Intrinsic noise is influenced by promoter structure and effects expression at each gene independently. In contrast, global extrinsic noise effects expression of all genes in a cell equally due to fluctuations in environment, cell state, or general transcriptional machinery. Pathway specific extrinsic noise

affects expression of particular genes by altering specific pathways, such as changes in abundance of transcription factors or signaling pathway components.

All three types of noise contribute to overall gene expression to some degree, but the contributions vary depending on the organism, environment, and specific gene. The contributions of intrinsic and extrinsic noise can be parsed using a dual reporter system (Elowitz et al., 2002). In this system, two fluorescent reporters under placed under the control of identical regulatory elements and the correlation in their expression is measured by microscopy or flow cytometry. When expression of the reporters are plotted against each other, the distribution along the positive diagonal represents extrinsic noise, as both genes were effected equally. Any distribution orthogonal to the diagonal represents intrinsic noise which effects each promoter differently (Figure 6A). Intrinsic noise is generally a small contribution to the overall noise in eukaryotic promoters. This is true in the yeast GAL1 promoter where very little intrinsic noise is detected (Raser and O 'Shea, 2004) (Figure 6B). Extrinsic noise can be further broken into its components by placing two reporters under the control of two separate regulatory elements. The contribution of global extrinsic noise was measured in this way in disome yeast strains which have an increase in total noise in expression at the GAL1-10 promoter (Figure 6C). Overall, there is little correlation between GAL1-10 promoter driven YFP and mCherry driven by the TDH3 promoter, indicating a generally low contribution of global extrinsic noise (Beach et al., 2017). Disome IX, which is the focus of work presented in this thesis, had a lower correlation between the promoters than euploid yeast, predicting that pathway specific extrinsic noise is the primary contribution to increased noise is Disome IX.

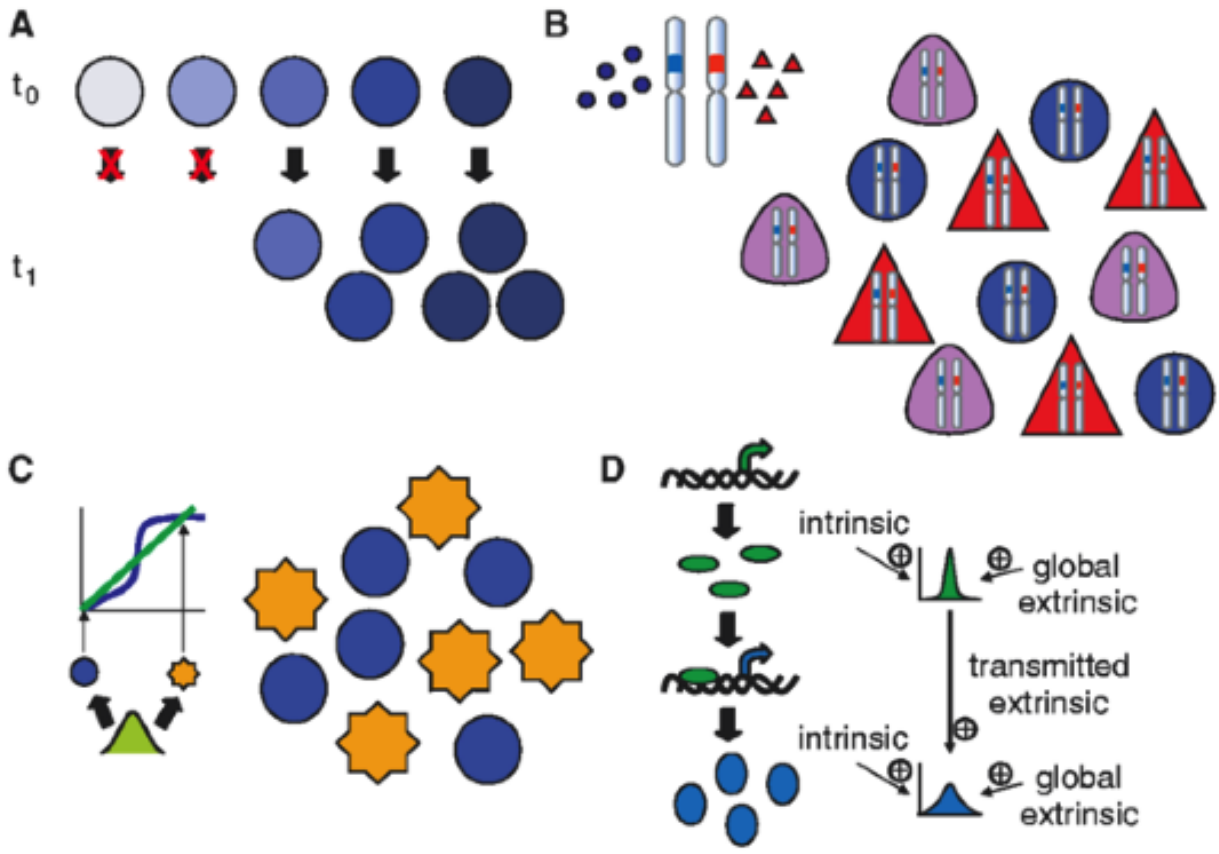

Figure 5. Phenotypic consequences of gene expression noise

(A) Small fluctuations in gene expression can alter reproductive fitness. (B) In heterozygous diploids, noise in gene expression can produce phenotypes that look like both homozygotes and heterozygotes, resulting in a heterogeneous population. (C) In genes which have a distinct phenotype threshold, noise can lead to multiple distinct phenotypes. (D) Small instances of noise in gene expression can propagate through signaling pathways to result in greater noise in expression of other genes. (Figure adapted from Raser and O 'Shea, 2005)

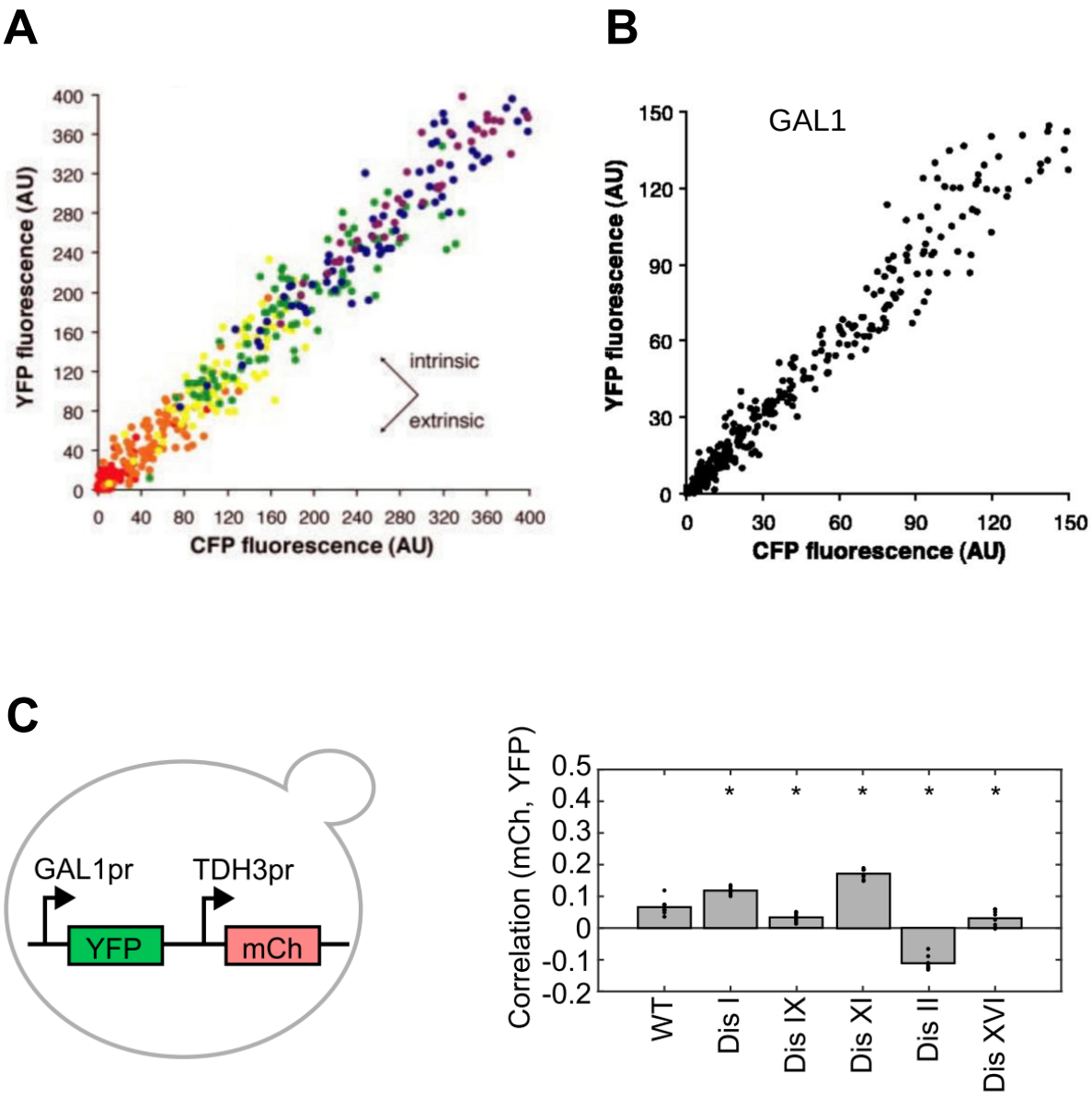

Figure 6. Intrinsic and extrinsic noise

(A) The contributions of intrinsic and extrinsic noise can be measured by the correlation in expression of two reporters driven by identical promoters. The distribution along the diagonal represents extrinsic noise which affects both reporters equally. Distribution along the

perpendicular axis represents intrinsic noise which affects each reporter independently. (B) Dual reporters reveal that extrinsic noise is the major source of noise at the GAL1-10 promoter. (C) Correlation between dual reporters driven by separate reporters distinguish between global and pathway specific extrinsic noise. Global extrinsic noise at the GAL1-10 promoter is a minor contributor is euploid and disome yeast. (Figures A-B are adapted from Raser and O'Shea, 2004, C is adapted from Beach et al., 2017)

THE YEAST GALACTOSE PATHWAY

The GAL1-10 promoter

The GAL1-10 promoter is a well-studied transcriptional promoter in yeast which regulates expression of the galactokinase Gal1 (Figure 7). Gal1 is an essential component of the Leloir pathway which converts galactose into glucose-6-phosphate for use in glycolysis. Glucose, the preferred sugar source for *S. cerevisiae*, does not require such conversion, so GAL1 is only expressed when glucose is unavailable and the less efficient galactose is the main carbon source. Promoter induction is regulated by two intersecting pathways, galactose activation and glucose repression, which together form a robust on/off switch (Reviewed in Timson, 2007).

The GAL1-10 promoter is composed of four upstream activating sequences (UAS), which serve as binding sites for the transcriptional activator Gal4, and an upstream regulatory sequence (URS) which binds the repressor Mig1. The GAL UAS is a 17 base pair consensus sequence, each UAS site contains 11-14 matches to the consensus sequence. There are UASs in the promoters of many structural and regulatory GAL genes. GAL5, GAL80, and GAL3 promoters each contain 1 UAS, GAL2 and GAL7 have 2 each, and the GAL1-10 promoter contains 4 (Johnston, 1987; Lohr et al., 1995). Affinity for Gal4 varies across UAS sites, leading to varied promoter activation. The URS lies between the UAS and TATA box in the GAL1-10 promoter, serving as a binding site for Mig1 in response to glucose, and preventing promoter induction (Flick and Johnston, 1990; Nehlin et al., 1991). The URS is a 17 base pair sequence containing a core GGGG motif, and has been identified in the GAL1-10 and GAL4 promoters.

Glucose repression

When glucose is available, the glucose repression pathway prevents induction of the GAL1-10 promoter. This regulation is primarily controlled by the localization of repressor Mig1 (Nehlin et al., 1991). In the absence of glucose, Mig1 is phosphorylated by kinase Snf1, sequestering it to the cytoplasm. When glucose is present, Mig1 is relieved of Snf1 repression and rapidly relocalizes to the nucleus where it can bind the URS and prevent assembly of transcriptional machinery at the promoter (DeVit et al., 1997; Ozcan and Johnston, 1999). Mig1 also acts to repress the galactose activation pathway by repressing transcription of GAL4 and GAL3, two positive regulators of the GAL1-10 promoter (Nehlin et al., 1991).

Galactose activation

When galactose is the primary carbon source, the induction of the GAL1-10 promoter is activated through a galactose sensitive signaling pathway. This activation occurs through activity of Gal4, a transcription factor which is constitutively bound to UAS regulatory elements in the promoter. When active, Gal4 recruits transcriptional machinery to the promoter. Gal4 directly interacts with subunits of Mediator and SAGA, allowing for the formation of preinitiation complex (PIC) at the promoter, and ultimately transcription (Bhaumik et al., 2003; Reeves and Hahn, 2005). Gal4 activation is repressed by Gal80 and activated by Gal3 (Johnston, 1987; Lohr et al., 1995; Traven et al., 2006).

Gal80 binds to Gal4 and inhibits its activity in non-inducing conditions (Torchia Robert W Hamilton et al., 1984). When Gal80 is bound to Gal4, Gal4 is unable to interact with SAGA or Mediator, meaning no PIC is formed at the promoter (Traven et al., 2006). In inducing

conditions, Gal80 repression is inhibited by Gal3 activity, however the exact mechanism of Gal3 activation remains a topic of debate.

Gal3 serves as the cell's galactose sensor, releasing Gal4 of Gal80 repression when galactose is present. Gal3 rapidly forms a complex with Gal80 in response to galactose, and this interaction is ATP dependent (Timson and Reece, 2002; Timson et al., 2002). The Gal3-Gal80 interaction is necessary for GAL gene activation, but there is conflicting evidence for where and when this interaction takes place. Early in vivo work suggests that a tripartite complex of Gal4-Gal3-Gal80 is formed at the promoter, and that Gal3 binding induces a conformational change in Gal80 which relieves repression (Platt and Reece, 1998). However, ChIP experiments show that, in inducing conditions, there is a decrease in Gal80 associated with the UAS, and no evidence of Gal3 at the UAS, indicating that Gal3-Gal80 interaction occurs outside of the nucleus (Peng and Hopper, 2002). Protein localization studies confirm that Gal3-Gal80 interactions occur throughout the cell, but also shows that Gal3 localizes to the nucleus in inducing conditions, suggesting that galactose bound Gal3 moves into the nucleus to bind Gal80 and release repression (Wightman et al., 2008). In contradiction to this conclusion, detailed imaging using a novel GAL gene array shows that Gal80 dissociates from Gal4 in response to galactose (Jiang et al., 2009). Furthermore, the kinetics of the proposed Gal3 and Gal80 trafficking are too slow to be responsible for the rapid induction of the promoter which occurs upon the switch to galactose containing media. Instead, nuclear Gal3 is essential for promoter induction, indicating that interaction Gal3 interacts with Gal4 associated Gal80, dissociating it from the promoter (Egriboz et al., 2011).

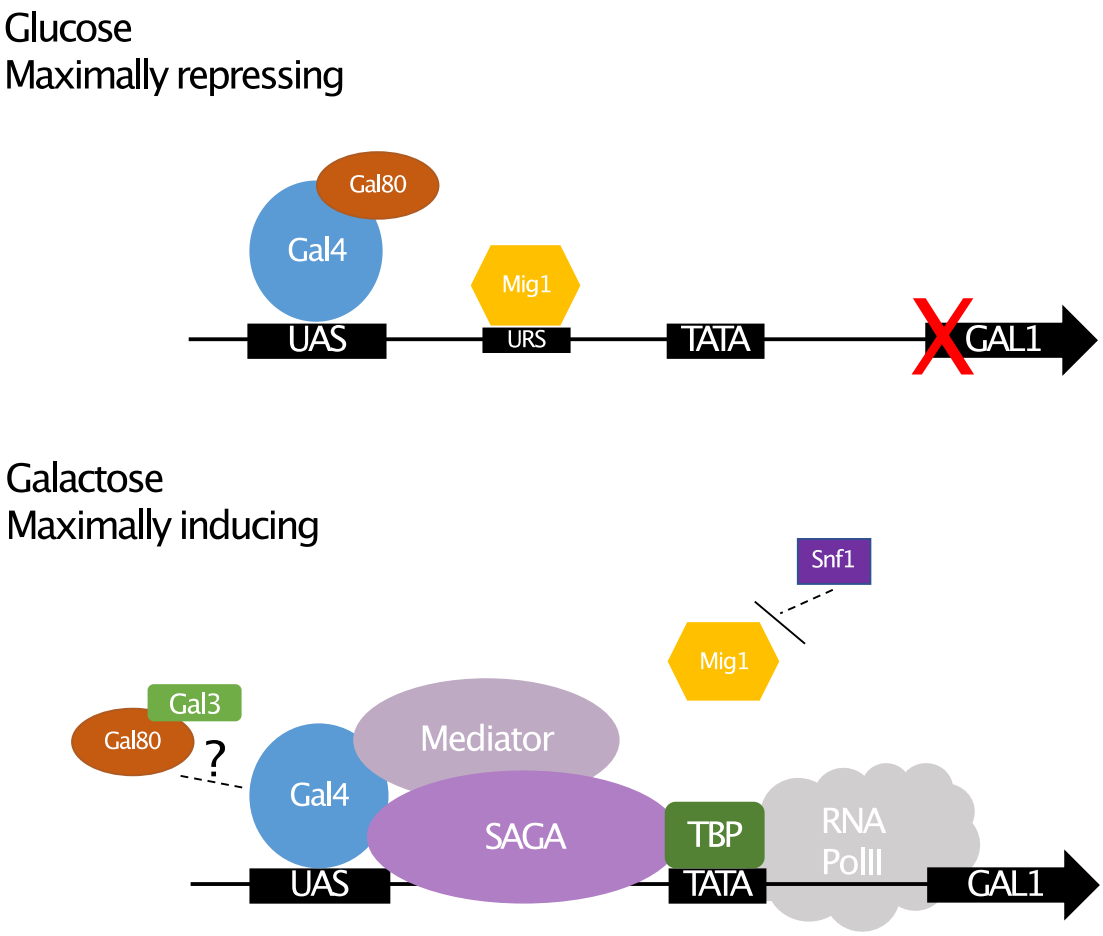

Figure 7. Galactose signaling pathway

Under maximally repressing conditions where glucose is the only carbon source, Mig1 is bound to the URS, preventing assembly of transcriptional machinery. In the absence of galactose, Gal80 is binds to inhibits Gal4. Under maximally inducing conditions where galactose is the only carbon source, Gal3 binds Gal80 preventing repression of Gal4 by an unknown mechanism. In the absence of glucose, Snf1 phosphorylates Mig1, preventing its nuclear localization. Gal4 is able to recruit Mediator and SAGA to the promoter and assembly of a preinitiation complex and transcription can begin.

Hexose transporters

Activation and repression of the GAL1-10 promoter relies on the cell sensing the sugars in the environment. Rather than an absolute threshold of glucose or galactose concentration, sensing is based on the ratio of glucose: galactose outside of the cell as the two sugars compete for transport into the cell via hexose transporters (Escalante-Chong et al., 2015).

Budding yeast have a large number of highly redundant hexose transporters, Hxt1-17 and Gal2, which act through facilitated diffusion to allow hexose sugars into the cell (Figure 8). No single hexose transporter is essential, many coincidental deletions are necessary to produce strains defective in transport for specific hexose sugars (Wieczorke et al., 1999). Despite the high degree of functional overlap, each hexose transporter plays a role is establishing efficient hexose transport, with each transporter has varying affinity for different hexose sugars. This is most well studied in transport of glucose; Hxt1, 2, 3, 4, 6, and 7 transport glucose with varying affinities (Maier et al., 2002; Ozcan and Johnston, 1999; Reifenberger et al., 1997). Expression and localization of these transporters to the membrane changes in response to environmental glucose concentrations. Hxt1 is a low affinity transporter and is the major transporter when glucose concentrations are high. Hxt3 has an intermediate glucose affinity and is expressed in both high and low concentrations of glucose. Higher affinity transporters Hxt4 and Hxt2 are expressed in lower glucose concentrations. Hxt6 and Hxt7 have the highest affinity for glucose and are both strongly induced in low glucose and repressed in high glucose. The complex regulation of glucose transporters is done by two interconnected pathways; Rgt1/Snf3 glucose induction, and Snf1/Mig1 glucose repression (Kim et al., 2013). As well as expression, localization of transporters to the membrane is regulated in response to changing glucose

concentrations; upon glucose depletion, Hxt1 is internalized by endocytosis and targeted for degradation (Roy et al., 2014).

Galactose is transported primarily by the galactose permease Gal2. Expression of GAL2 is sensitive to galactose as its promoter contains two Gal4 UAS sites (Lohr et al., 1995). Gal2 is a high affinity hexose transporter, having equal affinity for galactose and glucose, comparable to that of Hxt6 and Hxt7 (Maier et al., 2002). Despite having the highest affinity for galactose of any of the hexose transporters, Gal2 is not required for galactose transport. Yeast lacking GAL2 are viable but exhibit slowed growth in galactose medium (Ozcan and Johnston, 1999; Tschopp et al., 1986). Additionally, Gal2 is not required for glucose: galactose ratio sensing, indicating that glucose and galactose compete for transport through other hexose transporters as well (Escalante-Chong et al., 2015).

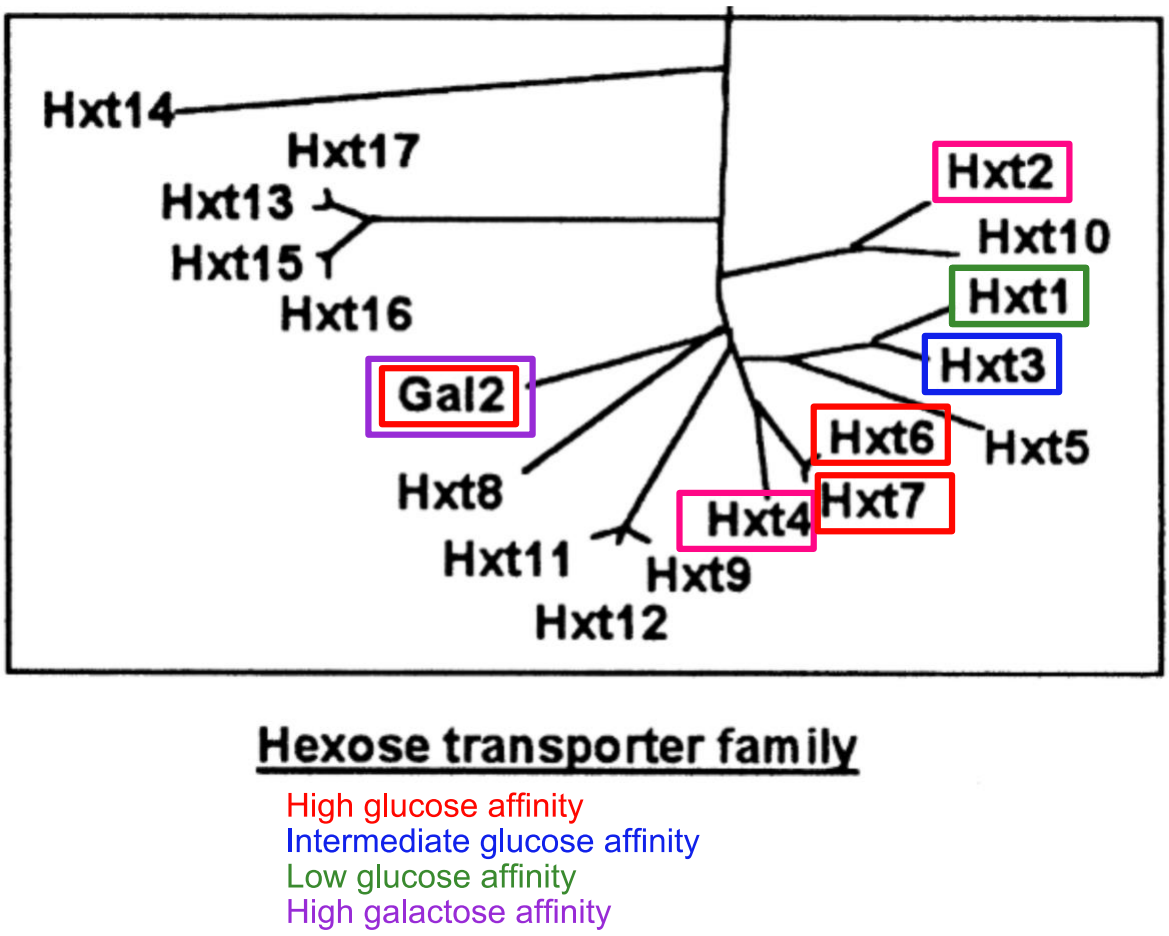

Figure 8. Yeast hexose transporter family

Phylogeny of hexose transporters in S. cerevisiae. Relative affinities for transport of glucose and galactose are highlighted (Figure adapted from Wieczorke et al., 1999)

CONCLUDING REMARKS

Phenotypic variability is a commonly noted feature of aneuploidies, particularly in human trisomies where clinical presentation varies greatly between individuals. This variability is often attributed to genetic heterogeneity. However, work for our lab and presented in this thesis show that phenotypic variability can be a consequence of aneuploidy itself.

This thesis describes my work to understand the mechanism by which an additional copy of chromosome IX in yeast produces variability in induction of the GAL1-10 promoter. By narrowing my focus to variability in a specific pathway caused by a specific aneuploidy, I am able to identify how defects in an essential cellular process brought about by altered gene dosage can induce variability in a signaling pathway, ultimately producing a phenotype of variability. I show that the previously identified endocytic defect in Disome IX yeast results in altered localization of hexose transporters to the plasma membrane. I hypothesize that this disruption of hexose transport leads to variability in hexose sugar uptake and induction of the GAL1-10 promoter.

REFERENCES

Arias, A.M., and Hayward, P. (2005). Filtering transcriptional noise during development: concepts and mechanisms. Nat. Rev. Genet. *7*, 34–44.

Arron, J.R., Winslow, M.M., Polleri, A., Chang, C.-P., Wu, H., Gao, X., Neilson, J.R., Chen, L., Heit, J.J., Kim, S.K., et al. (2006). NFAT dysregulation by increased dosage of DSCR1 and DYRK1A on chromosome 21. Nature *441*, 595–600.

Beach, R.R., Ricci-Tam, C., Brennan, C.M., Silberman, R.E., Springer, M., Amon, A., Moomau, C.A., Hsu, P.-H., and Hua, B. (2017). Aneuploidy Causes Non-genetic Individuality. Cell *169*, 229-242.e21.

Belichenko, N.P., Belichenko, P. V, Kleschevnikov, A.M., Salehi, A., Reeves, R.H., and Mobley, W.C. (2009). The "Down Syndrome Critical Region" Is Sufficient in the Mouse Model to Confer Behavioral, Neurophysiological, and Synaptic Phenotypes Characteristic of Down Syndrome. J. Neurosci. *29*, 5938–5948.

Bhaumik, S.R., Raha, T., Aiello, D.P., and Green, M.R. (2003). In vivo target of a transcriptional activator revealed by fluorescence resonance energy transfer. Genes Dev. *18*, 333–343.

Birkbak, N.J., Eklund, A.C., Li, Q., Mcclelland, S.E., Endesfelder, D., Tan, P., Tan, I.B., Richardson, A.L., Szallasi, Z., and Swanton, C. (2011). Paradoxical Relationship between Chromosomal Instability and Survival Outcome in Cancer.

Blank, H.M., Sheltzer, J.M., Meehl, C.M., and Amon, A. (2015). Mitotic entry in the presence of DNA damage is a widespread property of aneuploidy in yeast. Mol. Biol. Cell *26*, 1440–1451.

Bonney, M.E., Moriya, H., and Amon, A. (2015). Aneuploid proliferation defects in yeast are not driven by copy number changes of a few dosage-sensitive genes. Genes Dev. *29*, 898–903.

Brennan, C.M., Vaites, L.P., Wells, J.N., Santaguida, S., Paulo, J.A., Storchova, Z., Harper, J.W., Marsh, J.A., and Amon, A. (2019). Protein aggregation mediates stoichiometry of protein complexes in aneuploid cells. Genes Dev. *33*, 1031–1047.

Caba, L., Rusu, C., Butnariu, L., Panzaru, M., Braha, E., Volosciuc, M., Popescu, R., Gramescu, M., Bujoran, C., Martiniuc, V., et al. (2013). Phenotypic variability in Patau syndrome. Rev. Med. Chir. Soc. Med. Nat *117*, 321–327.

Chess, A., Simon, I., Cedar, H., and Axel, R. (1994). Allelic inactivation regulates olfactory receptor gene expression. Cell *78*, 823–834.

Cohen, W.I. (2003). Health Care Guidelines for Individuals with Down Syndrome—1999 Revision. Down Syndr. Visions 21st Century 237–245.

Deitz, S.L., and Roper, R.J. (2011). Trisomic and Allelic Differences Influence Phenotypic Variability During Development of Down Syndrome Mice. Genetics *189*, 1487.

Delabara, J.-M., Theophilea, D., Rahmanp, Z., Chettouha, Z., Blouina, J.-L., Prieur', M., Noelc, B.,

and Sinep, P.-M. (1993). Molecular Mapping of Twenty-Four Features of Down Syndrome on Chromosome 21.

Dephoure, N., Hwang, S., O'Sullivan, C., Dodgson, S.E., Gygi, S.P., Amon, A., and Torres, E.M. (2014). Quantitative proteomic analysis reveals posttranslational responses to aneuploidy in yeast. Elife *3*, 1–27.

DeVit, M., Waddle, J.A., and Johnston, M. (1997). Regulated Nuclear Translocation of the Migl Glucose Repressor. Mol. Biol. Cell *8*, 1603–1618.

Dodgson, S.E., Kim, S., Costanzo, M., Baryshnikova, A., Morse, D.L., Kaiser, C.A., Boone, C., Amon, A., Abe, F., Usui, K., et al. (2016). Chromosome-Specific and Global Effects of Aneuploidy in Saccharomyces cerevisiae. Genetics *202*, 1395–1409.

Doran, E., Keator, D., Head, E., Phelan, M.J., Kim, R., Totoiu, M., Barrio, J.R., Small, G.W., Potkin, S.G., and Lott, I.T. (2017). Down Syndrome, Partial Trisomy 21, and Absense of Alzheimer's Disease: The Role of APP. J. Alzheimer's Dis. *56*, 459–470.

Dunlevy, L., Bennett, M., Slender, A., Lana-Elola, E., Tybulewicz, V.L., Fisher, E.M.C., and Mohun, T. (2010). Down's syndrome-like cardiac developmental defects in embryos of the transchromosomic Tc1 mouse. Cardiovasc. Res. *88*, 287–295.

Egriboz, O., Jiang, F., and Hopper, J.E. (2011). Rapid GAL Gene Switch of Saccharomyces cerevisiae Depends on Nuclear Gal3, Not Nucleocytoplasmic Trafficking of Gal3 and Gal80. Genetics *189*, 825–835.

Elowitz, M.B., Levine, A.J., Siggia, E.D., and Swain, P.S. (2002). Stochastic Gene Expression in a Single Cell. Science (80-.). *297*, 1183–1186.

Escalante-Chong, R., Savir, Y., Carroll, S.M., Ingraham, J.B., Wang, J., Marx, C.J., Springer, M., and Johnson, A.D. (2015). Galactose metabolic genes in yeast respond to a ratio of galactose and glucose. Proc. Natl. Acad. Sci. *112*, 1636–1641.

Flick, J.S., and Johnston, M. (1990). Two Systems of Glucose Repression of the GAL] Promoter in Saccharomyces cerevisiae.

Fraser, H.B., Hirsh, A.E., Giaever, G., Kumm, J., and Eisen, M.B. (2004). Noise Minimization in Eukaryotic Gene Expression. PLoS Biol. *2*, 834–838.

Gasch, A.P., Spellman, P.T., Kao, C.M., Carmel-Harel, O., Eisen, M.B., Storz, G., Botstein, D., and Brown, P.O. (2000). Genomic Expression Programs in the Response of Yeast Cells to Environmental Changes □ D.

Hall, B. (1965). Delayed ontogenesis in human trisomy syndromes. Hereditas *52*, 334–344.

Hanahan, D., and Weinberg, R.A. (2000). The hallmarks of cancer. Cell *100*, 57–70.

Hanahan, D., and Weinberg, R.A. (2011). Hallmarks of cancer: the next generation. Cell *144*, 646–674.

Hartley, D., Blumenthal, T., Carrillo, M., DiPaolo, G., Esralew, L., Gardiner, K., Granholm, A., Iqbal, K., Krams, M., Lemere, C., et al. (2015). Down syndrome and Alzheimer's disease: Common pathways, common goals. Alzheimers. Dement. *11*, 700–709.

Hassold, T.J., and Jacobs, P.A. (1984). Trisomy in Man. Annu. Rev. Genet. *18*, 69–97.

Hill, C.A., Sussan, T.E., Reeves, R.H., and Richtsmeier, J.T. (2009). Complex contributions of Ets2 to craniofacial and thymus phenotypes of trisomic "Down syndrome" mice. Am. J. Med. Genet. A *149A*, 2158–2165.

Hsu, H.-F., and Hou, J.-W. (2007). Variable Expressivity in Patau Syndroe is Not All Related to Trisomy 13 Mosaicism. Am. J. Med. Genet. *Part A*, 1739–1748.

Jia, C.-W., Wang, L., Lan, Y.-L., Song, R., Zhou, L.-Y., Yu, L., Yang, Y., Liang, Y., Li, Y., Ma, Y.-M., et al. (2015). Aneuploidy in Early Miscarriage and its Related Factors. Chin. Med. J. (Engl). *128*, 2772.

Jiang, F., Frey, B.R., Evans, M.L., Friel, J.C., and Hopper, J.E. (2009). Gene Activation by Dissociation of an Inhibitor from a Transcriptional Activation Domain. Mol. Cell. Biol. *29*, 5604–5610.

Johnston, M. (1987). A Model Fungal Gene Regulatory Mechanism: the GAL Genes of Saccharomyces Cerevisiae. Microbiol. Rev. 458–476.

Kahlem, P. (2006). Gene-Dosage Effect on Chromosome 21 Transcriptome in Trisomy 21: Implication in Down Syndrome Cognitive Disorders. Behav. Genet. 2006 363 *36*, 416–428.

Kim, J.-H., Roy, A., Ii, D.J., and Cho, K.H. (2013). The glucose signaling network in yeast. Biochim. Biophysa Acta *1830*, 5204–5210.

Korbel, J.O., Tirosh-Wagner, T., Urban, A.E., Chen, X.-N., Kasowski, M., Dai, L., Grubert, F., Erdman, C., Gao, M.C., Lange, K., et al. (2009). The genetic architecture of Down syndrome phenotypes revealed by high-resolution analysis of human segmental trisomies. Proc. Natl. Acad. Sci. *106*, 12031–12036.

Korenberg, J.R., Kawashima, H., Pulst, S.-M., Lkeuchi, T., Ogasawara, N., Yamamoto, K., Schonberg, S.A., West, R., Allen, L., Magenis, E., et al. (1990). Molecular Definition of a Region of Chromosome 21 That Causes Features of the Down Syndrome Phenotype.

Letourneau, A., and Antonarakis, S.E. (2012). Genomic determinants in the phenotypic variability of Down syndrome (Elsevier Inc.).

Levy, S.F., Ziv, N., Siegal, M.L., and Hurst, L.D. (2012). Bet Hedging in Yeast by Heterogeneous, Age-Correlated Expression of a Stress Protectant. PLoS Biol *10*.

Li, H., Cherry, S., Klinedinst, D., DeLeon, V., Redig, J., Reshey, B., Chin, M.T., Sherman, S.L., Maslen, C.L., and Reeves, R.H. (2012). Genetic modifiers predisposing to congenital heart disease in the sensitized Down syndrome population. Circ. Cardiovasc. Genet. *5*, 301–308.

Lin, H.-Y., Lin, S.-P., Chen, Y.-J., Hung, H.-Y., Kao, H.-A., Hsu, C.-H., Chen, M.-R., Chang, J.-H., Ho,

C.-S., Huang, F.-Y., et al. (2006). Clinical Characteristics and Survival of Trisomy 18 in a Medical Center in Taipei, 1988-2004. Am. J. Med. Genet. *Part A*, 945–951.

Lohr, D., Venkov, P., and Zlatanova, A.J. (1995). Transcriptional regulation in the yeast GAL gene family: a complex genetic network. FASEB J. *9*, 777–787.

Lorke, D. (1994). Developmental characteristics of trisomy 19 mice. Acta Anat. (Basel). *150*, 159–169.

Maier, A., Volker, B., Boles, E., and Fuhrmann, G.F. (2002). Characterisation of glucose transport in Saccharomyces cerevisiae with plasma membrane vesicles (countertransport) and intact cells (initial uptake) with single Hxt1, Hxt2, Hxt3, Hxt4, Hxt6, Hxt7 or Gal2 transporters. FEMS Yeast Res. *2*, 539–550.

Maslen, C.L., Babcock, D., Robinson, S.W., Bean, L.J.H., Dooley, K.J., Willour, V.L., and Sherman, S.L. (2006). CRELD1 Mutations Contribute to the Occurrence of Cardiac Atrioventricular Septal Defects in Down Syndrome. Am. J. Med. Genet. Part A *140*, 2501–2505.

Maurici, D., Perez-Atayde, A., Grier, H.E., Baldini, N., Serra, M., and Fletcher, J. (1998). Frequency and implications of chromosome 8 and 12 gains in Ewing sarcoma. Cancer Genet. Cytogenet. *100*, 106–110.

Nehlin, J.O., Carlberg, M., and Ronne, H. (1991). Control of yeast GAL genes by MIG 1 repressor: a transcriptional cascade in the glucose response. EMBO J. *10*, 3373–3377.

Olson, L.E., Roper, R.J., Baxter, L.L., Carlson, E.J., Epstein, C.J., and Reeves, R.H. (2004). Down Syndrome Mouse Models Ts65Dn, Ts1Cje, and Ms1Cje/Ts65Dn Exhibit Variable Severity of Cerebellar Phenotypes. Dev. Dyn. *230*, 581–589.

Olson, L.E., Roper, R.J., Sengstaken, C.L., Peterson, E.A., Aquino, V., Galdzicki, Z., Siarey, R., Pletnikov, M., Moran, T.H., and Reeves, R.H. (2007). Trisomy for the Down syndrome “critical region” is necessary but not sufficient for brain phenotypes of trisomic mice. Hum. Mol. Genet. *16*, 774–782.

Oromendia, A.B., Dodgson, S.E., and Amon, A. (2012). Aneuploidy causes proteotoxic stress in yeast. Genes Dev. *26*, 2696–2708.

Ozcan, S., and Johnston, M. (1999). Function and regulation of yeast hexose transporters. Microbiol. Mol. Biol. Rev. *63*, 554–569.

Ozery-Flato, M., Linhart, C., Trakhtenbrot, L., Izraeli, S., and Shamir, R. (2011). Large-scale analysis of chromosomal aberrations in cancer karyotypes reveals two distinct paths to aneuploidy. Genome Biol. *12*.

Peng, G., and Hopper, J.E. (2002). Gene activation by interaction of an inhibitor with a cytoplasmic signaling protein. Proc. Natl. Acad. Sci. *99*, 8548–8553.

Peres, E., Savasan, S., Cushing, B., Abella, S., and Mohamed, A. (2004). Chromosome analyses of 16 cases of Wilms tumor: different pattern in unfavorable histology. Cancer Genet. Cytogenet. *148*, 66–70.

Pfau, S.J., and Amon, A. (2012). Chromosomal instability and aneuploidy in cancer: From yeast to man. EMBO Rep. *13*, 515–527.

Platt, A., and Reece, R.J. (1998). The yeast galactose genetic switch is mediated by the formation of a Gal4p–Gal80p–Gal3p complex. EMBO J. *17*, 4086–4091.

Potter, H. (2016). Beyond Trisomy 21: Phenotypic Variability in People with Down Syndrome Explained by Further Chromosome Mis-segregation and Mosaic Aneuploidy. J Down Syndr Chromosom Abnorm. *2*.

Pritchard, M.A., and Kola, I. (1999). The "gene dosage effect" hypothesis versus the "amplified developmental instability" hypothesis in Down syndrome. Mol. Biol. Down Syndr. 293–303.

Rachidi, M., and Lopes, C. (2007). Mental retardation in Down syndrome: From gene dosage imbalance to molecular and cellular mechanisms. Neurosci. Res. *59*, 349–369.

Rachidi, M., and Lopes, C. (2008). Mental retardation and associated neurological dysfunctions in Down syndrome: a consequence of dysregulation in critical chromosome 21 genes and associated molecular pathways. Eur. J. Paediatr. Neurol. *12*, 168–182.

Raj, A., and Van Oudenaarden, A. (2008). Stochastic gene expression and its consequences. Cell *135*, 216–226.

Raser, J.M., and O 'shea, E.K. (2005). Noise in Gene Expression: Origins, Consequences, and Control. Science (80-.). *309*, 2010–2013.

Raser, J.M., and O 'Shea, E.K. (2004). Control of Stochasticity in Eukaryotic Gene Expression. Science (80-.). *304*, 1811–1814.

Reeves, W.M., and Hahn, S. (2005). Targets of the Gal4 Transcription Activator in Functional Transcription Complexes. Mol. Cell. Biol. *25*, 9092–9102.

Reifenberger, E., Boles, E., and Ciriacy, M. (1997). Kinetic characterization of individual hexose transporters of Saccharomyces cerevisiae and their relation to the triggering mechanisms of glucose repression. Eur. J. Biochem. *245*, 324–333.

Roizen, N.J., and Patterson, D. (2003). Down's syndrome. Lancet *361*, 1281–1289.

Roper, R.J., and Reeves, R.H. (2006). Understanding the Basis for Down Syndrome Phenotypes. PLoS Genet. *2*.

Rovelet-Lecrux, A., Hannequin, D., Raux, G., Le Meur, N., Laquerrière, A., Vital, A., Dumanchin, C., Feuillette, S., Brice, A., Vercelletto, M., et al. (2006). APP locus duplication causes autosomal dominant early-onset Alzheimer disease with cerebral amyloid angiopathy. Nat. Genet. *38*, 24–26.

Roy, A., Kim, Y.B., Cho, K.H., and Kim, J.H. (2014). Glucose starvation-induced turnover of the yeast glucose transporter Hxt1. Biochim. Biophys. Acta - Gen. Subj. *1840*, 2878–2885.

Serizawa, S., Miyamichi, K., and Sakano, H. (2004). One neuron-one receptor rule in the mouse

olfactory system. Trends Genet. *20*, 648–653.

Shapiro, B.L. (1975). Amplified developmental instability in Down's syndrome. Ann. Hum. Genet. *38*, 429–437.

Shapiro, B.L. (1994). The Environmental Basis of the Down Syndrome Phenotype. Dev. Med. Child Neurol. *36*, 84–90.

Sheltzer, J.M., Blank, H.M., Pfau, S.J., Tange, Y., George, B.M., Humpton, T.J., Brito, I.L., Hiraoka, Y., Niwa, O., and Amon, A. (2011). Aneuploidy Drives Genomic Instability in Yeast. Science (80-.). *333*, 1026–1030.

Sheltzer, J.M., Torres, E.M., Dunham, M.J., and Amon, A. (2012). Transcriptional consequences of aneuploidy. Proc. Natl. Acad. Sci. U. S. A. *109*, 12644–12649.

Siegel, J.J., and Amon, A. (2012). New insights into the troubles of aneuploidy. Annu. Rev. Cell Dev. Biol. *28*, 189–214.

Smith, A.J. de, Trewick, A.L., and Blakemore, A.I.F. (2010). Implications of copy number variation in people with chromosomal abnormalities: potential for greater variation in copy number state may contribute to variability of phenotype. Hugo J. *4*, 1.

Springer, M., Weissman, J.S., and Kirschner, M.W. (2010). A general lack of compensation for gene dosage in yeast. Mol. Syst. Biol. *6*, 368.

Stingele, S., Stoehr, G., Peplowska, K., Cox, J., Mann, M., and Storchova, Z. (2012). Global analysis of genome, transcriptome and proteome reveals the response to aneuploidy in human cells. Mol. Syst. Biol. *8*.

Su, X.A., Ma, D., Parsons, J. V, Replogle, J.M., Amatruda, J.F., Whittaker, C.A., Stegmaier, K., and Amon, A. (2021). RAD21 is a driver of chromosome 8 gain in Ewing sarcoma to mitigate replication stress. Genes Dev. *35*, 556–572.

Terhorst, A., Sandikci, A., Keller, A., Whittaker, C.A., Dunham, M.J., and Amon, A. (2020). The environmental stress response causes ribosome loss in aneuploid yeast cells. Proc. Natl. Acad. Sci. *117*, 17031–17040.

Thorburn, R.R., Gonzalez, C., Brar, G.A., Christen, S., Carlile, T.M., Ingolia, N.T., Sauer, U., Weissman, J.S., and Amon, A. (2013). Aneuploid yeast strains exhibit defects in cell growth and passage through START. Mol. Biol. Cell *24*, 1274–1289.

Timson, D.J. (2007). Galactose Metabolism in Saccharomyces cerevisiae. Dyn. Biochem. Process Biotechnol. Mol. Biol. 63–73.

Timson, D.J., and Reece, R.J. (2002). Kinetic analysis of yeast galactokinase: implications for transcriptional activation of the GAL genes. Biochimie *84*, 265–272.

Timson, D.J., Ross, H.C., and Reece, R.J. (2002). Gal3p and Gal1p interact with the transcriptional repressor Gal80p to form a complex of 1:1 stoichiometry. Biochem. J. *363*, 515–520.

Torchia Robert W Hamilton, T.E., Cano, C.L., and Hopper, J.E. (1984). Disruption of Regulatory Gene GAL80 in Saccharomyces cerevisiae: Effects on Carbon-Controlled Regulation of the Galactose/Melibiose Pathway Genes.

Torres, E.M., Sokolsky, T., Tucker, C.M., Chan, L.Y., Boselli, M., Dunham, M.J., and Amon, A. (2007). Effects of Aneuploidy on Cellular Physiology and Cell Division in Haploid Yeast. Science (80-.). *317*, 916–924.

Torres, E.M., Dephoure, N., Panneerselvam, A., Tucker, C.M., Whittaker, C.A., Gygi, S.P., Dunham, M.J., and Amon, A. (2010). Identification of Aneuploidy- Tolerating Mutations. Cell *143*, 71–83.

Torres, E.M., Springer, M., and Amon, A. (2016). No current evidence for widespread dosage compensation in S. Cerevisiae. Elife *5*.

Traven, A., Jelicic, B., and Sopta, M. (2006). Yeast Gal4: a transcriptional paradigm revisited. EMBO Rep. *7*, 496–499.

Tschopp, J.F., Emr, S.D., Field, C., and Schekman, R. (1986). GAL2 Codes for a Membrane-Bound Subunit of the Galactose Permease in Saccharomyces cerevisiae.

De Vita, S., Canzonetta, C., Mulligan, C., Delom, F., Groet, J., Baldo, C., Vanes, L., Dagna-Bricarelli, F., Hoischen, A., Veltman, J., et al. (2010). Trisomic dose of several chromosome 21 genes perturbs haematopoietic stem and progenitor cell differentiation in Down's syndrome. Oncogene *29*, 6102.

Weaver, B.A., and Cleveland, D.W. (2006). Does aneuploidy cause cancer? Curr. Opin. Cell Biol. *18*, 658–667.

Wieczorke, R., Krampe, S., Weierstall, T., Freidel, K., Hollenberg, C.P., and Boles, E. (1999). Concurrent knock-out of at least 20 transporter genes is required to block uptake of hexoses in Saccharomyces cerevisiae. FEBS Lett. *464*, 123–128.

Wightman, R., Bell, R., and Reece, R.J. (2008). Localization and Interaction of the Proteins Constituting the GAL Genetic Switch in Saccharomyces cerevisiae. Eukaryot. Cell *7*, 2061–2068.

Zhu, J., Pavelka, N., Bradford, W.D., Rancati, G., and Li, R. (2012). Karyotypic determinants of chromosome instability in Aneuploid budding yeast. PLoS Genet. *8*.

Chapter 2: Variability in GAL1-10 promoter induction in aneuploid yeast

Moomau CA, Moretto F, Amon A

CAM and AA designed the experiments.

FM performed and analyzed experiments in Figure 1D.

CAM performed and analyzed all other experiments.

ABSTRACT

By studying the GAL signaling pathway in Disome IX cells and screening chromosome IX for genes which increase GAL1pr variability, we find that the endocytosis defect in Disome IX can increase variability in sugar uptake and promoter variability. We show that gene dosage can lead to variability. In this case, Disome IX increases the dosage of multiple genes involved in inhibiting endocytosis. This leads to an endocytic defect that impacts the surface localization of hexose transporters, which ultimately leads to variability in uptake of hexose sugars and thus variability in induction of the GAL1-10 promoter.

INTRODUCTION

Aneuploidy, an imbalanced karyotype caused by the gain or loss of one or more chromosome(s), is associated with many fitness defects including reduced proliferation, proteotoxic stress, genomic instability, and activation of stress response signatures (Santaguida and Amon, 2015). In humans, aneuploidy contributes to pathology; it is a hallmark of cancer, with over 90% of solid tumors having altered karyotypes (Weaver and Cleveland, 2006) and the leading cause of miscarriage (Hassold and Jacobs, 1984). The most common human aneuploidy is trisomy 21, or Down syndrome, accounting for about 1 in 750 - 1000 live births. Down syndrome is associated with high rates of miscarriage, shortened life span, cognitive disability, characteristic facial morphology, hypotonia, Alzheimer's disease, congenital heart disease, and leukemia along with over 80 other clinical features. Notably, the incidence and severity of a majority of those phenotypes is highly variable (Roper and Reeves, 2006). It has long been assumed that this phenotypic variability is due to genetic heterogeneity among individuals. However, work in genetically homogenous populations of aneuploid yeast and trisomic mice suggests that phenotypic variability is a consequence of aneuploidy itself (Beach et al., 2017).

How aneuploidy leads to specific phenotypes is a topic of much discussion. Some phenotypes are thought to be the general consequence of an imbalanced karyotype, such as proteotoxicity and a distinct gene-expression signature (Dephoure et al., 2014; Oromendia et al., 2012; Stingele et al., 2012; Terhorst et al., 2020). Other phenotypes seem to be the consequence of altered gene dosage due to gain or loss of specific chromosome, such as the endocytic defect in Disome IX yeast, radicicol resistance in Disome XV yeast, and predisposition

to Alzheimer's in human trisomy 21 (Chen et al., 2012; Dodgson et al., 2016; Doran et al., 2017; Rovelet-Lecrux et al., 2006).

Aneuploid yeast are more variable in cell cycle length, stress response activation, and GAL1-10 promoter induction than their euploid counterparts. Variability in S phase duration is due to stochastic DNA damage in aneuploid cells, a general feature of aneuploidy (Beach et al., 2017). However, not all yeast disomes studied have increased variability in stress response and promoter induction, meaning these phenotypes are likely to be the consequence of altered dosage of genes on specific chromosomes rather than a general effect of aneuploidy. Here, we show that the endocytic defect in haploid yeast harboring and additional copy of chromosome IX (Disome IX) is sufficient to increase variability in induction at the GAL1-10 promoter.

The GAL pathway is a well understood signaling pathway in budding yeast which modulates expression of the galactokinase Gal1 according to the sugars in the environment. Expression at the GAL1-10 promoter is strongly repressed and activated depending on the specific sugars available in the environment. Transcription is repressed when cells are grown with glucose, the preferred carbon source for budding yeast. The promoter is activated when galactose is the dominant sugar source, requiring Gal1 for metabolism.

Variability in transcriptional induction at the *GAL1* promoter can be measured with a fluorescent reporter construct, GAL1pr-YFP, in which activation of the GAL1-10 promoter drives YFP expression (Escalante-Chong et al., 2015). Induction of gene expression downstream of the promoter can be measured by flow cytometry, and the standard deviation of YFP expression serves as a measure of gene expression variability driven by the promoter (Figure 1A). Beach et

al show many disomes are variable in GAL1pr-YFP induction, with disomes IX, II, and XIII having a significantly higher standard deviation than euploid yeast after an 8-hour exposure to galactose. The magnitude of this increase in standard deviation depends on which chromosome is present as an extra copy and does not scale with the size of the chromosome. Disomes I and XI have no difference in variability compared to euploid cells, suggesting that this phenotype may be caused by the increased dosage of specific genes on each chromosome rather than a broader consequence of excess DNA content. To investigate how the addition of a specific chromosome can increase variability in transcriptional responses, we focused on studying haploid yeast containing an additional copy of chromosome IX (Disome IX). Chromosome IX is relatively small and does not contain any of the main members of the GAL signaling pathway, making it a good candidate to study this phenomenon of aneuploid associated variability in gene expression.

RESULTS

Induction of the GAL1-10 promoter is variable in disomes IX and XIII

Expression of GAL1pr-YFP is more variable in Disome IX and Disome XIII than in euploid cells. Both disomes have a slightly lower mean induction than WT, and an increased standard deviation and coefficient of variation (Figure 1B). To check that this is not due to genetic heterogeneity within the disome strain stocks evaluated, clones from single colonies of WT and Disome IX yeast were generated. GAL1pr-YFP variability was measured in eight separate colonies from each strain. Single colonies of disome IX yeast have the same phenotype as the mixed stock; they are more variable in GAL1pr-YFP than WT colonies, meaning the variability in expression driven by the GAL1 promoter is not due to genetic heterogeneity within the disome strains (Figure 1C).

To see if GAL promoter variability is evident at the RNA level, transcripts of reporter RNA were measured by single-molecule fluorescent in situ hybridization (smFISH) (Rahman and Zenklusen, 2013). There are fewer transcripts per cell of YFP driven by the GAL1-10 promoter in Disome IX than WT euploid yeast, and GAL transcription is more variable within the disome population (Figure 1D). This suggests that in the case of disome IX, variability in expression occurs at the level of promoter activation itself, with or without a contribution from post-transcriptional processes.

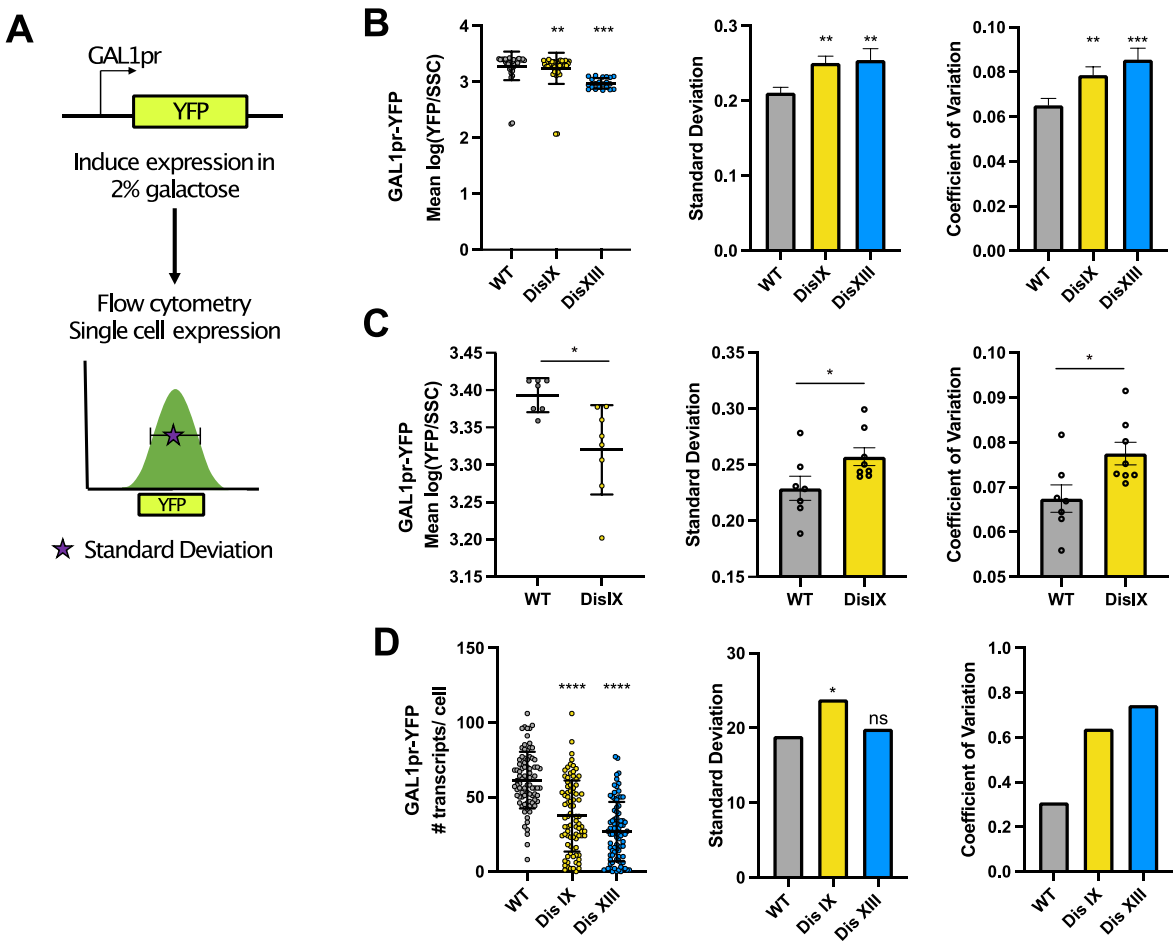

Figure 1. GAL1-10 promoter variability

(A) GAL1-10 promoter induction is measured using a fluorescent reporter GAL1pr-YFP integrated at the HO locus. (B) WT (AA38340), Disome IX (AA38344), and Disome XIII (AA38346) yeast containing integrated GAL1pr-YFP reporter were induced in galactose for 8 hours and reporter induction (left), standard deviation (center), and coefficient of variation (right) were measured. (C) Induction, standard deviation, and coefficient of variation of GAL1pr-YFP in 8 seperate colonies of WT and Disome IX strains induced in galactose for 8 hours. (D) Number (left), standard deviation (center), and coefficient of variation (right) of GAL1pr-YFP RNA transcripts per cell measured by smFISH in WT, Disome IX, and Disome XIII yeast. (B-C) Error

bars represent standard error of the mean. Asteriks (*) represent statistical significance of Disomes compared to WT, calculated by Wilcoxon rank-sum test. (D) Significance was calculated by Welch's t-test (left) and F test to compare variance (middle).

Expression of GAL pathway components are not more variable in disomes

We next began looking at levels of key components of the GAL pathway to see if variability in expression of factors in the galactose sensing pathway upstream of GAL1-10 promotor activation contribute to variability in GAL1-10 driven expression. Endogenous GAL4, GAL80, GAL3, HXT1, and GAL2 were tagged with GFP (Figure 2A). Gal4 is the transcriptional activator which is constitutively bound to the GAL1 promoter at the upstream activating sequence (UAS) and recruits transcriptional machinery in the presence of galactose. Gal80 is a repressor which binds Gal4 and inhibits its activity when there is no galactose in the cell. Gal3 serves as a galactose sensor, binding to Gal80 and preventing its repressor activity when galactose is present. Hxt1 and Gal2 are two of 18 hexose transporters through which galactose enters the cell.

Expression of these GFP tagged proteins were measured by flow cytometry (Figure 2B). Levels of the activators Gal4 and Gal3 are slightly reduced in disomes, which correlates with the slightly lower induction of GAL1pr-YFP. Gal80 expression is lower in Disome XIII, this is likely due to dosage compensation as the GAL80 gene is on chromosome XIII, and only one copy is tagged. However, there are no significant differences in the standard deviation of any of the pathway components measured (Figures 2C-2G). The modest increase in standard deviation of Gal2, Gal80, and Gal4 in Disome IX is consistent with variability in expression from the GAL1-10 promoter as those genes all have a GAL UAS in their promoter. However, unlike the GAL1-10 promoter which contains 4 UASs, GAL2 has only 2, and GAL80 and GAL4 each have just one UAS, which suggests why the effect is much smaller.

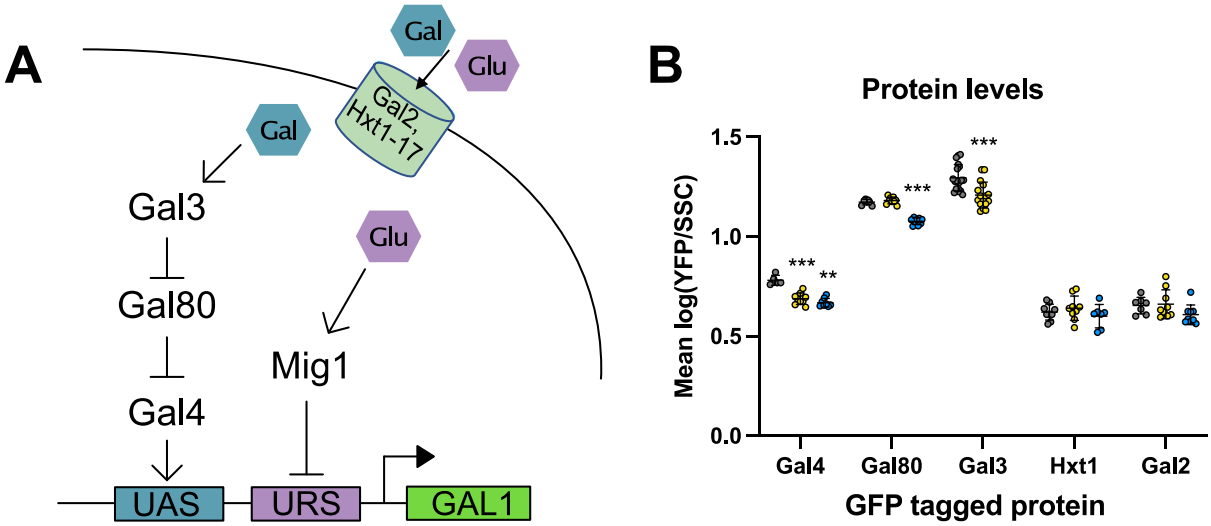
A
Gal
Glu
Gal2, Hxt1-17
Gal
Gal3
Glu
Gal80
Mig1
Gal4
UAS
URS
GAL1
B
Protein levels
Mean log(YFP/SSC)
1.5
1.0
0.5
0.0
***
**
***
***
Gal4
Gal80
Gal3
Hxt1
Gal2
GFP tagged protein

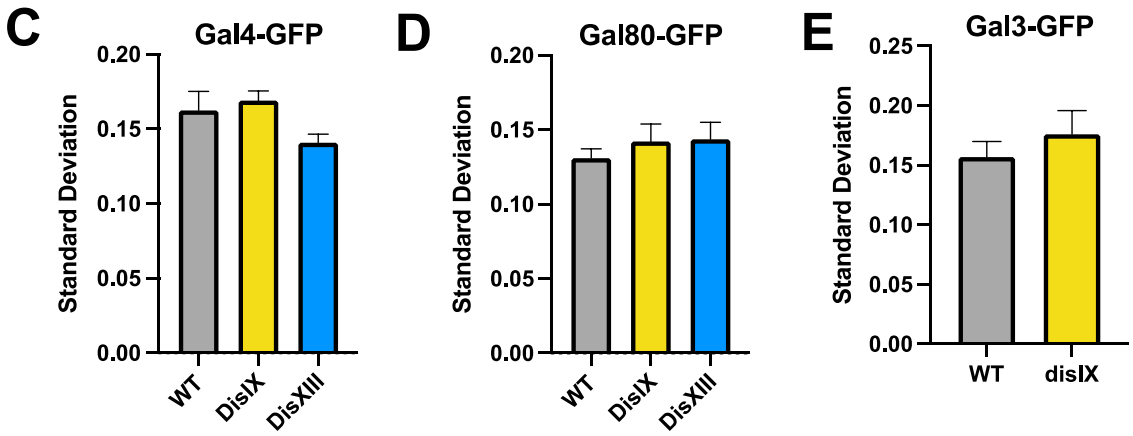
C
Gal4-GFP
D
Gal80-GFP
E
Gal3-GFP
Standard Deviation
0.20
0.15
0.10
0.05
0.00
0.25
WT
DisIX
DisXIII
disIX

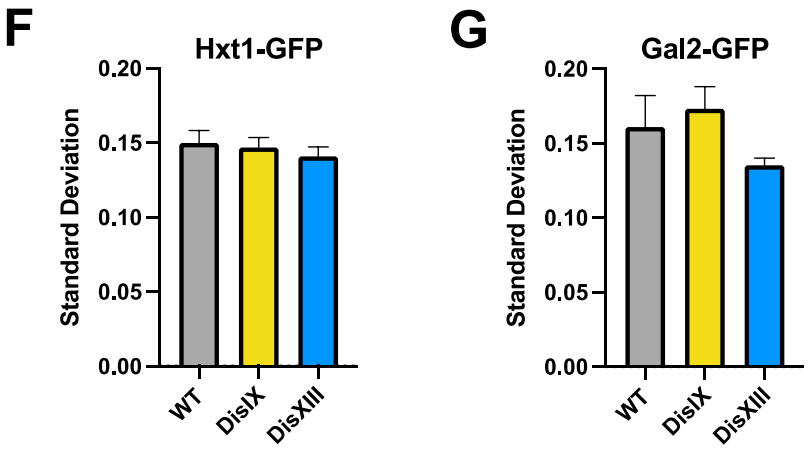
F
Hxt1-GFP
G
Gal2-GFP
Standard Deviation
0.20
0.15
0.10
0.05
0.00
WT
DisIX
DisXIII

Figure 2. Variability in expression of GAL pathway components

(A) Diagram of the GAL1-10 promoter and Galactose signaling pathway. Galactose is transported into the cell and allows Gal4 bound to the upstream activating sequence (UAS) to recruit transcriptional machinery to the promoter. Glucose enters the cell and allows Mig1 to block transcription at the upstream regulatory sequence (URS). (B) Expression of GFP tagged components of the galactose pathway; Gal4, Gal80, Gal3, Hxt1, and Gal2. Gray circles are euploid WT, yellow circles are Disome IX, and blue circles are Disome XIII (Strains: AA4143, AA4144, AA4145, AA4146, AA4147, AA4148, AA4149, AA4150, AA4151, AA4152, AA4153, AA4154, AA4155, AA4156). (C-G) Standard deviation of expression of each pathway component. Error bars represent standard error of the mean. Asteriks (*) represent statistical significance of Disomes compared to WT, calculated by Wilcoxon rank-sum test.

Disome IX yeast exhibit variability in glucose uptake

Rather than variability in expression of the pathway members themselves causing variable expression from the GAL1-10 promoter, variability could arise based on a variability in input to the pathway – hexose transport. The promoter GAL1-10 promoter is sensitive to the ratio of glucose and galactose in the cell (Escalante-Chong et al., 2015). These sugars enter the cell through hexose transporters, which passively transport sugars into the cell by facilitated diffusion. Budding yeast have 18 highly redundant hexose transporters, Hxt1-17 and Gal2. Each transporter has varying affinities for different hexose sugars, and their expression is regulated according to the concentration of sugars available in the environment (Reifenberger et al., 1997). Gal2 is the major galactose transporter, it has the highest affinity for galactose of any of the transporters, but also has a high affinity for glucose, highlighting the strong preference for glucose when this suggest is present as a carbon source. Hxt1 is a low affinity glucose transporter and is a major transporter for sugars when glucose is abundant.

To measure glucose transport, WT and Disome IX yeast were cultured in glucose containing media and incubated with a commercially available fluorescent glucose analog, 2-NBDGlucose (2-(N-(7-Nitrobenz-2-oxa-1,3-diazol-4-yl) Amino)-2-Deoxyglucose) which is known to be internalized into yeast via hexose transporter (Roy et al., 2015). Glucose uptake into individual cells can be measured by microscopy (Figure 3A). WT and Disome IX cells consistently take up the same amount of glucose, with the mean fluorescence per cell increasing at the same rate in both strains from 2 to 32-minutes after 2-NBDGlucose addition (Figure 3B). However, as the time of exposure to 2NBDGlucose increases, a difference in standard deviation arises between Disome IX and WT. After 24 minutes of exposure to 2-NBDGlucose, the standard

deviation of uptake in Disome IX is almost 30% higher than that of the euploid WT strain (Figure 3C-D).

To assess whether this variability represents an increased propensity for specific cells to take in more or less glucose, glucose uptake was measured in individual cells in two independent experiments. Cells were incubated with 2-NBDGlucose for 4 minutes, then incubated in media containing glucose and no fluorescent molecule for 30 minutes, then once again incubated with 2-NBDGlucose for 4 minutes (Figure 3E). In euploid WT cells, there was a weak positive correlation between the first and second glucose uptake measurement in each cell (R^2= 0.5081). In Disome IX cells, this correlation was much weaker (R^2= 0.1358). These data suggest individual disome cells may be variable in how much glucose they take up at any given time, rather than each cell having its own consistent rate of glucose uptake that varies more in Disome IX cells.

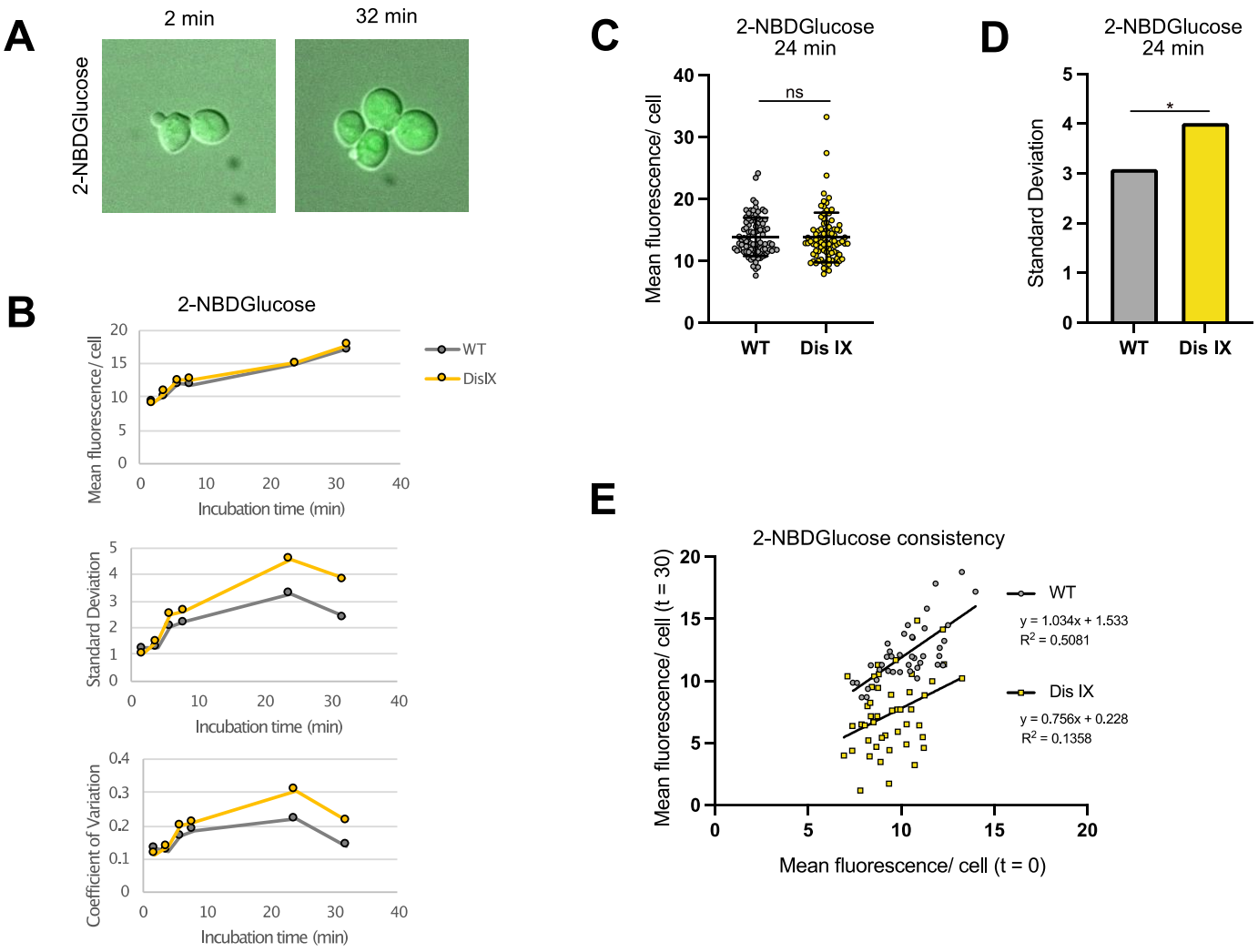

Figure 3. Glucose uptake in euploid and Disome IX yeast

(A) Yeast were grown incubated with fluorescent glucose analog 2-NBDGlucose for 2 and 32 minutes and uptake measured by microscopy. (B) WT (AA38272, gray) and Disome IX (AA38274, yellow) yeast incubated with 2-NBDGlucose for 2-32 minutes. Mean fluorescence per cell (top), standard deviation (middle), and coefficient of variation (bottom) are plotted at each time point. (C) Mean fluorescence of single cells after 24 min incubation with 2-NBDGlucose.

Significance was calculated by Welch's t-test. (D) Standard deviation of data in C, steriks (*) represent statistical significance, calculated by F test. (E) Single cells were incubated with 2-NBDGlucose for 4 min and mean fluorescence is plotted on X-axis. After 30 minutes in plain media, cells were again incubated with 2-NBDGlucose for 4 minutes and the mean fluorescence of the same cells is plotted on the Y-axis. Linear regression and R^2 were calculated in GraphPad Prism.

Disome IX yeast exhibit variability in galactose uptake

To measure galactose transport, we used a fluorescent galactose analog, 2-NBDGalactose synthesized by General Synco Inc. Like 2-NBDGlucose, this analog is taken up by cells and can be measured by microscopy (Figure 4A). To check that this new analog competes with galactose for transport into cells, WT yeast were cultured in galactose media then incubated in media containing 60 μM of 2-NBDGalactose and varying concentrations of galactose. The fluorescence per cell is negatively correlated with the concentration of galactose in the media (Fig 4B), with 2-NBDGalactose uptake reducing by over 40% when 1% galactose was added to media. This indicates that 2-NBDGalactose uptake is reflective of galactose uptake.

To measure galactose transport, WT and disome IX cells were cultured in galactose containing media and then exposed to 2-NBDGalactose. As in glucose uptake experiments, WT and Disome IX cells consistently take up the same amount of galactose, with the mean fluorescence per cell increasing at the same rate in both strains from 2 to 32-minutes after 2-NBDGlucose addition (Figure 4C). However, a difference in standard deviation arises between Disome IX and WT cells as the time of exposure to 2-NBDGalactose increases. After 24 minutes of exposure to 2-NBDGalactose, the standard deviation of uptake in Disome IX is over 35% higher than that of the euploid WT strain (Figure 4D-E).

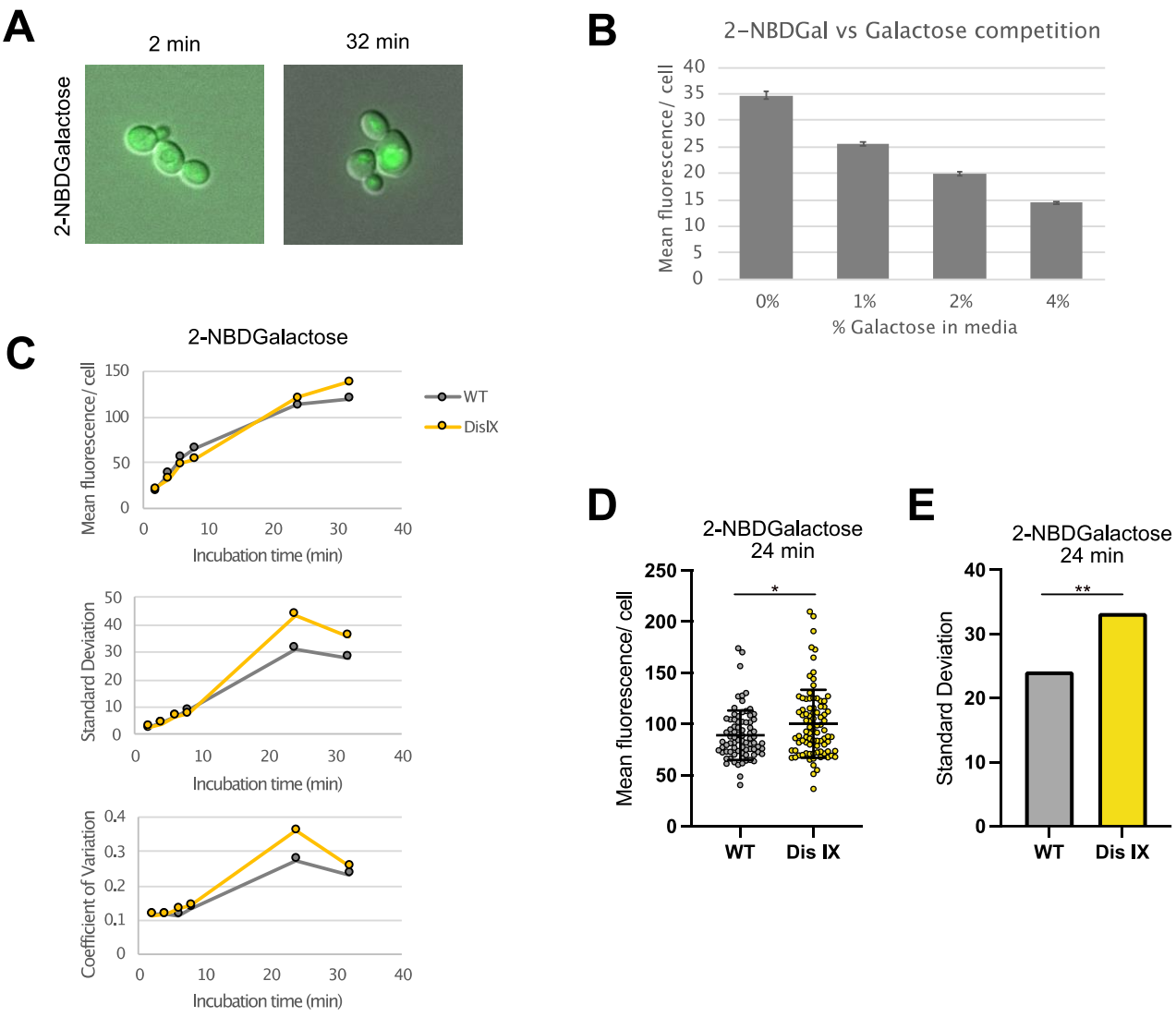

Figure 4. Galactose uptake in euploid and Disome IX yeast

(A) Yeast were grown incubated with fluorescent glucose analog 2-NBDGalactose for 2 and 32 minutes and uptake measured by microscopy. (B) WT yeast (AA38272) were grown up in galactose medium and incubated for 16 min with 2-NBDGalactose and 0-4% Galactose. Uptake of 2-NBDGalactose is measured as mean fluorescence per cell. (C) WT (AA38272, gray) and Disome IX (AA38274, yellow) yeast incubated with 2-NBDGalactose for 2-32 minutes. Mean fluorescence per cell (top), standard deviation (middle), and coefficient of variation (bottom)

are plotted at each time point. (D) Mean fluorescence of single cells after 24 min incubation with 2-NBDGalactose. Asteriks (*) represent statistical significance, calculated by Welch's t-test. (E) Standard deviation of data in D, asteriks (*) represent statistical significance, calculated by F test.

A screen of chromosome IX for genes involved in driving variability in GAL1-10 promoter expression

To investigate increased variability in expression driven by GAL1-10 in disome IX yeast is caused by an additional copy of a specific gene(s), chromosome IX was screened for genes which increase GAL1pr-YFP variability in single extra copy. To simulate the disome state for each gene along chromosome IX, euploid cells containing the GAL1pr-YFP reporter were transformed with from the Molecular Barcoded Yeast (MoBY) ORF Library, which contain single ORFs and are maintained in single copy (Ho et al., 2009). These transformants were then cultured in galactose and promoter induction measured by flow cytometry (Figure 5A). ORFs were then ranked by standard deviation of promoter induction; standard deviations ranged from .190 to .410 (Figure 5B). The distribution of the standard deviations is skewed to the right (mean = .262, median = .257), with 46% of the total range in standard deviation containing just 10% of the ORFs. These top 10% were considered "hits" (Figure 5C). The corresponding library plasmids were sequenced to confirm the identity of the ORF contained in the plasmid (Table 1). Of the 17 MoBY plasmids sequenced, 7 did not contain the expected ORF, and at least 5 of the "hits" were actually a mixture of plasmids containing different ORFs. It is unclear if this contamination is present throughout the MoBY library, or just in the lab stocks screened; however, when screening for variable expression it is expected that heterogenous plasmid stocks would be identified with higher frequency.

Single Disome IX deletions have little effect on GAL1pr-YFP variability

Screen hits were deleted from the extra copy of Disome IX to determine if this affected variability in expression of GAL1pr-YFP in this aneuploidy context. While the screen identifies candidate genes that could increase the standard deviation of GAL1pr-YFP expression in euploid cells, deletion of these same genes from Disome IX had no effect on the standard deviation of GAL1pr-YFP expression in Disome IX yeast. These data suggest that most of the hits are at best sufficient to induce GAL1pr-YFP expression variability, but are not necessary to explain the variability in GAL1pr-YFP expression in Disome IX yeast (Figure 4D). There were three deletions which did result in a significantly lower standard deviation than the full Disome IX; por2Δ, aim21Δ, and irr1Δ, but none reduced the standard deviation to euploid levels.

Two genes which did not show up as hits in the chromosome IX screen, QDR2 and CKA1, were also deleted from Disome IX cells. Standard deviation of GAL1pr-YFP was not changed in Disome IX cka1Δ, as expected. Surprisingly, Disome IX qdr2Δ has a lower standard deviation, similar to that of por2Δ, aim21Δ, and irr1Δ. This discrepancy highlights the important distinction between adding and subtracting genes. Increasing the dosage of one gene in the context of euploidy is not an exact opposite to reducing gene dosage in the context of disomy. The former, as in the screen, asks if the addition of one gene is sufficient to alter GAL1 promoter induction. The latter asks if the gene is necessary for disome IX to reach its increased standard deviation. As we observed, not all genes which are sufficient to induce variability are necessary and vice-versa.

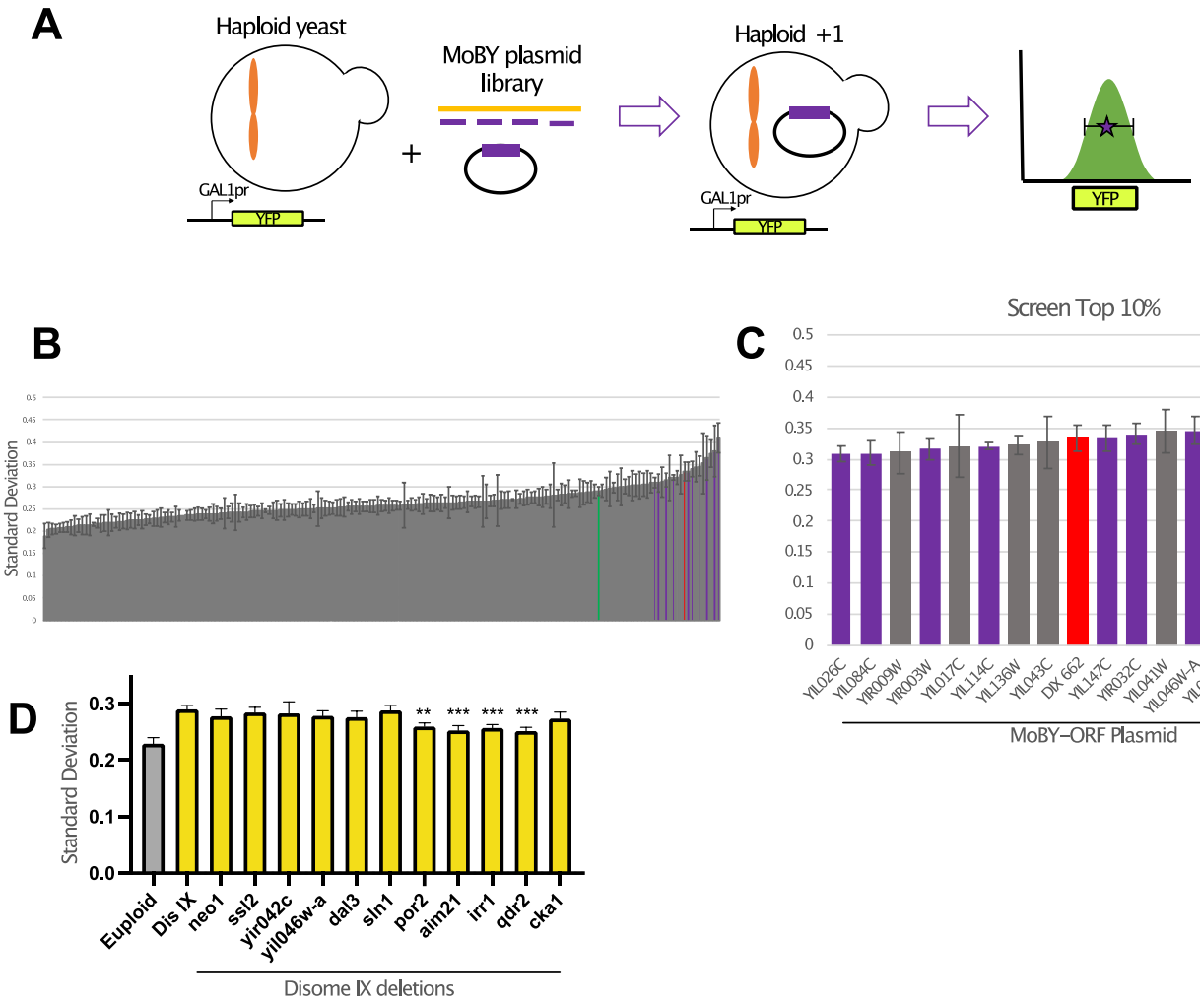
A
Haploid yeast
MoBY plasmid library
Haploid +1
GAL1pr
YFP
GAL1pr
YFP
YFP
B
Standard Deviation
C
Screen Top 10%
YIL026C
YIL084C
YIR009W
YIR003W
YIL017C
YIL114C
YIL136W
YIL043C
DIX 6G2
YIL147C
YIR032C
YIL041W
YIL046W-A
YIL041W
YIR042C
YIL173W
YIL143C
YIL048W
MoBY–ORF Plasmid
D
Standard Deviation
Euploid
Dis IX
neo1
ssl2
yir042c
yil046w-a
dal3
sln1
por2
aim21
irr1
qdr2
cka1
Disome IX deletions

Figure 5. Chromosome IX screen for GAL1pr-YFP variability

(A) Haploid yeast containing GAL1pr-YFP reporter were transformed with MoBY-ORF library plasmids and induction of the promoter was measured after 8 hours in galactose. (B) The average standard deviation of GAL1pr-YFP across all replicates is plotted for yeast transformed with each plasmid. Each bar corresponds to a different ORF in chromosome IX. Green bar is WT control transformed with marker matched vector. Red bar is Disome IX control transformed with marker match vector. Purple bars correspond to hits. Error bars represent the standard error of the mean. (C) Zoomed in view of B, the top 10% of ORFs are shown labeled with SGD IDs. Purple bars are plasmids whose ORFs were confirmed by sequencing (see Table 1). (D) Hits identified in the screen were deleted in Disome IX, restoring them to single copy and GAL1pr-YFP is measured (Strains: AA38340, AA38344, AA41867, AA41869, AA41870, AA41871, AA41872, AA41873, AA41874, AA41875, AA41876, AA41877, AA41878). Asterisks (*) represent significance of Disome IX deletions compared to full Disome IX calculated by Wilcoxon rank-sum test.

Database ID	Gene	SD	MoBY plasmid sequence (by colony)				
			1	2	3	4	5
YIL048W	NEO1	0.4096	NEO1	NEO1	NEO1	NEO1	NEO1
YIL143C	SSL2	0.3795	SSL2	SSL2	SSL2	SSL2	SSL2
YIL173W	VTH1	0.3739	SGN1	CSM2	--	--	--
YIR042C	YIR042C	0.3652	YIR042C	YIR042C	YIR042C	--	YIR042C
YIL041W (1)	GVP36	0.3523	YLR118C	YLR118C	YLR118C	YLR118C	YLR118C
YIL046W-A	YIL046W-A	0.3460	YIL046W-A	--	YIL046W-A	YIL046W-A	YIL046W-A
YIL041W (2)	GVP36	0.3443	BUR2	--	--	--	--
YIR032C	DAL3	0.3397	DAL3	DAL3	--	DAL3	DAL3
YIL147C	SLN1	0.3339	SLN1	SLN1	SLN1	SLN1	SLN1
YIL043c	CBR1	0.3272	AGE2	AGE2	AGE2	--	SNL1
YIL136W	OM45	0.3212	RPL2A	--	--	HIS5	--
YIL114C	POR2	0.3209	POR2	POR2	--	POR2	POR2
YIL017C	VID28	0.3203	MRPL6	THP2	AGE2	AGE2	VID28
YIR003W	AIM21	0.3154	AIM21	AIM21	AIM21	AIM21	--
YIR009W	MSL1	0.3107	COA1	YJL193W	MSL1	MSL1	--
YIL084C	SDS3	0.3088	SDS3	SDS3	SDS3	SDS3	SDS3
YIL026C	IRR1	0.3087	IRR1	--	IRR1	--	IRR1

Table 1. Sequencing of screen hit plasmids

MoBY plasmids corresponding to the top 10% of standard deviations in the screen were extracted from 5 colonies and sequenced by Quintara.

Addition of two endocytic genes increases GAL1pr-YFP variability in euploid cells

Notably, two of the hits identified in the screen – NEO1 and AIM21 – are genes involved in endocytosis. NEO1 encodes a flippase involved in establishing membrane asymmetry (Takar et al., 2016). AIM21 is part of a complex which inhibits actin assembly, regulating actin levels between cables and patches, increasing monomer pools and allowing for more efficient endocytosis (Shin et al., 2018). These hits suggest that perturbing endocytosis by increasing expression of endocytic genes on chromosome IX can contributes to variability in expression from the GAL1-10 promoter. This hypothesis is further supported by previous findings that Disome IX yeast have an endocytic defect (Dodgson et al., 2016). This defect in endocytosis in Disome IX yeast is exacerbated by deletion of the endocytic scaffold gene EDE1, and can be largely rescued by deleting one copy of PRK1, a gene on chromosome IX which inhibits endocytosis (Dodgson et al., 2016).

To determine whether reduced endocytosis in disome IX contributes to increased variability in GAL1pr-YFP expression, GAL1pr-YFP variability was measured in endocytosis mutants (Figure 6A). Reducing endocytic efficiency in euploid cells by deletion of EDE1 is sufficient to increase GAL1pr-YFP variability to Disome IX. Rescuing disome IX's endocytic defect by deletion of one copy of PRK1 does not return GAL1pr-YFP variability to euploid levels. Endocytic efficiency is inversely correlated with standard deviation. The standard deviation of GAL1pr-YFP expression almost doubles in Disome IX ede1Δ cells which have impaired endocytosis. These data suggest that inhibiting endocytosis can increase GAL promoter variability, but it is not the sole source of variability in disome IX yeast.

Variability in hexose uptake is affected by endocytosis mutations. Euploid ede1Δ yeast exhibit more variability in 2-NBDGlucose uptake that WT yeast (Figures 6B-C). The differences in 2-NBDGalactose variation are small, and not statistically significant; however, the pattern mimics that of GAL1pr-YFP variability in the same strains, with WT ede1Δ having increased standard deviation, and Disome IX prk1Δ/PRK1 slightly reducing the observed variability in uptake (Figures 6D-E). These data support the idea that at least some of the noise observed in expression from the GAL1-10 promoter originates with variable uptake of glucose and galactose through hexose transporters, and that an endocytosis defect in Disome IX may contribute to this variability.

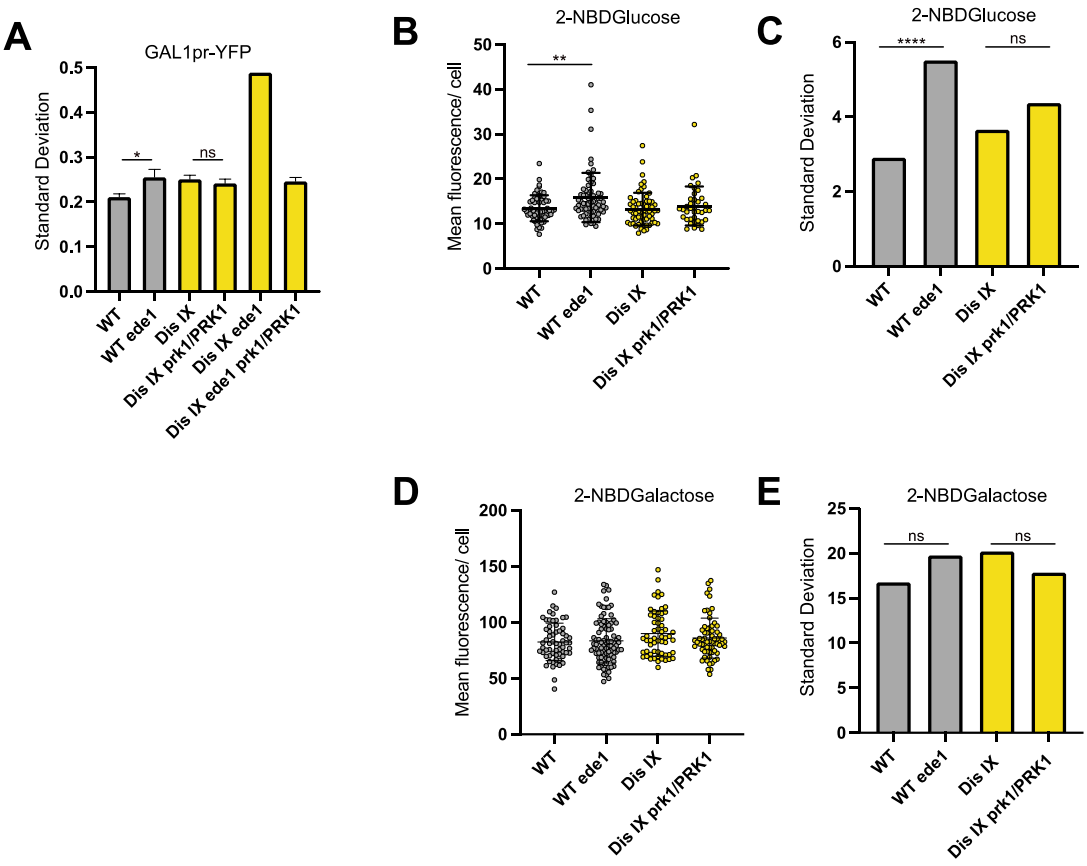

Figure 6. GAL pathway variability in endocytosis mutants

(A) Standard deviation of GAL1pr-YFP was measured in WT and Disome IX yeast with endocytosis mutations (Strains: AA38340, AA41879, A38344, AA41882, AA41883, AA41884). Error bars are the standard error of the mean. Asterisks (*) represent significance between indicated strains calculated by Wilcoxon rank-sum test. (B-E) Uptake and standard deviation of 2-NBDGlucose and 2-NBDGalactose in euploid and Disome IX endocytosis mutants (Strains: AA38272, AA37945 AA38278, AA37950). Asteriks (*) represent statistical significance, calculated by Welch's t-test (B,D) and F-test (C,E).

Endocytosis relates to GAL1-10 promoter variability through hexose uptake

Because addition of chromosome IX and deletion of EDE1 both appear to increase hexose uptake variability, but the expression of transporters Hxt1 and Gal2 are not altered in Disome IX, we hypothesized that disrupting endocytosis alters the localization of hexose transporters. The concentration of different transporters at the membrane changes with the concentration of sugars in the environment, and this balance is maintained in part by endocytosis. For example, yeast internalize Hxt1 in an endocytosis dependent manner when glucose is not available (Roy et al., 2014). To test this hypothesis, the localization of two major hexose transporters, Hxt1 and Gal2, were assessed. Endogenous Hxt1 and Gal2 were tagged with the fluorophore mNeonGreen in euploid and disome IX yeast, and the yeast were cultured in glucose or galactose before imaging. The concentration of the transporters at the plasma membrane was measured for each cell and variability in localization is measured by the standard deviation of each strain (Figure 7A). There is no difference in concentration or in variability of either transporter in euploid and Disome IX cells that were cultured in glucose (Figures 7B-C, 8A-B). Differences emerge when cells are grown in galactose. There is no difference in variability of Hxt1 localization, but the overall concentration of Hxt1 at the membrane is lower in Disome IX cells than euploid (Figure 7D-E). There is no measurable difference in Gal2 localization in Disome IX. However, Disome IX ede1Δ cells have a lower concentration of Gal2 at the membrane than WT cells (Figure 8C-D). Overall, cells with reduced endocytic efficiency have fewer hexose transporters at the membrane.

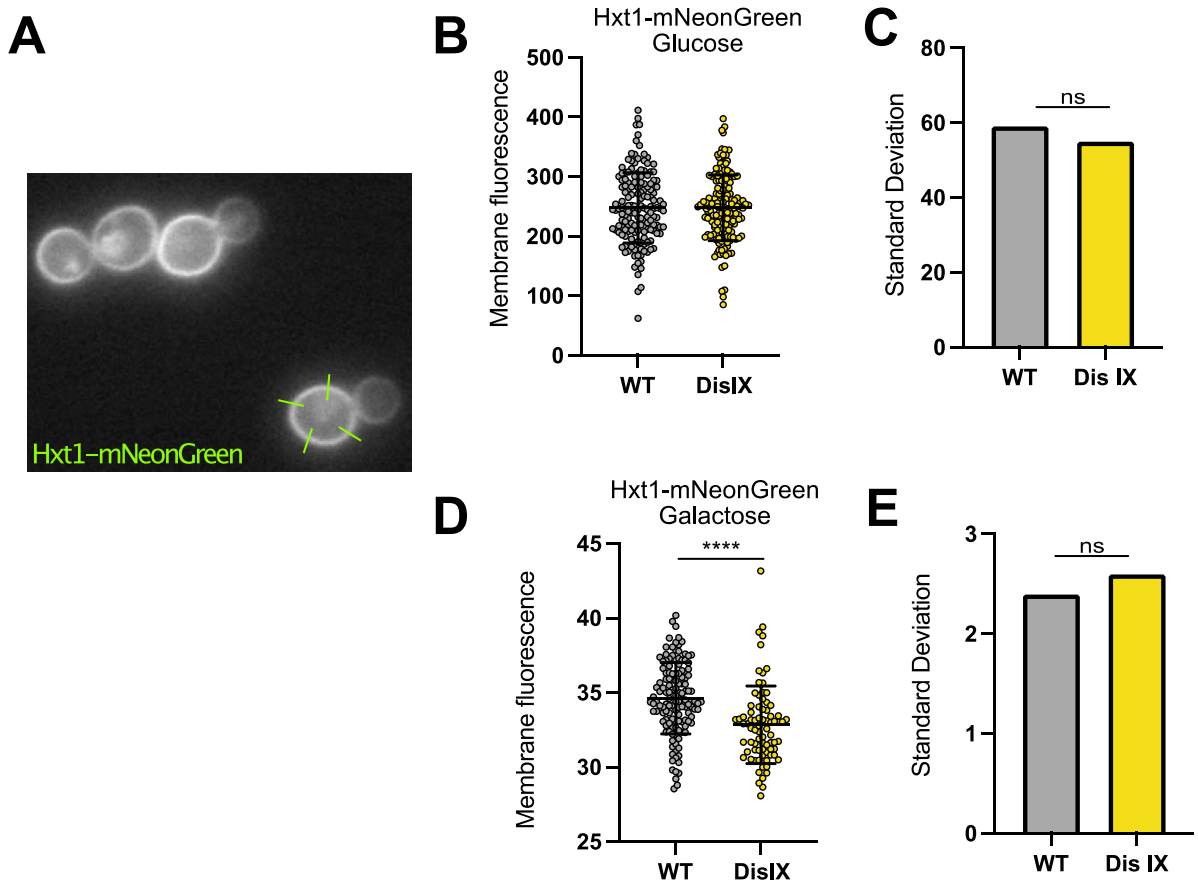

Figure 7. Hxt1-mNeonGreen localization

(A) Endogenous Hxt1 was labeled with fluorescent tag mNeonGreen. Membrane localization was measured by taking the average maximum value of four lines drawn intersecting the membrane of each cell. (A-B) Concentration (B) and standard deviation (C) of Euploid (AA41885) and Disome IX (AA41886) yeast grown in glucose. (C-D) Concentration (D) and standard deviation (E) of Euploid and Disome IX yeast grown in galactose. Asteriks (*) represent statistical significance, calculated by Welch's t-test (B,D) and F-test (C,E).

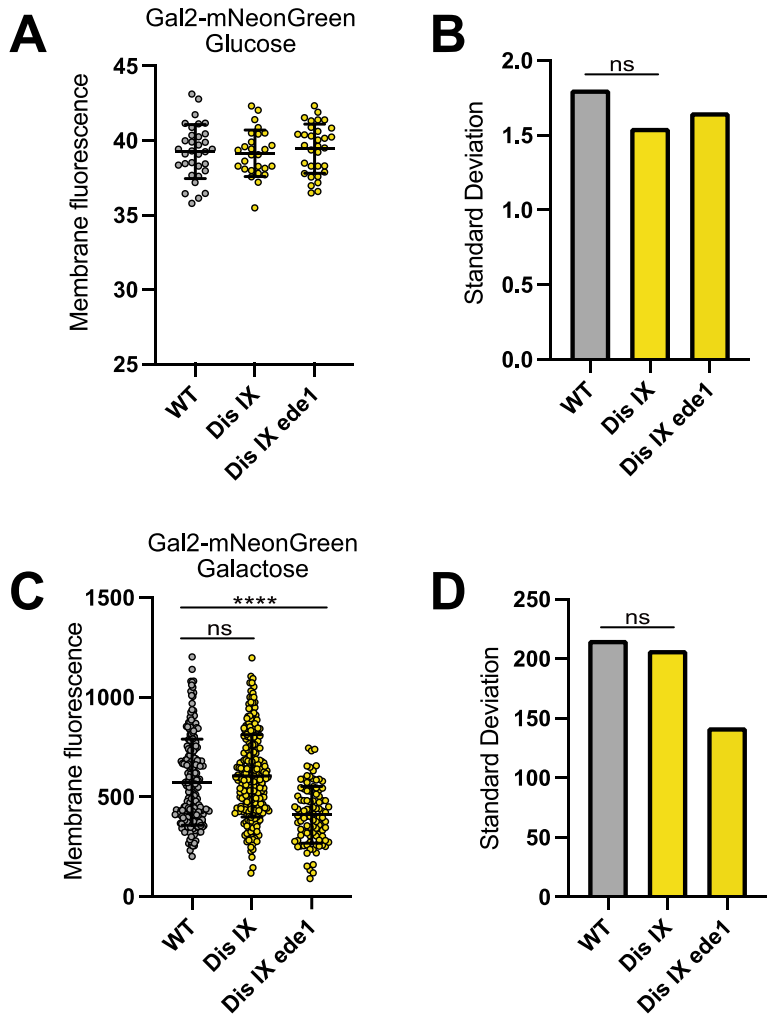

Figure 8. Hxt1-mNeonGreen localization

Endogenous Gal2 was labeled with fluorescent tag mNeonGreen. Membrane localization was measured by taking the average maximum value of four lines drawn intersecting the membrane of each cell. (A-B) Concentration (A) and standard deviation (B) of Euploid (AA41887), Disome IX (AA41888), and Disome IX ede1Δ (AA41889) yeast grown in glucose. (C-D) Concentration (C) and standard deviation (D) of Euploid and Disome IX yeast grown in galactose. Asteriks (*) represent statistical significance, calculated by Welch's t-test (A,C) and F-test (B,D).

DISCUSSION

Reducing endocytosis leads to an increase in variability at the GAL1-10 promoter in budding yeast. Genetically altering the efficiency of endocytosis by deletion of EDE1, or addition of NEO1, AIM21, or the entirety of chromosome IX increases the variability of induction at the GAL1-10 promoter and uptake of hexose sugars. However, the endocytic defect in Disome IX is not the only reason Disome IX yeast exhibit GAL pathway variability, as rescuing the endocytic defect by deletion of PRK1 does not restore variability to euploid levels.

The role of hexose transport

Endocytosis helps to establish the correct balance of hexose transporters at the membrane in response to changing sugar availability, thus effecting the input to the GAL pathway (Roy et al., 2014). Therefore, it makes sense that the localization of hexose transporters Hxt1 and Gal2 are altered in endocytosis mutants. There is less Hxt1 at the membrane in Disome IX cells cultured in galactose. However, there is no such difference in Gal2 localization in Disome IX ede1Δ cells which have an even greater endocytic defect; Gal2 concentration at the membrane drops significantly. Together, this data points to an overall reduction in hexose transporters at the membrane when endocytosis is less efficient. This is a bit counterintuitive as endocytosis internalizes transporters, targeting them for degradation, so one might expect to see more transporters on the membrane when this process is disrupted. However, there are two reasons this may not be the case. First, glucose and galactose uptake are regulated by a complex balance of several transporters, only two of which are measured in

these studies. Second, disrupting endocytosis will alter membrane trafficking, and without membrane turn over there may be fewer transporters available on the cell membrane.

The difference in transporter localization, without itself being variable could introduce variability into transcription driven by the GAL pathway. Without the correct balance of hexose transporters at the membrane, the concentration of sugars within the cell will be altered. With fewer transporters, there is more competition for transport into the cell, leading to variability in the concentration of sugars in the cell which will propagate through the GAL pathway, ultimately resulting in variability in expression from the GAL1-10 promoter.

Gene dosage and variability

Broadly, variability is a feature of aneuploidy across species. There is a huge amount of variability among people with trisomy 21 Down Syndrome in conditions like congenital heart defects, onset of Alzheimer's associated dementia, and leukemia. In mice, the Down syndrome model Ts65Dn have similarly variable phenotypes. Trisomy 19 mouse embryos are variable in morphology, including a higher standard deviation of nuchal edema thickness than euploid embryos (Beach et al., 2017). Aneuploid yeast are more variable in cell cycle length, transcriptional induction, and stress response. Together, this would suggest that something about the state of aneuploidy itself, rather than the specific changes in gene dosage, leads to variability. However, when this broad phenotype of noise is broken down into its parts, it is possible to identify specific genetic drivers of this variability. I have shown that disrupting the essential cellular process of endocytosis results in transcriptional noise in yeast. While this does not account for all of the GAL pathway noise observed in Disome IX yeast, it does demonstrate

that altering the dosage of one or a few specific genes can result in increased variability in pathway output.

Other yeast disomes exhibit the same, or even greater, variability in expression from the GAL1-10 promoter. However, it is unlikely that this phenotype has the same cause in all the disomes. Each disomy means increased dosage of a distinct set of genes, which I hypothesize would disrupt regulation of different cellular processes. Many different disomes may ultimately lead to the same phenotype of GAL pathway variability, but this is likely happening through different mechanisms. This is supported by the fact the standard deviation in GAL1pr-YFP does not correlate to the size of the chromosome that is in excess. If the phenotype were caused only by increased gene dosage, it would be expected that larger chromosomes would have the largest effect, and this is not the case. For example, Disome XI, which is larger than Disome IX, has no increase in GAL1pr-YFP variability. Taken together, these data provide further evidence that phenotypic variability in aneuploidy is not necessarily the result of genetic heterogeneity, but rather can be a consequence of the aneuploidy itself.

MATERIALS AND METHODS

Yeast Strains and Plasmids

All yeast strains are derivatives of W303 and listed in Supplemental Table S1. Deletions and fluorescent tags were generated using a PCR based method (Longtine et al., 1998). Plasmids used in strain construction are listed in Supplemental Table S2. Primers used in strain construction are listed in Supplemental Table S3.

GAL1-10 promoter Induction

Yeast were inoculated from selective plates with histidine dropout (-his) and 200 µg/mL Geneticin (G418) into 1 mL liquid G418/-his medium with 2% glucose in 96-well deep well plates and grown up for 24 hours shaking at 30˚. To ensure cultures are in log phase and the GAL1-10 promoter is neither induced nor repressed, yeast were grown out in SC media with 2% raffinose at serial dilutions 1:100 to 1:400. Raffinose outgrowth plates were incubated at 30˚ for 16-18 hours. The cultures of each strain with an OD_{600} closest to 0.1 were pelleted, washed twice then resuspended 1:1 in SC without sugar, the diluted 1:100 into 500 µL of SC media containing 2% Galactose. Yeast were incubated shaking at 30˚ for 8 hours before promoter induction is measured.

Flow Cytometry

After 8 hour induction, activation of the GAL1-10 promoter was measured by flow cytometry. Cells are pelleted, washed twice and resuspended in Tris-EDTA pH 7.5 (TE) and transferred to 96 well CELLTREAT plates. Samples were run on a Stratedigm s1000EX cytometer

with FSC/SSC threshold of 200 and PMT gain settings of FITC 2.0%, FSC 33.5%, and SSC 55.3%. Flow cytometry data was analyzed using a custom MATLAB code modified from code shared by Mike Springer (Beach et al., 2017). YFP values were normalized to cell size by dividing by SSC values, and rescaled by an arbitrary factor of $10^{3.5}$. Only samples in which over 5000 cells were counted were included in analysis.

Uptake of hexose sugars

Cultures were inoculated from G418/-his plates into liquid G418/-his medium with 2% glucose and grown shaking at 30˚ for 1-2 hours. This culture was then added to 15 mL of SC 2% Raffinose and grown shaking at room temperature overnight (16-20 hours). The culture was then filtered through a Supor 450 membrane disc filter and washed with SC media containing no sugar. For glucose uptake assays, 1 OD of cells were resuspended in 10 mL of SC media with 2% Glucose and allowed to grow at room temperature for 4-6 hours. For galactose uptake assays, 2 OD of cells were resuspended in 10mL of synthetic complete media with 2% Galactose and grown 4-6 hours. After 4-6 hour incubation, 100uL of culture were added to culture inlet wells of a CellASIC ONIX Y04C microfluidic plate. Using the CellASIC ONIX microfluidic platform, cells were loaded into the plate at 8psi for 5 seconds. SC with 60 mg/ml of 2-NBDGlucose or 2-NBDGalactose were flowed across the cells at 2psi for 2-32 minutes, followed by PBS at 2psi for 4 minutes. Cells were then imaged using a Zeiss Axio Observer-Z1 microscope with a 63X objective and a Hamamatsu ORCA-AG digital camera. 8 stacks were acquired 1 micron apart and maximally projected. Hexose uptake was measured using ImageJ. The largest ellipse possible was drawn within each cell and mean fluorescent intensity was measured within that area.

Chromosome IX screen

WT yeast containing the GAL1pr-YFP reporter were transformed with plasmids from the MoBY-ORF plasmid collection corresponding to ORFs within chromosome IX. Yeast were cultured as described above, except synthetic dropout media lacking uracil was used to maintain plasmids. After 8 hours in 2% galactose, induction of GAL1pr-YFP was measured by flow cytometry, as described above. The screen was repeated 8 times and the standard deviations were averaged across runs for each plasmid to establish final values for each ORF, standard deviation for each ORF is listed in Supplemental table 4.

Localization of hexose transporters

Yeast containing Hxt1-mNeonGreen or Gal2-mNeonGreen were grown up in raffinose, filtered, and resuspended into either glucose or galactose containing media and imaged as previously described in “uptake of hexose sugars”. Cells were imaged on CellASIC ONIX Y04C microfluidic plates with media flowing constantly at 2 psi.

Membrane localization was measured using ImageJ. The line tool was used to measure the maximum fluorescent intensity across the membrane in four locations around the cell. Those four measurements were averaged to produce a single “membrane concentration” value for each cell.

Supplemental Table S1. Yeast strains used in this study

Strain (AA)	Disome	Genotype
37945	-	MATa, ade2-1, leu2-3, ura3, trp1-1, his3-11,15, can1-100, GAL, [phi+], ade1::HIS3, lys2::KanMX6, ede1::NAT
37950	IX	MATa, ade2-1, leu2-3, ura3, trp1-1, his3-11,15, can1-100, GAL, [phi+], xxx::KAN, xxx::HIS3 (markers inserted on chromosome IX; 342433-342832 deleted between FAA3 and URM1 on chromosome IX), prk1::NAT/PRK1
38272	-	MATa, ade2-1, leu2-3, ura3, trp1-1, his3-11,15, can1-100, GAL, [phi+], ade1::HIS3, lys2::KanMX6
38278	IX	MATa, ade2-1, leu2-3, ura3, trp1-1, his3-11,15, can1-100, GAL, [phi+], xxx::KAN, xxx::HIS3 (markers inserted on chromosome IX; 342433-342832 deleted between FAA3 and URM1 on chromosome IX)
38340	-	MATa, ade2-1, leu2-3, ura3, trp1-1, his3-11,15, can1-100, GAL, [phi+], ade1::HIS3, lys2::KanMX6, ho::GAL1pr-YFP:HYGRO
38344	IX	MATa, ade2-1, leu2-3, ura3, trp1-1, his3-11,15, can1-100, GAL, [phi+], xxx::KAN, xxx::HIS3 (markers inserted on chromosome IX; 342433-342832 deleted between FAA3 and URM1 on chromosome IX), ho::GAL1pr-YFP:HYGRO
38346	XIII	MATalpha, ade2-1, leu2-3, ura3, trp1-1, his3-11,15, can1-100, GAL, [phi+], xxx::KAN, xxx::HIS3 (markers inserted on chromosome XIII; 309200-309300 deleted between SPO20 and YMR018W on chromosome XIII), ho::GAL1pr-YFP:HYGRO
41838	-	MATalpha, ade2-1, leu2-3, ura3, trp1-1, his3-11,15, can1-100, GAL, [phi+], GAL80-GFP:TRP1
41839	-	MATalpha, ade2-1, leu2-3, ura3, trp1-1, his3-11,15, can1-100, GAL, [phi+], HXT1-GFP:TRP1
41840	-	MATalpha, ade2-1, leu2-3, ura3, trp1-1, his3-11,15, can1-100, GAL, [phi+], GAL2-GFP:TRP1
41841	-	MATalpha, ade2-1, leu2-3, ura3, trp1-1, his3-11,15, can1-100, GAL, [phi+], GAL4-GFP:TRP1
41842	-	MATalpha, ade2-1, leu2-3, ura3, trp1-1, his3-11,15, can1-100, GAL, [phi+], GAL3-GFP::TRP
41843	-	MATa, ade2-1, leu2-3, ura3, trp1-1, his3-11,15, can1-100, GAL, [phi+], ade1::HIS3, lys2::KanMX6, GAL4-GFP:TRP1
41844	IX	MATalpha, ade2-1, leu2-3, ura3, trp1-1, his3-11,15, can1-100, GAL, [phi+], xxx::KAN, xxx::HIS3 (markers inserted on chromosome IX; 342433-342832 deleted between FAA3 and URM1 on chromosome IX), GAL4-GFP::TRP1
41845	XIII	MATalpha, ade2-1, leu2-3, ura3, trp1-1, his3-11,15, can1-100, GAL, [phi+], xxx::KAN, xxx::HIS3 (markers inserted on chromosome XIII; 309200-309300 deleted between SPO20 and YMR018W on chromosome XIII), GAL4-GFP:TRP1

41846	-	MATa, ade2-1, leu2-3, ura3, trp1-1, his3-11,15, can1-100, GAL, [phi+], ade1::HIS3, lys2::KanMX6, GAL80-GFP:TRP1
41847	IX	MATalpha, ade2-1, leu2-3, ura3, trp1-1, his3-11,15, can1-100, GAL, [phi+], xxx::KAN, xxx::HIS3 (markers inserted on chromosome IX; 342433-342832 deleted between FAA3 and URM1 on chromosome IX), GAL80-GFP:TRP1
41848	XIII	MATalpha, ade2-1, leu2-3, ura3, trp1-1, his3-11,15, can1-100, GAL, [phi+], xxx::KAN, xxx::HIS3 (markers inserted on chromosome XIII; 309200-309300 deleted between SPO20 and YMR018W on chromosome XIII), GAL80-GFP:TRP1
41849	-	MATalpha, ade2-1, leu2-3, ura3, trp1-1, his3-11,15, can1-100, GAL, [phi+], ade1::HIS3, lys2::KanMX6, GAL3-GFP:TRP1
41850	IX	MATa, ade2-1, leu2-3, ura3, trp1-1, his3-11,15, can1-100, GAL, [phi+], xxx::KAN, xxx::HIS3 (markers inserted on chromosome IX; 342433-342832 deleted between FAA3 and URM1 on chromosome IX), GAL3-GFP:TRP1
41851	-	MATa, ade2-1, leu2-3, ura3, trp1-1, his3-11,15, can1-100, GAL, [phi+], ade1::HIS3, lys2::KanMX6, HXT1-GFP:TRP1
41852	IX	MATalpha, ade2-1, leu2-3, ura3, trp1-1, his3-11,15, can1-100, GAL, [phi+], xxx::KAN, xxx::HIS3 (markers inserted on chromosome IX; 342433-342832 deleted between FAA3 and URM1 on chromosome IX), HXT1-GFP:TRP1
41853	XIII	MATa, ade2-1, leu2-3, ura3, trp1-1, his3-11,15, can1-100, GAL, [phi+], xxx::KAN, xxx::HIS3 (markers inserted on chromosome XIII; 309200-309300 deleted between SPO20 and YMR018W on chromosome XIII), HXT1-GFP:TRP1
41854	-	MATallpha, ade2-1, leu2-3, ura3, trp1-1, his3-11,15, can1-100, GAL, [phi+], ade1::HIS3, lys2::KanMX6, GAL2-GFP:TRP1
41855	IX	MATalpha, ade2-1, leu2-3, ura3, trp1-1, his3-11,15, can1-100, GAL, [phi+], xxx::KAN, xxx::HIS3 (markers inserted on chromosome IX; 342433-342832 deleted between FAA3 and URM1 on chromosome IX), GAL2-GFP::TRP1
41856	XIII	MATalpha, ade2-1, leu2-3, ura3, trp1-1, his3-11,15, can1-100, GAL, [phi+], xxx::KAN, xxx::HIS3 (markers inserted on chromosome XIII; 309200-309300 deleted between SPO20 and YMR018W on chromosome XIII), GAL2-GFP:TRP1
41857	-	MATalpha, ade2-1, leu2-3, ura3, trp1-1, his3-11,15, can1-100, GAL, [phi+], aim21::TRP1
41858	-	MATalpha, ade2-1, leu2-3, ura3, trp1-1, his3-11,15, can1-100, GAL, [phi+], qdr2::TRP1
41859	-	MATalpha, ade2-1, leu2-3, ura3, trp1-1, his3-11,15, can1-100, GAL, [phi+], yil046w-a::TRP1
41860	-	MATalpha, ade2-1, leu2-3, ura3, trp1-1, his3-11,15, can1-100, GAL, [phi+], dal3::TRP1
41861	-	MATalpha, ade2-1, leu2-3, ura3, trp1-1, his3-11,15, can1-100, GAL, [phi+], por2::TRP1

41862	IX	MATa, ade2-1, leu2-3, ura3, trp1-1, his3-11,15, can1-100, GAL, [phi+], xxx::KAN, xxx::HIS3 (markers inserted on chromosome IX; 342433-342832 deleted between FAA3 and URM1 on chromosome IX), neo1::TRP1
41863	IX	MATa, ade2-1, leu2-3, ura3, trp1-1, his3-11,15, can1-100, GAL, [phi+], xxx::KAN, xxx::HIS3 (markers inserted on chromosome IX; 342433-342832 deleted between FAA3 and URM1 on chromosome IX), ssl2::TRP1
41864	IX	MATa, ade2-1, leu2-3, ura3, trp1-1, his3-11,15, can1-100, GAL, [phi+], xxx::KAN, xxx::HIS3 (markers inserted on chromosome IX; 342433-342832 deleted between FAA3 and URM1 on chromosome IX), sln1::TRP1
41865	-	MATalpha, ade2-1, leu2-3, ura3, trp1-1, his3-11,15, can1-100, GAL, [phi+], cka1::TRP1
41866	IX	MATa, ade2-1, leu2-3, ura3, trp1-1, his3-11,15, can1-100, GAL, [phi+], xxx::KAN, xxx::HIS3 (markers inserted on chromosome IX; 342433-342832 deleted between FAA3 and URM1 on chromosome IX), irr1::TRP1
41867	IX	MATa, ade2-1, leu2-3, ura3, trp1-1, his3-11,15, can1-100, GAL, [phi+], xxx::KAN, xxx::HIS3 (markers inserted on chromosome IX; 342433-342832 deleted between FAA3 and URM1 on chromosome IX), neo1::TRP1, ho::GAL1pr-YFP:HYGRO
41868	IX	MATa, ade2-1, leu2-3, ura3, trp1-1, his3-11,15, can1-100, GAL, [phi+], xxx::KAN, xxx::HIS3 (markers inserted on chromosome IX; 342433-342832 deleted between FAA3 and URM1 on chromosome IX), ho::GAL1pr-YFP:HYGRO, neo1::TRP1
41869	IX	MATalpha, ade2-1, leu2-3, ura3, trp1-1, his3-11,15, can1-100, GAL, [phi+], xxx::KAN, xxx::HIS3 (markers inserted on chromosome IX; 342433-342832 deleted between FAA3 and URM1 on chromosome IX), ho::GAL1pr-YFP:HYGRO, ssl2::TRP1
41870	IX	MATa, ade2-1, leu2-3, ura3, trp1-1, his3-11,15, can1-100, GAL, [phi+], xxx::KAN, xxx::HIS3 (markers inserted on chromosome IX; 342433-342832 deleted between FAA3 and URM1 on chromosome IX), ho::GAL1pr-YFP:HYGRO, yir042c::TRP1
41871	IX	MATa, ade2-1, leu2-3, ura3, trp1-1, his3-11,15, can1-100, GAL, [phi+], xxx::KAN, xxx::HIS3 (markers inserted on chromosome IX; 342433-342832 deleted between FAA3 and URM1 on chromosome IX), ho::GAL1pr-YFP:HYGRO, yil046w-a::TRP1
41872	IX	MATalpha, ade2-1, leu2-3, ura3, trp1-1, his3-11,15, can1-100, GAL, [phi+], xxx::KAN, xxx::HIS3 (markers inserted on chromosome IX; 342433-342832 deleted between FAA3 and URM1 on chromosome IX), ho::GAL1pr-YFP:HYGRO, dal3::TRP1
41873	IX	MATa, ade2-1, leu2-3, ura3, trp1-1, his3-11,15, can1-100, GAL, [phi+], xxx::KAN, xxx::HIS3 (markers inserted on chromosome IX; 342433-342832 deleted between FAA3 and URM1 on chromosome IX), ho::GAL1pr-YFP:HYGRO, sln1::TRP1

41874	IX	MATalpha, ade2-1, leu2-3, ura3, trp1-1, his3-11,15, can1-100, GAL, [phi+], xxx::KAN, xxx::HIS3 (markers inserted on chromosome IX; 342433-342832 deleted between FAA3 and URM1 on chromosome IX), ho::GAL1pr-YFP:HYGRO, por2::TRP1
41875	IX	MATa, ade2-1, leu2-3, ura3, trp1-1, his3-11,15, can1-100, GAL, [phi+], xxx::KAN, xxx::HIS3 (markers inserted on chromosome IX; 342433-342832 deleted between FAA3 and URM1 on chromosome IX), ho::GAL1pr-YFP:HYGRO, aim21::TRP1
41876	IX	MATalpha, ade2-1, leu2-3, ura3, trp1-1, his3-11,15, can1-100, GAL, [phi+], xxx::KAN, xxx::HIS3 (markers inserted on chromosome IX; 342433-342832 deleted between FAA3 and URM1 on chromosome IX), ho::GAL1pr-YFP:HYGRO, irr1::TRP1
41877	IX	MATalpha, ade2-1, leu2-3, ura3, trp1-1, his3-11,15, can1-100, GAL, [phi+], xxx::KAN, xxx::HIS3 (markers inserted on chromosome IX; 342433-342832 deleted between FAA3 and URM1 on chromosome IX), ho::GAL1pr-YFP:HYGRO, qdr2::TRP1
41878	IX	MATalpha, ade2-1, leu2-3, ura3, trp1-1, his3-11,15, can1-100, GAL, [phi+], xxx::KAN, xxx::HIS3 (markers inserted on chromosome IX; 342433-342832 deleted between FAA3 and URM1 on chromosome IX), ho::GAL1pr-YFP:HYGRO, cka1::TRP1
41879	-	MATalpha, ade2-1, leu2-3, ura3, trp1-1, his3-11,15, can1-100, GAL, [phi+], ade1::HIS3, lys2::KanMX6, ho::GAL1pr-YFP:HYGRO, ede1::NAT
41880	-	MATa, ade2-1, leu2-3, ura3, trp1-1, his3-11,15, can1-100, GAL, [phi+], ade1::HIS3, lys2::KanMX6, ho::GAL1pr-YFP:HYGRO, prk1::NAT
41881	-	MATalpha, ade2-1, leu2-3, ura3, trp1-1, his3-11,15, can1-100, GAL, [phi+], ade1::HIS3, lys2::KanMX6, ho::GAL1pr-YFP:HYGRO, ede1::NAT, prk1::NAT
41882	IX	MATalpha, ade2-1, leu2-3, ura3, trp1-1, his3-11,15, can1-100, GAL, [phi+], xxx::KAN, xxx::HIS3 (markers inserted on chromosome IX; 342433-342832 deleted between FAA3 and URM1 on chromosome IX), ho::GAL1pr-YFP:HYGRO, prk1::NAT
41883	IX	MATa, ade2-1, leu2-3, ura3, trp1-1, his3-11,15, can1-100, GAL, [phi+], xxx::KAN, xxx::HIS3 (markers inserted on chromosome IX; 342433-342832 deleted between FAA3 and URM1 on chromosome IX), ho::GAL1pr-YFP:HYGRO, ede1::NAT
41884	IX	MATalpha, ade2-1, leu2-3, ura3, trp1-1, his3-11,15, can1-100, GAL, [phi+], xxx::KAN, xxx::HIS3 (markers inserted on chromosome IX; 342433-342832 deleted between FAA3 and URM1 on chromosome IX), ho::GAL1pr-YFP:HYGRO, prk1::NAT, ede1::NAT
41885	-	MATa, ade2-1, leu2-3, ura3, trp1-1, his3-11,15, can1-100, GAL, [phi+], ade1::HIS3, lys2::KanMX6, HXT1-mNeonGreen-KanMX6
41886	IX	MATa, ade2-1, leu2-3, ura3, trp1-1, his3-11,15, can1-100, GAL, [phi+], xxx::KAN, xxx::HIS3 (markers inserted on chromosome IX; 342433-342832

		deleted between FAA3 and URM1 on chromosome IX), HXT1-mNeonGreen-KanMX6
41887	-	MATa, ade2-1, leu2-3, ura3, trp1-1, his3-11,15, can1-100, GAL, [phi+], ade1::HIS3, lys2::KanMX6, GAL2-mNeonGreen-KanMX6
41888	IX	MATa, ade2-1, leu2-3, ura3, trp1-1, his3-11,15, can1-100, GAL, [phi+], xxx::KAN, xxx::HIS3 (markers inserted on chromosome IX; 342433-342832 deleted between FAA3 and URM1 on chromosome IX), GAL2-mNeonGreen-KanMX6
41889	IX	MATalpha, ade2-1, leu2-3, ura3, trp1-1, his3-11,15, can1-100, GAL, [phi+], xxx::KAN, xxx::HIS3 (markers inserted on chromosome IX; 342433-342832 deleted between FAA3 and URM1 on chromosome IX), GAL2-mNeonGreen-KanMX6, ede1::NAT

Supplemental Table S2. Plasmids used in this study

Plasmid	Vector	E coli marker	Yeast marker	Source
A247	pFA6a-TRP1	Kan	TRP	(Longtine et al., 1998)
A249	pFA6a-GFP(S65T)-TRP1	Kan	TRP	(Longtine et al., 1998)
A2765	pFA6a-7mNeonGreen-KAN	Amp	Kan	

Supplemental Table S3. Primers used in this study to generate strains. Primers were used in deletion or C terminal tagging of endogenous yeast genes. Primers were designed with homology to genes listed and plasmids as described in (Longtine et al., 1998), and the primer sequences used (F1, F2, and R1) are listed.

Gene	Primer	Sequence
NEO1	F1	AGAAAGGGGTATCAGTGTGCACGGAAAACTTCAGAGACAACGGATCCCCGGGTTAATTAA
NEO1	R1	TAATCCGTTGAAGCAACAAGAAAAATCCAAACCAATTGAAGAATTCGAGCTCGTTTAAAC
AIM21	F1	TTGGTGATCTAACAGGAAATCTATTTTGACCGATTATACACGGATCCCCGGGTTAATTAA
AIM21	R1	TTGTAAATCTGCCAATTTGTTCAGTACGCTCTGCTTCAAAGAATTCGAGCTCGTTTAAAC
QDR2	F1	TTTAGTAGAAACTCTGCTCTCAAACTTGAGTACTGCAACGCGGATCCCCGGGTTAATTAA
QDR2	R1	CTTATCACACCAATTCCTCTTTCTCGGTAGTGGAGCGATCGAATTCGAGCTCGTTTAAAC
YIL046W-A	F1	AACACAAGGCTATTGTATTGCACTAAACGGGCAAGAAGCCCGGATCCCCGGGTTAATTAA
YIL046W-A	R1	ACGATACAGACTGCAAGGTTGCTTTCTTCTTACGCTGATGGAATTCGAGCTCGTTTAAAC
DAL3	F1	ATGCTTATCTTGTAGGGCAAAAAATCTTTGAAGCAAAGATCGGATCCCCGGGTTAATTAA
DAL3	R1	ACATGAACATTTACATATTTACTTCGCCCACAGTCGCAGAGAATTCGAGCTCGTTTAAAC
SSL2	F1	AGTAGCATCTACTGACGTTGGAATCAGTGGAAGATAAATCCGGATCCCCGGGTTAATTAA
SSL2	R1	ATGATATATAATACCCGAGCAATCTACAGCAAAGCTCAGCGAATTCGAGCTCGTTTAAAC
POR2	F1	AGGAATTGCATGAAGAGGAAAGTGTTAGAAATTACCTACGCGGATCCCCGGGTTAATTAA
POR2	R1	CCTGAGAAATATGAATTGGTGTGAAGCAGCGTATGTGTGAGAATTCGAGCTCGTTTAAAC
SLN1	F1	CGTTGGGTATAATCTACTTTGTTTTGATTTAACAATACAACGGATCCCCGGGTTAATTAA
SLN1	R1	TTATGCATATAAGTCAACGCGTAGCGGTGGTATTACGCGCGAATTCGAGCTCGTTTAAAC

GAL3	F2	AGTTTCGAAGCCTGCCTTGGGTACTTGTTTGTACGAACAACGGATCCCCGGGTTAATTAA
GAL3	R1	CTATGGTTGCATCGGATGCTGGAATGGGTTCTATTGGACTGAATTCGAGCTCGTTTAAAC
IRR1	F1	AGGCGATTGACCTGAGAACAAGAGCTCGGACGAAGGTAACCGGATCCCCGGGTTAATTAA
IRR1	R1	GAGCAATAAGTCTGACGTATATCTTTTCCCGAATTCGAGCTCGTTTAAAC
CKA1	F1	CAAAAATAGGGGGTTGTAGAAGGAATATTTGATTCGAACTCGGATCCCCGGGTTAATTAA
CKA1	R1	TTAAATCTATTAGAATTAAGTACAATTGTACAGATGGTAAGAATTCGAGCTCGTTTAAAC
GAL2	F2	ACAACATGACGACAAACCGTGGTACAAGGCCATGCTAGAACGGATCCCCGGGTTAATTAA
GAL2	R1	TCATGAAAAATTAAGAGAGATGATGGAGCGTCTCACTTCAGAATTCGAGCTCGTTTAAAC
HXT1	F2	TGATGACCAACCATTTTACAAGAGTTTGTTTAGCAGGAAACGGATCCCCGGGTTAATTAA
HXT1	R1	ATTAAATACTGTATAAGTCATTAAAATATGCATATTGAGCGAATTCGAGCTCGTTTAAAC
GAL4	F2	ATTCGATGATGAAGATACCCCACCAAACCCAAAAAAAGAGCGGATCCCCGGGTTAATTAA
GAL4	R1	TGCACAGTTGAAGTGAACTTGCGGGGTTTTTCAGTATCTAGAATTCGAGCTCGTTTAAAC
GAL80	F2	CTCCACATTAAACGTTAGCAATATCTCGCATTATAGTTTACGGATCCCCGGGTTAATTAA
GAL80	R1	TTTTTATAACGTTCGCTGCACTGGGGGCCAAGCACAGGGCGAATTCGAGCTCGTTTAAAC

Supplemental Table S4. Chromosome IX MoBY-ORF screen for GAL1pr-YFP variability. Standard deviation of GAL1pr-YFP in all MoBY-ORF plasmids screened, listed from highest to lowest standard deviation. Column 1 lists the Saccharomyces Genome Database ID for each plasmid. Column 2 lists the number of replicates measured for each plasmid which met criteria for inclusion in the screen (ie. At least 5000 particles measured by flow cytometry). Column 3 lists the mean of the standard deviations of all distributions measured for each plasmid. Column 4 lists the standard error of the mean in column 3.

Saccharomyces Genome Database ID	n	Average Standard Deviation	SEM
TYIL048W	11	0.409553494	0.03404598
YIL143C	7	0.379549229	0.057391973
YIL173W	6	0.373873207	0.030149054
YIR042C	8	0.365209845	0.050216209
YIL041W	7	0.352303547	0.068706161
YIL046W-A	13	0.346023463	0.021814741
YIL041W	8	0.344333733	0.034130857
YIR032C	16	0.33965727	0.016728618
YIL147C	11	0.333902125	0.020427139
dIX 662	12	0.333757572	0.021544584
YIL043C	6	0.32720234	0.042451113
YIL136W	8	0.321178404	0.015512967
YIL114C	10	0.320939417	0.006151207
YIL017C	8	0.320276993	0.050326294
YIR003W	12	0.315425458	0.015794316
YIR009W	8	0.310746294	0.033440879
YIL084C	8	0.308823766	0.019755292
YIL026C	15	0.308732602	0.011730084
YIR010W	8	0.308631319	0.021524068
YIL022W	6	0.305250675	0.030731394
YIL069C	7	0.304905022	0.025546019
YIL011W	6	0.303136026	0.030929538
YIL004C	8	0.302535727	0.024895923
YIR004W	8	0.302522386	0.032970457

YIR017C	8	0.301118858	0.021260615
YIR036C	8	0.299738918	0.016308527
YIL159W	8	0.299224912	0.042422393
YIR021W	8	0.298254413	0.029726719
YIL158W	4	0.297168968	0.011715119
YIR016W	8	0.294908765	0.038791301
YIL068C	8	0.294494705	0.026099723
YIL021W	8	0.291048327	0.013946231
WT 662	15	0.290918867	0.009531176
YIR007W	7	0.289977027	0.015078118
YIR014W	8	0.288227764	0.024527383
YIL160C	8	0.287551798	0.021509207
YIL105C	8	0.285703777	0.026771978
YIL010W	8	0.285593029	0.031085573
YIL110W	6	0.28493576	0.007088493
YIL123W	8	0.284312028	0.008070006
YIR037W	8	0.283739437	0.031376318
YIL031W	8	0.282814829	0.02007151
YIL109C	8	0.282285457	0.025015842
YIL113W	7	0.281298962	0.012457984
YIL005W	2	0.280796538	0.072035236
YIL020C	8	0.278607014	0.026042923
YIL036W	8	0.27779475	0.015815955
YIL014W	6	0.276834141	0.02277679
YIL162W	4	0.276748427	0.018717696
YIL135C	7	0.27646911	0.013699811
YIL122W	8	0.276139581	0.012945042
YIL003W	8	0.276039559	0.017167391
YIL073C	7	0.273187486	0.016470717
YIL128W	8	0.272454853	0.011083262
YIL067C	8	0.271677465	0.020068243
YIL074C	2	0.270653783	0.001853072
YIR035C	8	0.270376316	0.019016532
YIR031C	8	0.270052719	0.017474457
YIL061C	4	0.270014342	0.019859735
YIL126W	2	0.269079168	0.057362454
YIL132C	8	0.268755456	0.013412996
YIL045W	8	0.267483568	0.012385389
YIL040W	6	0.267307415	0.038354873

YIL085C	3	0.267037317	0.057219393
YIL039W	6	0.266607225	0.012580394
YIL140W	8	0.266398892	0.014116471
YIL108W	8	0.266384739	0.011291963
YIR034C	8	0.266265623	0.023683291
YIL077C	8	0.264821424	0.01321133
YIL055C	8	0.264545723	0.015424589
YIR025W	8	0.264100482	0.013663225
YIL008W	6	0.263841985	0.016494317
YIL016W	8	0.263822388	0.035468823
YIL127C	8	0.263805415	0.012918056
YIL007C	8	0.263192993	0.01934713
YIL089W	8	0.263115749	0.014461962
YIL102C	8	0.263084028	0.01801934
YIR001C	8	0.26296135	0.019093172
YIL152W	8	0.262935345	0.010756563
YIL145C	2	0.260890388	0.023438692
YIR006C	7	0.260624455	0.015817354
YIL052C	4	0.260325456	0.011537223
YIL111W	8	0.260253486	0.01500435
YIL060W	8	0.259215059	0.00889345
YIL164C	3	0.258985995	0.050628768
YIL153W	8	0.258213178	0.009334792
YIR018W	8	0.25791155	0.010484191
YIL166C	8	0.257753451	0.011797151
YIR033W	8	0.257704014	0.017831662
YIL070C	8	0.257682923	0.011741703
YIL103W	8	0.257498695	0.013287788
YIL024C	8	0.257282519	0.021155505
YIL155C	6	0.256104616	0.014561452
YIL149C	8	0.255909593	0.014145488
YIL006W	8	0.255805025	0.01078495
YIR005W	8	0.255688173	0.011581838
YIL124W	8	0.255542118	0.017008109
YIL056W	8	0.255491016	0.011451935
YIL092W	8	0.255110625	0.016246411
YIL053W	6	0.255033324	0.009191085
YIL104C	8	0.254225572	0.021897191
YIL157C	8	0.253930256	0.019384223

YIL121W	6	0.252440969	0.018541983
YIR013C	8	0.252075557	0.012968316
YIL133C	8	0.251953095	0.015713845
YIL062C	5	0.251601072	0.017117579
YIL029C	8	0.251097723	0.022915105
YIL002W-A	2	0.251091951	0.03955194
YIL095W	8	0.250819435	0.009232724
YIL139C	8	0.250410636	0.021778806
YIR028W	8	0.250014919	0.016296398
YIL106W	8	0.249093465	0.015098062
YIR026C	8	0.248983397	0.018747427
YIL101C	8	0.248724031	0.013508276
YIL050W	8	0.24854392	0.012283292
YIL064W	8	0.248220728	0.01493852
YIR024C	4	0.248170858	0.0227411
YIR039C	2	0.247620402	0.014291093
YIL057C	6	0.24697948	0.021856905
YIL165C	4	0.246907435	0.018895351
YIL120W	4	0.246203419	0.0085327
YIL066C	8	0.246193013	0.003652007
YIL148W	7	0.246081154	0.016761036
YIL034C	8	0.245317524	0.010197994
YIR015W	8	0.245233173	0.013777676
YIL075C	8	0.244338056	0.012815424
YIL088C	4	0.242844742	0.018748468
YIR011C	4	0.242760185	0.011491319
YIL037C	6	0.242492502	0.021563223
YIR022W	5	0.242391184	0.040751338
YIR012W	4	0.242266361	0.021376108
YIL076W	8	0.241898484	0.013814628
YIL047C	3	0.241067664	0.034306287
YIL154C	8	0.239569648	0.012214607
YIL150C	3	0.239299991	0.016760151
YIL138C	2	0.238997665	0.021522714
YIL079C	8	0.238997539	0.0152575
YIL074C	6	0.238781921	0.009968094
YIL051C	8	0.23877463	0.013521719
YIL063C	3	0.23865078	0.01438838
YIL044C	8	0.237284026	0.013954834

YIL097W	4	0.236171691	0.011684203
YIR023W	8	0.235843747	0.010456514
YIL019W	1	0.235095369	
YIL117C	8	0.23485128	0.012460405
YIL115C	3	0.232936576	0.022355997
YIL065C	8	0.232210616	0.010112386
YIL142W	4	0.232026568	0.016414359
YIL035C	8	0.230760937	0.011557821
YIR027C	4	0.230639147	0.021632133
YIL098C	8	0.22967495	0.017809814
YIL096C	4	0.227973765	0.01608345
YIL015W	5	0.226387208	0.009149823
YIL093C	4	0.226095294	0.011981074
YIL091C	4	0.225790172	0.020388712
YIL090W	4	0.225044825	0.01080938
YIL078W	4	0.225019598	0.018868149
YIL072W	8	0.224667188	0.016521148
YIL118W	4	0.223066898	0.019687077
YIL071C	4	0.22199187	0.016052811
YIL146C	4	0.221556108	0.01891177
YIL083C	8	0.220046672	0.012054339
YIL042C	4	0.219458004	0.019636349
YIR008C	2	0.219366535	0.027940028
YIR029W	6	0.218344543	0.017332964
YIL023C	6	0.217735236	0.019212021
YIL116W	4	0.217731462	0.010145119
YIL094C	2	0.215317977	0.003701198
YIL121W	2	0.214080545	0.02339947
YIL033C	4	0.213462057	0.020663279
YIL009W	5	0.213103864	0.019999307
YIL161W	4	0.212864056	0.014868934
YIL099W	2	0.211994137	0.022040385
YIL046W	8	0.209154336	0.016508078
YIL049W	8	0.208857737	0.01148344
YIL002C	8	0.20852202	0.010215943
YIR030C	8	0.207873496	0.009719558
YIL027C	4	0.205316098	0.010353605
YIL158W	4	0.205156184	0.012699839
YIR038C	3	0.203023415	0.015750916

YIL009C-A	2	0.1895295	0.028632432

ACKNOWLEDGMENTS

We thank Michael Springer and Chiara Ricci-Tam for reagents, time, resources, and thoughts throughout this work. We thank Folkert van Werven for his early thoughts on this project. This work was funded in part by a National Science Foundation Graduate Research Fellowship (DGE1122374 to CAM). AA is an investigator of the Howard Hughes Medical Institute.

References

Beach, R.R., Ricci-Tam, C., Brennan, C.M., Silberman, R.E., Springer, M., Amon, A., Moomau, C.A., Hsu, P.-H., and Hua, B. (2017). Aneuploidy Causes Non-genetic Individuality. Cell *169*, 229-242.e21.

Chen, G., Bradford, W.D., Seidel, C.W., and Li, R. (2012). Hsp90 Stress Potentiates Rapid Cellular Adaptation through Induction of Aneuploidy. Nature *482*, 246.

Dephoure, N., Hwang, S., O'Sullivan, C., Dodgson, S.E., Gygi, S.P., Amon, A., and Torres, E.M. (2014). Quantitative proteomic analysis reveals posttranslational responses to aneuploidy in yeast. Elife *3*, 1–27.

Dodgson, S.E., Kim, S., Costanzo, M., Baryshnikova, A., Morse, D.L., Kaiser, C.A., Boone, C., Amon, A., Abe, F., Usui, K., et al. (2016). Chromosome-Specific and Global Effects of Aneuploidy in Saccharomyces cerevisiae. Genetics *202*, 1395–1409.

Doran, E., Keator, D., Head, E., Phelan, M.J., Kim, R., Totoiu, M., Barrio, J.R., Small, G.W., Potkin, S.G., and Lott, I.T. (2017). Down Syndrome, Partial Trisomy 21, and Absense of Alzheimer's Disease: The Role of APP. J. Alzheimer's Dis. *56*, 459–470.

Escalante-Chong, R., Savir, Y., Carroll, S.M., Ingraham, J.B., Wang, J., Marx, C.J., Springer, M., and Johnson, A.D. (2015). Galactose metabolic genes in yeast respond to a ratio of galactose and glucose. Proc. Natl. Acad. Sci. *112*, 1636–1641.

Hassold, T.J., and Jacobs, P.A. (1984). Trisomy in Man. Annu. Rev. Genet. *18*, 69–97.

Ho, C.H., Magtanong, L., Barker, S.L., Gresham, D., Nishimura, S., Natarajan, P., Koh, J.L.Y., Porter, J., Gray, C.A., Andersen, R.J., et al. (2009). A molecular barcoded yeast ORF library enables mode-of-action analysis of bioactive compounds.

Longtine, M.S., Mckenzie III, A., Demarini, D.J., Shah, N.G., Wach, A., Brachat, A., Philippsen, P., and Pringle, J.R. (1998). Additional modules for versatile and economical PCR-based gene deletion and modification in Saccharomyces cerevisiae. Yeast *14*, 953–961.

Oromendia, A.B., Dodgson, S.E., and Amon, A. (2012). Aneuploidy causes proteotoxic stress in yeast. Genes Dev. *26*, 2696–2708.

Rahman, S., and Zenklusen, D. (2013). Single-Molecule Resolution Fluorescent In Situ Hybridization (smFISH) in the Yeast S. cerevisiae. In Imaging Gene Expression: Methods and Protocols, Methods in Molecular Biology, Y. Shav-Tal, ed. (Springer Science + Business Media), pp. 33–46.

Reifenberger, E., Boles, E., and Ciriacy, M. (1997). Kinetic characterization of individual hexose transporters of Saccharomyces cerevisiae and their relation to the triggering mechanisms of glucose repression. Eur. J. Biochem. *245*, 324–333.

Roper, R.J., and Reeves, R.H. (2006). Understanding the Basis for Down Syndrome Phenotypes. PLoS Genet. *2*.

Rovelet-Lecrux, A., Hannequin, D., Raux, G., Le Meur, N., Laquerrière, A., Vital, A., Dumanchin, C., Feuillette, S., Brice, A., Vercelletto, M., et al. (2006). APP locus duplication causes autosomal dominant early-onset Alzheimer disease with cerebral amyloid angiopathy. Nat. Genet. *38*, 24–26.

Roy, A., Kim, Y.B., Cho, K.H., and Kim, J.H. (2014). Glucose starvation-induced turnover of the yeast glucose transporter Hxt1. Biochim. Biophys. Acta - Gen. Subj. *1840*, 2878–2885.

Roy, A., Dement, A.D., Cho, K.H., and Kim, J.H. (2015). Assessing glucose uptake through the yeast hexose transporter 1 (Hxt1). PLoS One *10*.

Santaguida, S., and Amon, A. (2015). Short- and long-term effects of chromosome mis-segregation and aneuploidy. Nat. Rev. Mol. Cell Biol. *16*, 473–485.

Shin, M., van Leeuwen, J., Boone, C., and Bretscher, A. (2018). Yeast Aim21/Tda2 both regulates free actin by reducing barbed end assembly and forms a complex with Cap1/Cap2 to balance actin assembly between patches and cables. Mol. Biol. Cell *29*, 923–936.

Stingele, S., Stoehr, G., Peplowska, K., Cox, J., Mann, M., and Storchova, Z. (2012). Global analysis of genome, transcriptome and proteome reveals the response to aneuploidy in human cells. Mol. Syst. Biol. *8*.

Takar, M., Wu, Y., and Graham, T.R. (2016). The Essential Neo1 Protein from Budding Yeast Plays a Role in Establishing Aminophospholipid Asymmetry of the Plasma Membrane *.

Terhorst, A., Sandikci, A., Keller, A., Whittaker, C.A., Dunham, M.J., and Amon, A. (2020). The environmental stress response causes ribosome loss in aneuploid yeast cells. Proc. Natl. Acad. Sci. *117*, 17031–17040.

Weaver, B.A., and Cleveland, D.W. (2006). Does aneuploidy cause cancer? Curr. Opin. Cell Biol. *18*, 658–667.

Chapter 3: Conclusions and Future Directions

SUMMARY OF KEY CONCLUSIONS

Multiple genes on chromosome IX can increase GAL1pr-YFP variability

By screening chromosome IX, I identified several genes which lead to variability at the GAL1-10 promoter in single extra copy. Among screen hits there are a few themes that arise (Table 1): NEO1 and AIM21 are both involved in endocytosis, SLN1 and POR2 are involved in maintaining osmolarity, and SSL2, SDS3, and IRR1 are all known to relocalize to the cytosol in response to hypoxia. These overlaps in hits indicate potential cellular processes which will lead to variability when perturbed. However, the diversity of hits points to the fact that while many genes are sufficient to increase noise at the GAL1-10 promoter to some degree, none appear to be necessary, as multiple open reading frames (ORFs) are able to increase variability alone.

This is further supported by deletion of several of these genes from Disome IX cells. When I individually deleted the screen hits from Disome IX cells, only a handful reduce GAL promoter variability, and none restore variability to WT euploid levels. This means that while the addition of these single genes may be sufficient to increase variability in euploid cells, they are not necessary for variability in Disome IX.

I did not identify a single gene on chromosome IX that is wholly responsible for this phenotype. Instead, there are a number of genes which contribute to variability either redundantly or in combination. Previous work in aneuploid yeast has distinguished between phenotypes which are the result of the addition of a few dosage sensitive genes and those which occur by mass action of dosage increase in several genes (Bonney et al., 2015; Dodgson et al., 2016). The lack of correlation between degree of aneuploidy and standard deviation in

GAL1pr-YFP (discussed in greater detail later) indicates that it is more likely the former. It would be interesting to delete combinations or all of the hits in Disome IX cells to see if these few genes together are necessary to produce the full increase in standard deviation. Similarly, I would be interested in overexpressing multiple screen hits in euploid cells to see if their effect on GAL1pr variability is additive. These experiments would shed light on the question of how much of chromosome IX is necessary to cause this phenotype.

Gene	SGD Description
NEO1	Phospholipid translocase (flippase), role in phospholipid asymmetry of plasma membrane; involved in **endocytosis**, vacuolar biogenesis and Golgi to ER vesicle-mediated transport; localizes to endosomes and the Golgi apparatus
SSL2	Component of RNA polymerase transcription factor TFIIH holoenzyme; acts as dsDNA-dependent translocase in context of TFIIH, unwinds DNA strands during initiation and promotes transcription start site (TSS) scanning; **relocalizes to cytosol under hypoxia**
YIR042C	Putative protein of unknown function
YIL046W-A	Putative protein of unknown function; identified by expression profiling and mass spectrometry
DAL3	Ureidoglycolate lyase; converts ureidoglycolate to glyoxylate and urea in the third step of allantoin degradation; expression is sensitive to nitrogen catabolite repression
SLN1	Transmembrane histidine phosphotransfer kinase and **osmosensor**; regulates MAP kinase cascade; transmembrane protein with an intracellular kinase domain that signals to Ypd1p and Ssk1p, thereby forming a phosphorelay system similar to bacterial two-component regulators
POR2	Putative mitochondrial porin (voltage-dependent anion channel); not required for mitochondrial membrane permeability or mitochondrial **osmotic stability**
AIM21	Subunit of a complex that associates with actin filaments; inhibits barbed end F-actin assembly; elevates actin monomer pools to increase **endocytotic efficiency** and to regulate the distribution of actin between cables and patches
SDS3	Component of the Rpd3L histone deacetylase complex; required for its structural integrity and catalytic activity, involved in transcriptional silencing; **relocalizes to the cytosol in response to hypoxia**
IRR1	Subunit of the cohesin complex; **relocalizes to the cytosol in response to hypoxia**; essential

Table 1. Screen hits Brief descriptions of genes which appeared as hits in my screen of chromosome IX for increased GAL1pr-YFP variability. Descriptions are adapted from the Saccharomyces Genome Database (SGD). Common key words are highlighted in purple.

Uptake of hexose sugars adds to variability in the GAL pathway

To identify potential sources of variability at the GAL1-10 promoter, I surveyed upstream components of the galactose activation pathway for instances of variability in Disome IX yeast. There was no measurable variability in expression of the key signaling components Gal4, Gal80, and Gal3. There is also no variability in expression of hexose transporters Hxt1 and Gal2, however there is variability in their function of hexose transport. Disome IX yeast are variable in uptake of both glucose and galactose, measured by internalization of fluorescent analogs to those sugars.

To better establish the relationship between variability in hexose uptake and variability in promoter induction, I replaced the fluorophore in the reporter construct, generating GAL1pr-mCherry. This allows for simultaneous measurement of hexose uptake and promoter induction in single cells. Preliminary experiments show a positive, but weak correlation between galactose uptake and induction of GAL1pr-mCherry (Figure 1). This correlation is stronger in Disome IX cells than euploid, suggesting that as variability in hexose uptake increases, it becomes a larger component of the noise observed at the promoter. It would be interesting to suppress variability in hexose uptake by constitutive overexpression of hexose transporters and see if that suppresses noise at the promoter.

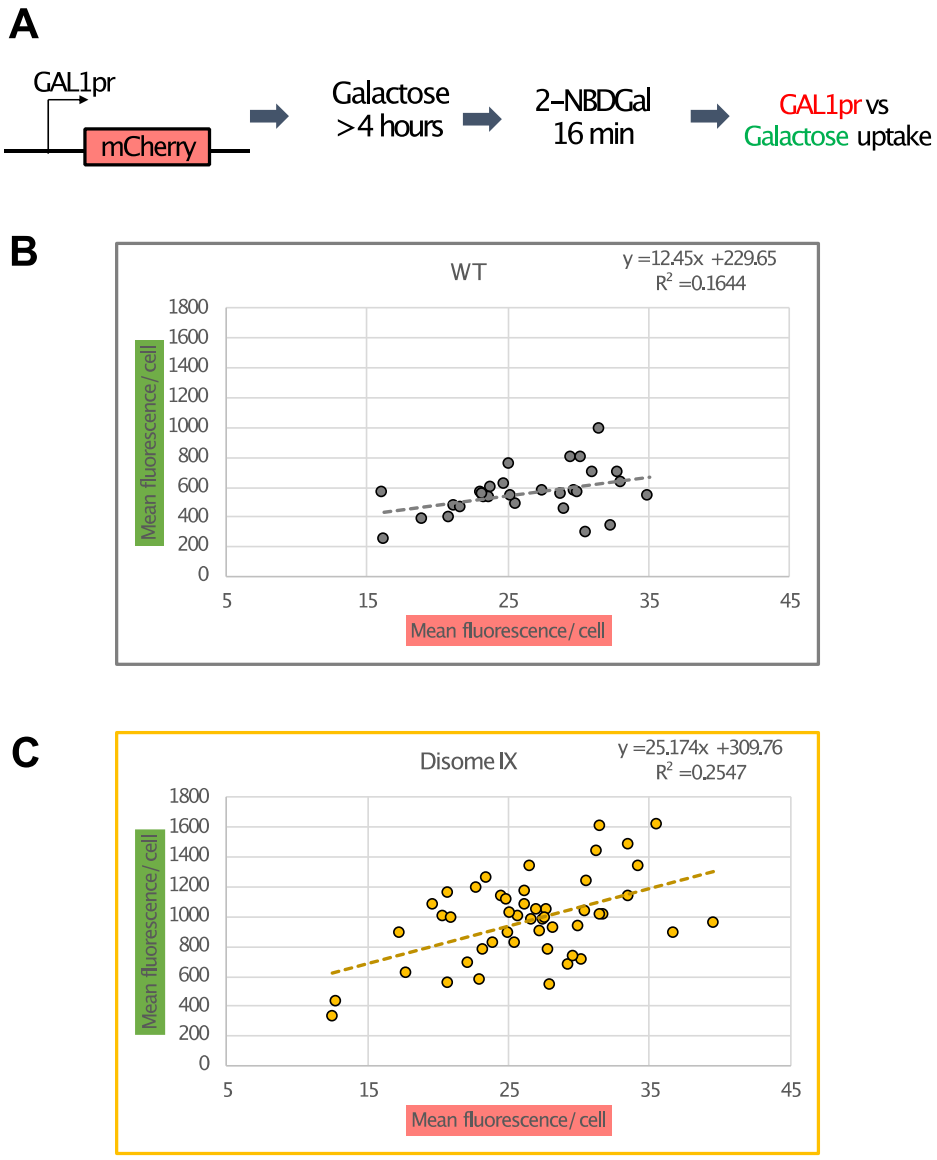

Figure 1. Correlation of galactose uptake and GAL1pr-mCherry

(A) Yeast containing GAL1pr-mCherry reporter were grown up in media containing galactose to induce expression at the GAL1-10 promoter. Yeast were then incubated with fluorescent galactose analog, 2-NBDGalactose. Galactose uptake a promoter induction were measured in single cells. Correlation is plotted in WT euploid (B) and Disome IX (C). Linear regression and R^2 values are listed on plots.

Inhibiting endocytosis increases GAL1-10 promoter variability

I have shown that disrupting endocytosis increases variability at the GAL1-10 promoter. Disome IX has an established endocytic defect which is rescued by deletion of one copy of PRK1, a gene on chromosome IX which inhibits endocytosis (Dodgson et al., 2016). This defect can be largely replicated in euploid yeast by deleting EDE1, which is involved in formation of early endocytic sites. The endocytic defect in disome IX is also exacerbated by EDE1 deletion (Figure 2). This defect, combined with the discovery of multiple endocytic genes in my screen of chromosome IX (Hua and Graham, 2003; Shin et al., 2018; Takar et al., 2016; Wicky et al., 2004), led to the hypothesis that endocytosis is involved in GAL pathway variability.

Using these endocytosis mutations, I was able to show that disrupting endocytosis by deletion of EDE1, addition of NEO1, addition of AIM21, or the addition of a full chromosome IX all increase the standard deviation of GAL1pr-YFP. The variability is even further increased in Disome IX ede1Δ. This inverse relationship between endocytosis and GAL1pr-YFP suggests that reduced endocytosis leads to increased variability in the GAL pathway. The same is true in uptake of hexose sugars; EDE1 deletion increases variability in glucose and galactose uptake. It will be important to measure variability in glucose and galactose uptake in euploid cells overexpressing NEO1 and AIM21 to confirm that these additions increase variability in the same way.

It seems that endocytic defect is not the only aspect of Disome IX which contributes to GAL pathway variability. While deleting one copy of PRK1 fully restores endocytosis to WT levels in Disome IX yeast, Disome IX prk1Δ/PRK1 yeast are still more variable in GAL1-10

promoter induction than euploid, with a potential slight reduction in GAL1pr-YFP standard deviation compared to Disome IX alone. Commonalities in the screen hits listed in Table 1 provide candidates for other sources of variability in Disome IX yeast which increase variability in the absence of endocytic defect.

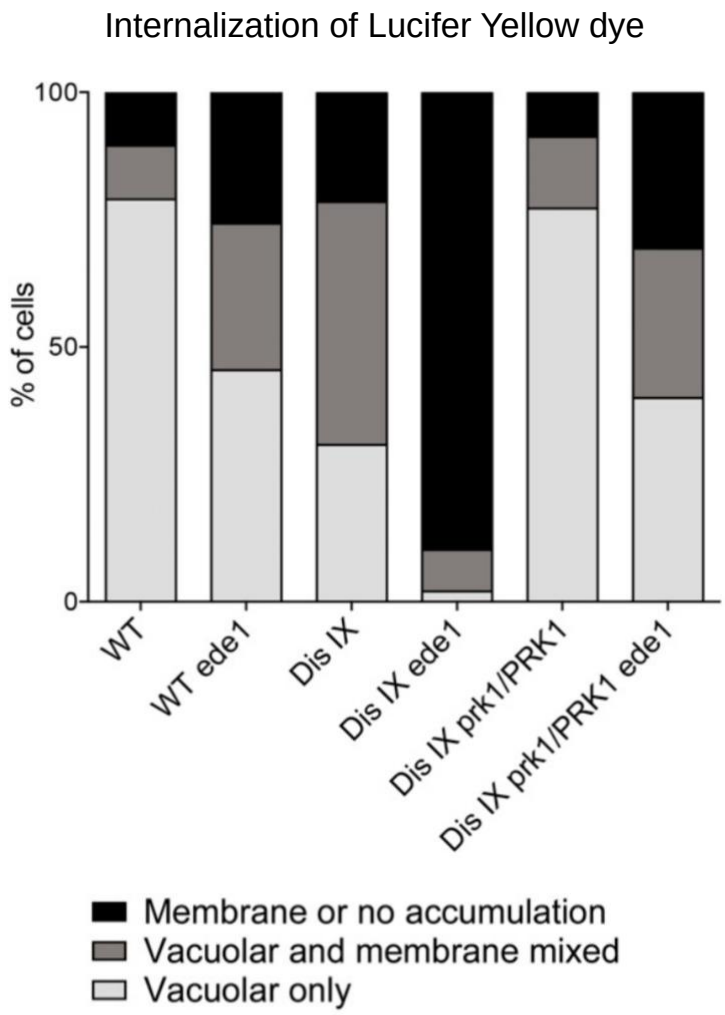

Figure 2. Disome IX endocytic defect

Yeast were incubated with Lucifer Yellow dye and imaged to determine efficiency of endocytosis. Disome IX cells are defective in endocytosis to a similar level to the deletion of EDE1. Disome IX ede1Δ are almost completely unable to internalized Lucifer Yellow. The defect in Disome IX is rescued by deletion of one copy of PRK1. The double mutant, Disome IX ede1Δ prk1Δ/PRK1 is restored to typical Disome IX levels. (Figure adapted from Dodgson et al. 2016)

Endocytosis defect alters localization of hexose transporters

I took two orthogonal approaches to understanding variability at the GAL1-10 promoter. A survey of the galactose signaling pathway found that Disome IX yeast are variable in uptake of hexose sugars. A screen of chromosome IX found that perturbing endocytosis increases GAL pathway variability. The localization of hexose transporters is at the intersection of these two discoveries. Budding yeast have a large family of hexose transporters with varying affinities for both glucose and galactose (Ozcan and Johnston, 1999; Reifenberger et al., 1997; Wieczorke et al., 1999). Competition between glucose and galactose for transport serves as the input for the GAL pathway (Escalante-Chong et al., 2015). Expression and localization of hexose transporters are regulated in response to the concentrations of sugars in the environment to maintain constant intracellular concentrations of sugars (Kim et al., 2013; Maier et al., 2002). Importantly, turnover of hexose transporters in response to changing environments occurs via endocytosis (Roy et al., 2014).

By studying localization of fluorescently tagged Hxt1 and Gal2, I found that inhibiting endocytosis lowers the concentration of hexose transporters on the cell membrane. There is less Hxt1 at the membrane in Disome IX cells. There is no measurable difference in Gal2 localization in Disome IX, but when endocytosis defect is exacerbated by deletion of EDE1, there is less Gal2 at the membrane. It is initially counterintuitive that inhibiting endocytosis would result in fewer transporters as endocytosis is responsible for removing them from the membrane. However, disrupting endocytosis alters the homeostasis between endocytosis and exocytosis which governs membrane transport (Feyder et al., 1980; Horák, 2003; Laidlaw and Macdonald, 2018; Ma and Burd, 2019). Therefore, I hypothesize that inefficient endocytosis

results in overall less membrane turnover, making the placement of hexose transporters on the membrane more difficult, ultimately leading to a lower concentration of transporters at the membrane. Overall, these finding lead to a model in which membrane trafficking is disrupted in Disome IX yeast, resulting in fewer hexose transporters at the plasma membrane, ultimately causing variability in hexose transport which propagates through the galactose signaling pathway producing noise in induction of the GAL1-10 promoter (Figure 3).

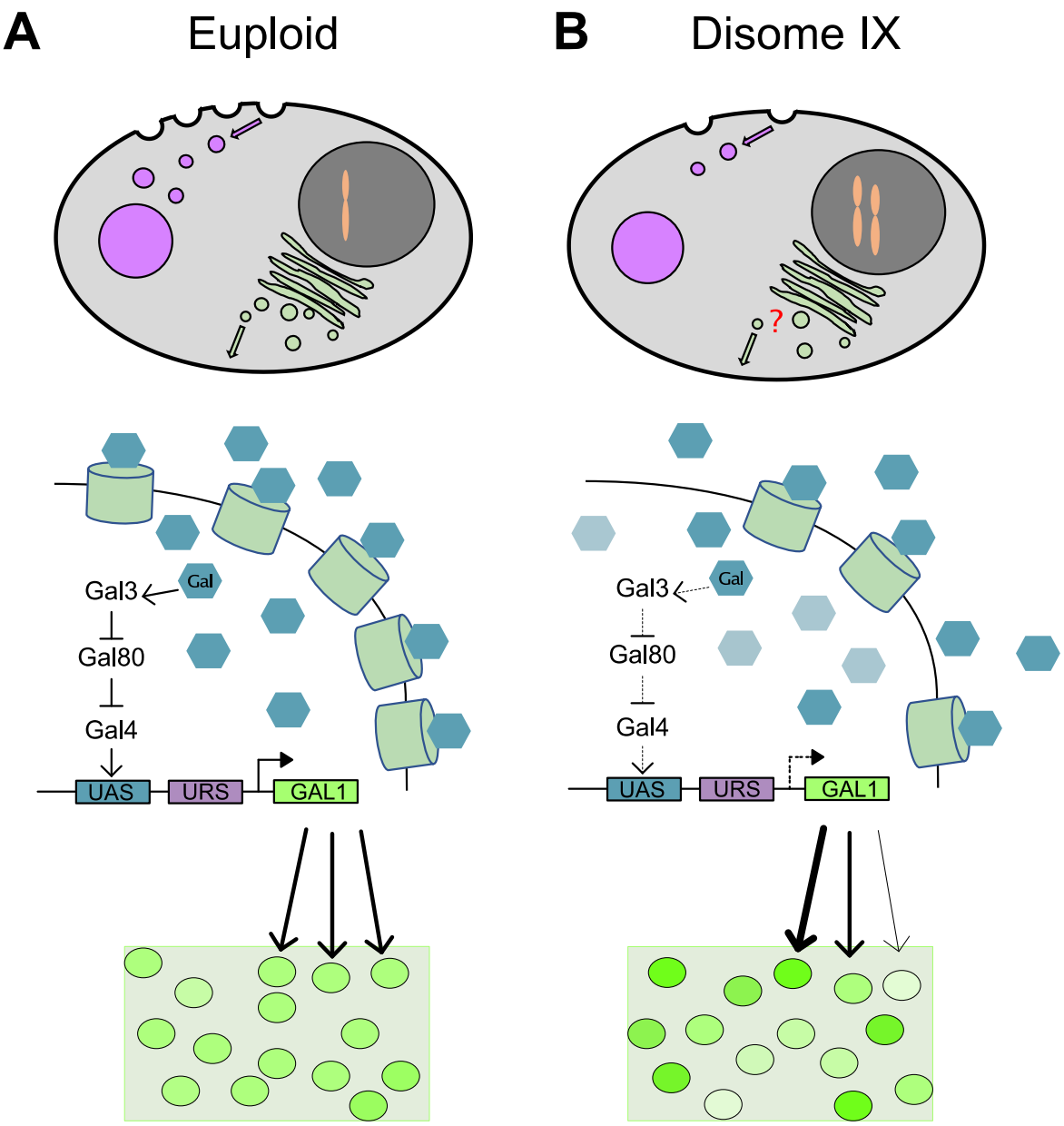

Figure 3. A model for GAL pathway variability through altered localization of hexose transporters

(A) In WT euploid yeast, hexose transporters are internalized and placed at the membrane in response to sugar concentrations in the environment through an established homeostasis in

membrane trafficking (top). Galactose enters the cell through transmembrane hexose transporters and signals the activation of the galactose signaling cascade (middle). Consistent hexose transporter leads to a consistent activation of the GAL1-10 promoter throughout a genetically homogenous population of yeast (bottom).

(B) In Disome IX yeast, endocytosis is inhibited, resulting in a disruption of membrane trafficking and the dysregulation of the localization of hexose transporters to the membrane (top). Extracellular galactose competes for entry into the cell through fewer transporters, leading to variability in the amount of galactose entering the cell (middle). Variability in galactose uptake propagates through the galactose signaling pathway, leading to inconsistent induction of the promoter and ultimately noise in expression of the YFP reporter (bottom).

Variability at the GAL1-10 promoter is unique to each disome

The mechanism by which variability in GAL1pr-YFP is increased is likely unique to each disome. Variability at the GAL1-10 promoter has been observed in disomes IX, VIII, II, XIII, and XVI. Although I have not definitively identified the full reason that Disome IX exhibits variability, I have shown that dosage of specific genes can alter variability, and also provided a mechanism through which that can happen. The endocytic defect in Disome IX is sufficient to cause increased variability in GAL1-10 promoter induction. Because this defect in endocytosis is unique to Disome IX, the GAL pathway must be perturbed in other ways in other disomes.

In Chapter 2, I showed that uptake of hexose sugars glucose and galactose is variable in Disome IX yeast. After 4-minute incubation with 2-NBDGlucose, Disomes IX, V, and XIII all have significantly higher standard deviation in glucose uptake than WT euploid yeast (Figure 4A-B). This variability does not always correlate with variability in GAL1pr-YFP (Figure 4C). Disome II has a significantly higher standard deviation than WT in GAL1pr-YFP induction, but there is no difference in glucose uptake.

Disome XIII, which does have an increase in glucose uptake variability comparable to Disome IX, does not have the differences in hexose transporter localization seen in Disome IX (Figure 5). Noise can be introduced to the promoter is a variety of ways and is the result of complex set of signals. Even though the ultimate phenotype of GAL promoter variability is common to multiple disomes, the mechanism is not.

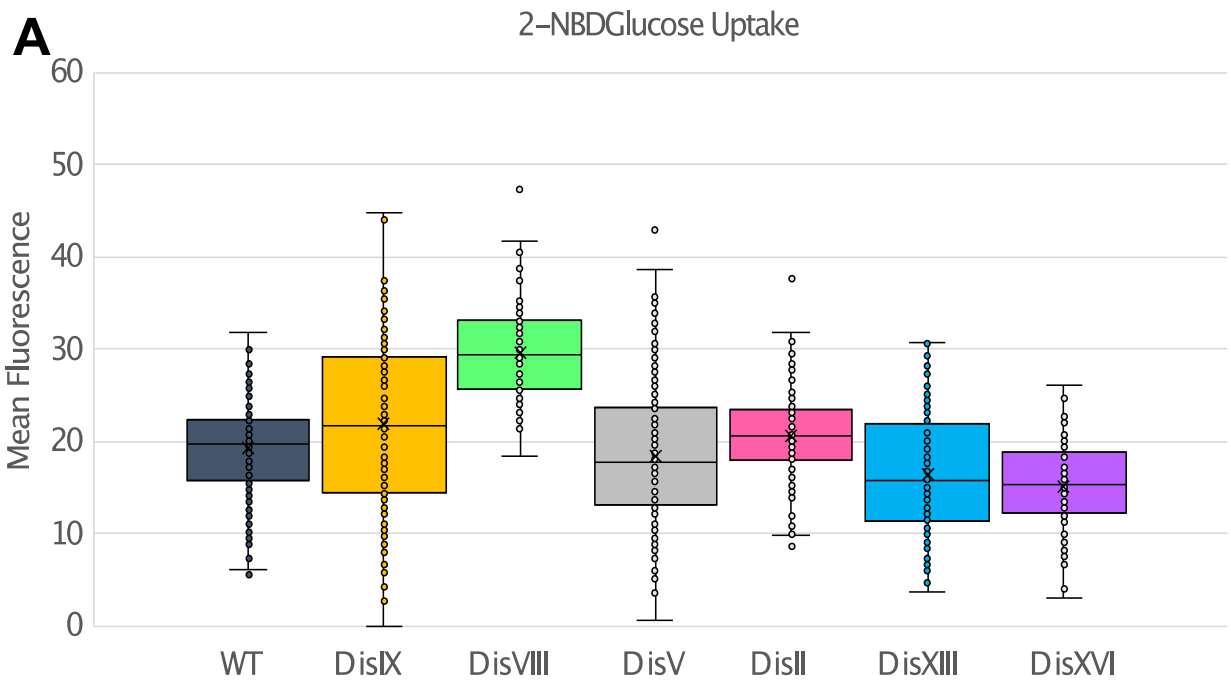
A
2–NBDGlucose Uptake
Mean Fluorescence
60
50
40
30
20
10
0
WT
DisIX
DisVIII
DisV
DisII
DisXIII
DisXVI

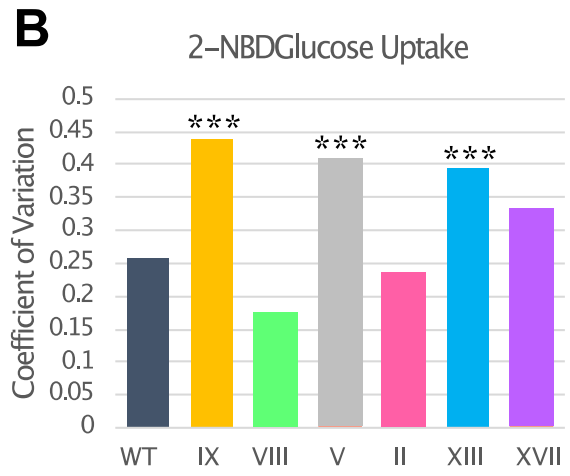
B
2–NBDGlucose Uptake
Coefficient of Variation
0.5
0.45
0.4
0.35
0.3
0.25
0.2
0.15
0.1
0.05
0
***
***
***
WT
IX
VIII
V
II
XIII
XVII

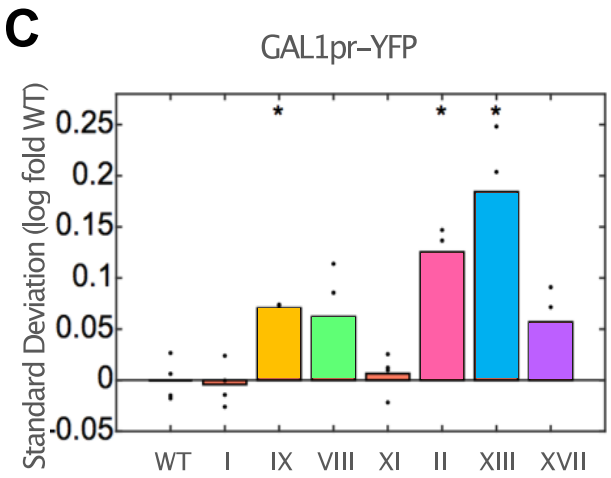
C
GAL1pr–YFP
Standard Deviation (log fold WT)
0.25
0.2
0.15
0.1
0.05
0
-0.05
WT
I
IX
VIII
XI
II
XIII
XVII

Figure 4. Glucose uptake variability in multiple disomes

(A) WT and Disome yeast were incubated with fluorescent glucose analog 2-NBDGlucose for 4 minutes and imaged. Mean fluorescence per cell is plotted for each strain with a box and whiskers plot overlaid to show distribution. (B) The coefficient of variation of each distribution shown in (A). (C) The standard deviation of GAL1pr-YFP of WT and disome yeast, adapted from Beach et al. 2017. Colors in A-C highlight disomes plotted on each graph for each of comparison.

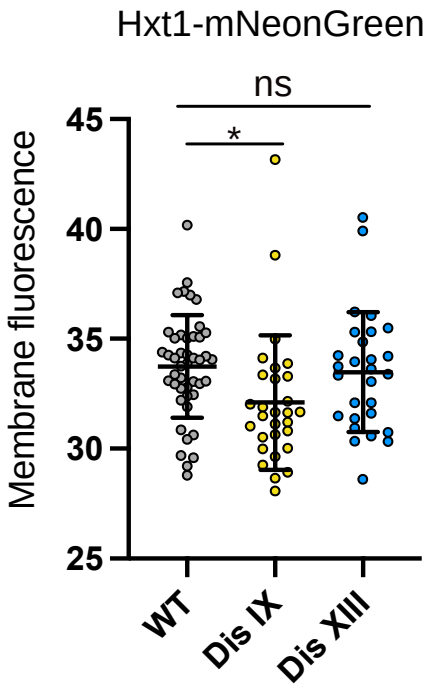

Figure 5. Hexose transporter localization in Disome XIII

WT and disome yeast were grown up in galactose media and imaged. The concentration of fluorescently tagged hexose transporter, Hxt1-mNeonGreen, was measured. Significance was calculated by Welch's t-test.

Phenotypic variability as a consequence of aneuploidy

Phenotypic variability is a feature of aneuploidy and is frequently noted in discussions of human trisomies (Caba et al., 2013; Callier et al., 2005; Hsu and Hou, 2007; Lin et al., 2006; Roper and Reeves, 2006). Speculation as to the source of this variability in trisomy 21, Down syndrome, has led to a number of theories largely based around genetic heterogeneity among individuals with Down syndrome. One hypothesis is that because aneuploidy causes genomic instability, there is more mosaicism in people with trisomies (Hsu and Hou, 2007; Potter, 2016; Sheltzer et al., 2011). Stochastic copy number variation (CNVs) across tissue and cell types may make some individuals more or less prone to certain phenotypes (Henrichsen et al., 2009; Potter, 2016). Another common hypothesis is that the typical array of mutations, SNPs, and CNVs expected in any population alters susceptibility to particular phenotypes. A lot of research has focused on identifying mutations which increase likelihood of certain Down syndrome traits (Kerstann et al., 2004; Letourneau and Antonarakis, 2012; Roper and Reeves, 2006). This has led to the discovery of mutations which pre dispose certain cardiac defects in Down Syndrome (Dunlevy et al., 2010; Li et al., 2012; Maslen et al., 2006). However, the work presented here adds to the evidence that phenotypic variability can be the result of aneuploidy itself regardless of genetic heterogeneity.

In yeast and mouse models of aneuploidy, phenotypic variability can be observed in genetically homogenous populations. Previous work from our lab shows that aneuploid yeast are variable in cell cycle length, stress response, and transcriptional activation. Non-genetic variability is evident in mice as well. Development of trisomic mouse embryos is variable, with an increased standard deviation of nuchal edema thickness in trisomy 19 embryos (Beach et al.,

2017). The Down syndrome mouse model, Ts65Dn, displays variability in cerebellar phenotypes compared to another model trisomic for fewer genes, Ts1Cje (Olson et al., 2004).

The differing mechanisms by which variability is produced in aneuploid yeast reveal that variability is not one general phenotype of aneuploidy, but a large category made up of several distinct phenotypes. Variability in S phase duration is the result of genomic instability, a common aneuploid phenotype (Blank et al., 2015; Sheltzer et al., 2011), and is rescued in all aneuploidies bypassing the DNA damage checkpoint (Beach et al., 2017). In contrast, my data shows that variability in promoter induction is the result of specific gene dosage effects. Phenotypes which are more variable in aneuploid populations represent complex phenotypes whose regulation is reliant upon dosage sensitive pathways.

Phenotypic variability is not always the result of genetic variability, and can be a consequence of aneuploidy itself. Therefore, searching for “susceptibility” mutations in human trisomies will not always yield meaningful results. In some cases, it may be more clinically relevant to investigate how the trisomy itself produces phenotypic variability.

REFERENCES

Beach, R.R., Ricci-Tam, C., Brennan, C.M., Silberman, R.E., Springer, M., Amon, A., Moomau, C.A., Hsu, P.-H., and Hua, B. (2017). Aneuploidy Causes Non-genetic Individuality. Cell *169*, 229-242.e21.

Blank, H.M., Sheltzer, J.M., Meehl, C.M., and Amon, A. (2015). Mitotic entry in the presence of DNA damage is a widespread property of aneuploidy in yeast. Mol. Biol. Cell *26*, 1440–1451.

Bonney, M.E., Moriya, H., and Amon, A. (2015). Aneuploid proliferation defects in yeast are not driven by copy number changes of a few dosage-sensitive genes. Genes Dev. *29*, 898–903.

Caba, L., Rusu, C., Butnariu, L., Panzaru, M., Braha, E., Volosciuc, M., Popescu, R., Gramescu, M., Bujoran, C., Martiniuc, V., et al. (2013). Phenotypic variability in Patau syndrome. Rev. Med. Chir. Soc. Med. Nat *117*, 321–327.

Callier, P., Faivre, L., Cusin, V., Marle, N., Thauvin-Robinet, C., Sandre, D., Rousseau, T., Sagot, P., Lacombe, E., Faber, V., et al. (2005). Microcephaly is not mandatory for the diagnosis of mosaic variegated aneuploidy syndrome. Am. J. Med. Genet. *137 A*, 204–207.

Dodgson, S.E., Kim, S., Costanzo, M., Baryshnikova, A., Morse, D.L., Kaiser, C.A., Boone, C., Amon, A., Abe, F., Usui, K., et al. (2016). Chromosome-Specific and Global Effects of Aneuploidy in Saccharomyces cerevisiae. Genetics *202*, 1395–1409.

Dunlevy, L., Bennett, M., Slender, A., Lana-Elola, E., Tybulewicz, V.L., Fisher, E.M.C., and Mohun, T. (2010). Down's syndrome-like cardiac developmental defects in embryos of the transchromosomic Tc1 mouse. Cardiovasc. Res. *88*, 287–295.

Escalante-Chong, R., Savir, Y., Carroll, S.M., Ingraham, J.B., Wang, J., Marx, C.J., Springer, M., and Johnson, A.D. (2015). Galactose metabolic genes in yeast respond to a ratio of galactose and glucose. Proc. Natl. Acad. Sci. *112*, 1636–1641.

Feyder, S., De Craene, J.-O., Bär, S., Bertazzi, D.L., and Friant, S. (1980). Membrane Trafficking in the Yeast Saccharomyces cerevisiae Model. Int. J. Mol. Sci *16*, 1509–1525.

Henrichsen, C.N., Chaignat, E., and Reymond, A. (2009). Copy number variants, diseases and gene expression. Hum. Mol. Genet. *18*, R1–R8.

Horák, J. (2003). The role of ubiquitin in down-regulation and intracellular sorting of membrane proteins: insights from yeast. Biochim. Biophys. Acta - Biomembr. *1614*, 139–155.

Hsu, H.-F., and Hou, J.-W. (2007). Variable Expressivity in Patau Syndroe is Not All Related to Trisomy 13 Mosaicism. Am. J. Med. Genet. *Part A*, 1739–1748.

Hua, Z., and Graham, T.R. (2003). Requirement for Neo1p in Retrograde Transport from the Golgi Complex to the Endoplasmic Reticulum. Mol. Biol. Cell *14*, 4971–4983.

Kerstann, K.F., Feingold, E., Freeman, S.B., Bean, L.J.H., Pyatt, R., Tinker, S., Jewel, A.H., Capone, G., and Sherman, S.L. (2004). Linkage Disequilibrium Mapping in Trisomic Populations:

Analytical Approaches and an Application to Congenital Heart Defects in Down Syndrome.

Kim, J.-H., Roy, A., Ii, D.J., and Cho, K.H. (2013). The glucose signaling network in yeast. Biochim. Biophysa Acta *1830*, 5204–5210.

Laidlaw, K.M.E., and Macdonald, C. (2018). Endosomal trafficking of yeast membrane proteins. Biochem. Soc. Trans. *46*, 1551–1558.

Letourneau, A., and Antonarakis, S.E. (2012). Genomic determinants in the phenotypic variability of Down syndrome (Elsevier Inc.).

Li, H., Cherry, S., Klinedinst, D., DeLeon, V., Redig, J., Reshey, B., Chin, M.T., Sherman, S.L., Maslen, C.L., and Reeves, R.H. (2012). Genetic modifiers predisposing to congenital heart disease in the sensitized Down syndrome population. Circ. Cardiovasc. Genet. *5*, 301–308.

Lin, H.-Y., Lin, S.-P., Chen, Y.-J., Hung, H.-Y., Kao, H.-A., Hsu, C.-H., Chen, M.-R., Chang, J.-H., Ho, C.-S., Huang, F.-Y., et al. (2006). Clinical Characteristics and Survival of Trisomy 18 in a Medical Center in Taipei, 1988-2004. Am. J. Med. Genet. *Part A*, 945–951.

Ma, M., and Burd, C.G. (2019). Retrograde trafficking and plasma membrane recycling pathways of the budding yeast Saccharomyces cerevisiae.

Maier, A., Volker, B., Boles, E., and Fuhrmann, G.F. (2002). Characterisation of glucose transport in Saccharomyces cerevisiae with plasma membrane vesicles (countertransport) and intact cells (initial uptake) with single Hxt1, Hxt2, Hxt3, Hxt4, Hxt6, Hxt7 or Gal2 transporters. FEMS Yeast Res. *2*, 539–550.

Maslen, C.L., Babcock, D., Robinson, S.W., Bean, L.J.H., Dooley, K.J., Willour, V.L., and Sherman, S.L. (2006). CRELD1 Mutations Contribute to the Occurrence of Cardiac Atrioventricular Septal Defects in Down Syndrome. Am. J. Med. Genet. Part A *140*, 2501–2505.

Olson, L.E., Roper, R.J., Baxter, L.L., Carlson, E.J., Epstein, C.J., and Reeves, R.H. (2004). Down Syndrome Mouse Models Ts65Dn, Ts1Cje, and Ms1Cje/Ts65Dn Exhibit Variable Severity of Cerebellar Phenotypes. Dev. Dyn. *230*, 581–589.

Ozcan, S., and Johnston, M. (1999). Function and regulation of yeast hexose transporters. Microbiol. Mol. Biol. Rev. *63*, 554–569.

Potter, H. (2016). Beyond Trisomy 21: Phenotypic Variability in People with Down Syndrome Explained by Further Chromosome Mis-segregation and Mosaic Aneuploidy. J Down Syndr Chromosom Abnorm. *2*.

Reifenberger, E., Boles, E., and Ciriacy, M. (1997). Kinetic characterization of individual hexose transporters of Saccharomyces cerevisiae and their relation to the triggering mechanisms of glucose repression. Eur. J. Biochem. *245*, 324–333.

Roper, R.J., and Reeves, R.H. (2006). Understanding the Basis for Down Syndrome Phenotypes. PLoS Genet. *2*.

Roy, A., Kim, Y.B., Cho, K.H., and Kim, J.H. (2014). Glucose starvation-induced turnover of the

yeast glucose transporter Hxt1. Biochim. Biophys. Acta - Gen. Subj. *1840*, 2878–2885.

Sheltzer, J.M., Blank, H.M., Pfau, S.J., Tange, Y., George, B.M., Humpton, T.J., Brito, I.L., Hiraoka, Y., Niwa, O., and Amon, A. (2011). Aneuploidy Drives Genomic Instability in Yeast. Science (80-.). *333*, 1026–1030.

Shin, M., van Leeuwen, J., Boone, C., and Bretscher, A. (2018). Yeast Aim21/Tda2 both regulates free actin by reducing barbed end assembly and forms a complex with Cap1/Cap2 to balance actin assembly between patches and cables. Mol. Biol. Cell *29*, 923–936.

Takar, M., Wu, Y., and Graham, T.R. (2016). The Essential Neo1 Protein from Budding Yeast Plays a Role in Establishing Aminophospholipid Asymmetry of the Plasma Membrane *.

Wicky, S., Schwarz, H., and Singer-Krüger, B. (2004). Molecular Interactions of Yeast Neo1p, an Essential Member of the Drs2 Family of Aminophospholipid Translocases, and Its Role in Membrane Trafficking within the Endomembrane System. Mol. Cell. Biol. *24*, 7402–7418.

Wieczorke, R., Krampe, S., Weierstall, T., Freidel, K., Hollenberg, C.P., and Boles, E. (1999). Concurrent knock-out of at least 20 transporter genes is required to block uptake of hexoses in Saccharomyces cerevisiae. FEBS Lett. *464*, 123–128.